Research Signpost
37/661 (2), Fort P.O.
Trivandrum-695 023
Kerala, India

Recent Developments in Wear Prevention, Friction and Lubrication, 2010: 45-136
ISBN: 978-81-308-0377-7 Editor: George K. Nikas

# 2. Rolling bearing life prediction, theory, and application

Erwin V. Zaretsky
*Chief Engineer (Structures and Materials), NASA Glenn Research Center, USA*

**Abstract.** A tutorial is presented outlining the evolution, theory, and application of rolling-element bearing life prediction from that of A. Palmgren, 1924, W. Weibull, 1939, G. Lundberg and A. Palmgren, 1947 and 1952, E. Ioannides and T. Harris, 1985, and E. Zaretsky, 1987. Comparisons are made between these life models. The Ioannides-Harris model without a fatigue limit is identical to the Lundberg-Palmgren model. The Weibull model is similar to that of Zaretsky if the exponents are chosen to be identical. Both the load-life and Hertz stress-life relations of Weibull, Lundberg and Palmgren, and Ioannides and Harris reflect a strong dependence on the Weibull slope. The Zaretsky model decouples the dependence of the critical shear stress-life relation from the Weibull slope. This results in a nominal variation of the Hertz stress-life exponent.

For 9th- and 8th-power Hertz stress-life exponents for ball and roller bearings, respectively, the Lundberg-Palmgren model best predicts life. However, for 12th- and 10th-power relations reflected by modern bearing steels, the Zaretsky model based on the Weibull equation is superior. Under the range of stresses examined, the use of a fatigue limit would suggest that (for most operating conditions under which a rolling-element bearing will operate) the bearing will not fail from classical rolling-element fatigue. Realistically, this is not the case. The use of a fatigue limit will significantly overpredict life over a range of normal operating Hertz stresses. (The use of ISO 281:2007 with a fatigue limit in these calculations would result in a bearing life approaching infinity.) Since the predicted lives of rolling-element bearings are high, the problem can become one of undersizing a bearing for a particular application.

Rules had been developed to distinguish and compare predicted lives to those actually obtained. Based upon field and test results of 51 ball and roller bearing sets, 98 percent of these bearing sets had acceptable life results using the Lundberg-Palmgren equations with life adjustment factors to predict bearing life. That is, they had lives equal to or greater than that predicted.

The Lundberg-Palmgren model was used to predict the life of a commercial turboprop gearbox. The life prediction was compared with the field lives of 64 gearboxes. From these results, the roller bearing lives exhibited a load-life exponent of 5.2, which correlated with

Correspondence/Reprint request: Dr. Erwin V. Zaretsky, Chief Engineer (Structures and Materials), NASA Glenn Research Center, USA

the Zaretsky model. The use of the ANSI/ABMA and ISO standards load-life exponent of 10/3 to predict roller bearing life is not reflective of modern roller bearings and will underpredict bearing lives.

# Introduction

By the close of the 19th century, the rolling-element bearing industry began to focus on sizing of ball and roller bearings for specific applications and determining bearing life and reliability. In 1896, R. Stribeck [1] in Germany began fatigue testing full-scale rolling-element bearings. J. Goodman [2] in 1912 in Great Britain published formulae based on fatigue data that would compute safe loads on ball and cylindrical roller bearings. In 1914, the "American Machinists Handbook" [3], devoted 6 pages to rolling-element bearings that discussed bearing sizes and dimensions, recommended (maximum) loading, and specified speeds. However, the publication did not address the issue of bearing life. During this time, it would appear that rolling-element bearing fatigue testing was the only way to determine or predict the minimum or average life of ball and roller bearings.

In 1924, A. Palmgren [4] in Sweden published a paper in German outlining his approach to bearing life prediction and an empirical formula based upon the concept of an $L_{10}$ life, or the time that 90 percent of a bearing population would equal or exceed without rolling-element fatigue failure. During the next 20 years he empirically refined his approach to bearing life prediction and matched his predictions to test data [5]. However, his formula lacked a theoretical basis or an analytical proof.

In 1939, W. Weibull [6,7] in Sweden published his theory of failure. Weibull was a contemporary of Palmgren and shared the results of his work with him. In 1947, Palmgren in concert with G. Lundberg, also of Sweden, incorporated his previous work along with that of Weibull and what appears to be the work of H. Thomas and V. Hoersch [8] into a probabilistic analysis to calculate rolling-element (ball and roller) life. This has become known as the Lundberg-Palmgren theory [9,10]. (In 1930, H. Thomas and V. Hoersch [8] at the University of Illinois, Urbana, developed an analysis for determining subsurface principal stresses under Hertzian contact [11]. Lundberg and Palmgren [9,10] do not reference the work of Thomas and Hoersch [8] in their papers.)

The Lundberg-Palmgren life equations have been incorporated into both the International Organization for Standardization (ISO) and the American National Standards Institute (ANSI)/American Bearing Manufacturers Association (ABMA)[1] standards for the load ratings and life of rolling-element [12 to 14] as well as in current bearing codes to predict life.

[1]ABMA changed their name from the Anti-Friction Bearing Manufacturers Association (AFBMA) in 1993.

In the post World War II era the major technology drivers for improving the life, reliability, and performance of rolling-element bearings have been the jet engine and the helicopter. By the late 1950s most of the materials used for bearings in the aerospace industry were introduced into use. By the early 1960s the life of most steels was increased over that experienced in the early 1940s primarily by the introduction of vacuum degassing and vacuum melting processes in the late 1950s [15].

The development of elastohydrodynamic (EHD) lubrication theory in 1939 by A. Ertel [16] and later A. Grubin [17] in 1949 in Russia showed that most rolling bearings and gears have a thin EHD film separating the contacting components. The life of these bearing and gears is a function of the thickness of the EHD film [15].

Computer programs modeling bearing dynamics that incorporate probabilistic life prediction methods and EHD theory enable optimization of rolling-element bearings based on life and reliability. With improved manufacturing and material processing, the potential improvement in bearing life can be as much as 80 times that attainable in the late 1950s or as much as 400 times that attainable in 1940 [15].

While there can be multifailure modes of rolling-element bearings, the failure mode limiting bearing life is contact (rolling-element) surface fatigue of one or more of the running tracks of the bearing components. Rolling-element fatigue is extremely variable but is statistically predictable depending on the material (steel) type, the processing, the manufacturing, and operating conditions [18].

Rolling-element fatigue life analysis is based on the initiation or first evidence of fatigue spalling on a loaded, contacting surface of a bearing. This spalling phenomenon is load cycle dependent. Generally, the spall begins in the region of maximum shear stresses, located below the contact surface, and propagates into a crack network. Failures other than that caused by classical rolling-element fatigue are considered avoidable if the component is designed, handled, and installed properly and is not overloaded [18]. However, under low EHD lubricant film conditions, rolling-element fatigue can be surface or near-surface initiated with the spall propagating into the region of maximum shearing stresses.

The database for ball and roller bearings is extensive. A concern that arises from these data and their analysis is the variation between life calculations and the actual endurance characteristics of these components. Experience has shown that endurance tests of groups of identical bearings under identical conditions can produce a variation in $L_{10}$ life from group to group. If a number of apparently identical bearings are tested to fatigue at a specific load, there is a wide dispersion of life among these bearings. For a group of 30 or more bearings, the ratio of the

longest to the shortest life may be 20 or more [18]. This variation can exceed reasonable engineering expectations.

# Bearing life theory

## Foundation for bearing life prediction

### Hertz contact stress theory

In 1917, Arvid Palmgren began his career at the A.–B. Svenska Kullager-Fabriken (SKF) bearing company in Sweden. In 1924 he published his paper [4] that laid the foundation for what later was to become known as the Lundberg-Palmgren theory [9]. Because the 1924 paper was missing two elements, it did not allow for a comprehensive rolling-element bearing life theory. The first missing element was the ability to calculate the subsurface principal stresses and hence, the shear stresses below the Hertzian contact of either a ball on a nonconforming race or a cylindrical roller on a race. The second missing element was a comprehensive life theory that would fit the observations of Palmgren. Palmgren discounted Hertz contact stress theory [11] and depended on the load-life relation for ball and roller bearings based on testing at SFK Sweden that began in 1910 [19]. Zaretsky discusses the 1924 Palmgren work in [20].

Palmgren did not have confidence in the ability of the Hertzian equations to accurately predict rolling bearing stresses. Palmgren [4] states, "The calculation of deformation and stresses upon contact between the curved surfaces…is based on a number of simplifying stipulations, which will not yield very accurate approximation values, for instance, when calculating the deformations. Moreover, recent investigations (circa 1919–1923) made at A.–B. Svenska Kullager-Fabriken (SKF) have proved through calculation and experiment that the Hertzian formulae will not yield a generally applicable procedure for calculating the material stresses.…As a result of the paramount importance of this problem to ball bearing technology, comprehensive in-house studies were performed at SKF in order to find the law that describes the change in service life that is caused by changing load, rpm, bearing dimensions, and the like. There was only one possible approach: tests performed on complete ball bearings. It is not acceptable to perform theoretical calculations only, since the actual stresses that are encountered in a ball bearing cannot be determined by mathematical means."

Palmgren later recanted his doubts about the validity of Hertz theory and incorporated the Hertz contact stress equation in his 1945 book [5]. In their 1947 paper [9], Lundberg and Palmgren state, "Hertz theory is valid under the

assumptions that the contact area is small compared to the dimensions of the bodies and that the frictional forces in the contact areas can be neglected. For ball bearings, with close conformity between rolling elements and raceways, these conditions are only approximately true. For line contact the limit of validity of the theory is exceeded whenever edge pressure occurs."

Lundberg and Palmgren exhibited a great deal of insight as to the other variables modifying the resultant shear stresses calculated from Hertz theory. They state [9], "No one yet knows much about how the material reacts to the complicated and varying succession of (shear) stresses which then occur, nor is much known concerning the effect of residual hardening stresses or how the lubricant affects the stress distribution within the pressure area. Hertz theory also does not treat the influence of those static stresses which are set up by the expansion or compression of the rings when they are mounted with tight fits." These effects are now understood, and life factors are currently being used to account for them so as to more accurately predict bearing life and reliability [18].

## Equivalent Load

Palmgren [4] recognized that it was necessary to account for combined and variable loading around the circumference of a ball bearing. He proposed a procedure in 1924 "to establish functions for the service life of bearings under purely radial load and to establish rules for the conversion of axial and simultaneous effective axial and radial loads into purely radial loads." Palmgren used Stribeck's equation [1] to calculate what can best be described as a stress on the maximum radially loaded ball-race contact in a ball bearing. The equation attributed to Stribeck by Palmgren is as follows:

$$k = \frac{5Q}{Zd^2} \tag{1}$$

where $Q$ is the total radial load on the bearing, $Z$ is the number of balls in the bearing, $d$ is the ball diameter, and $k$ is Stribeck's constant.

Palmgren modified Stribeck's equation to include the effects of speed and load as well as modifying the ball diameter relation. For brevity, this modification is not presented. It is not clear whether Palmgren recognized at that time that Stribeck's equation was valid only for a diametral clearance greater than zero with fewer than half of the balls being loaded. However, he stated that the corrected constant yielded good agreement with tests performed.

Palmgren [4] states, "It is probably impossible to find an accurate and, at the same time, simple expression for the ball pressure as a function of radial and axial pressure…" According to Palmgren, "Adequately precise results can be obtained by using the following equation:

$$Q = R + yA \tag{2}$$

where $Q$ is the imagined, purely radial load that will yield the same service life as the simultaneously acting radial and axial forces, $R$ is the actual radial load, and $A$ is the actual axial load." For ball bearings, Palmgren presented values of $y$ as a function of Stribeck's constant $k$. Palmgren stated that these values of $y$ were confirmed by test results [4].

By 1945, Palmgren [5] modified Eq. (2) as follows:

$$Q = P_{eq} = XF_r + YF_a \tag{3}$$

where

| | |
|---|---|
| $P_{eq}$ | the equivalent load |
| $F_r$ | the radial component of the actual load |
| $F_a$ | the axial component of the actual load |
| $X$ | a rotation factor |
| $Y$ | the thrust factor of the bearing |

The rotation factor $X$ is an expression for the effect on the bearing capacity of the conditions of rotation. The thrust factor $Y$ is a conversion value for thrust loads [5].

## Fatigue Limit

Palmgren [4] states that bearing "limited service life is primarily a fatigue phenomenon. However, under exceptional high loads there will be additional factors such as permanent deformations, direct fractures, and the like.…If we start out from the assumption that the material has a certain fatigue limit, meaning that it can withstand an unlimited number of cyclic loads on or below a certain, low level of load, the service life curve will be asymptotic. Since, moreover, the material has an elastic limit and/or fracture limit, the curve must yield a finite load even when there is only a single load value, meaning that the number of cycles equals zero. If we further assume that the curve has a profile of an exponential function, the

general equation for the relationship existing between load and number of load cycles prior to fatigue would read:

$$k = C(an + e)^{-x} + u \tag{4}$$

where $k$ is the specific load or Stribeck's constant, $C$ is the material constant, $a$ is the number of load cycles during one revolution at the point with the maximum load exposure, $n$ is the number of revolutions in millions, $e$ is the material constant that is dependent on the value of the elasticity or fracture limit, $u$ is the fatigue limit, and $x$ is an exponent."

According to Palmgren, "This exponent $x$ is always located close to 1/3 or 0.3. Its value will approach 1/3 when the fatigue limit is so high that it cannot be disregarded, and 0.3 when it is very low." Palmgren reported test results that support a value of $x$ = 1/3. Hence, Eq. (4) can be written as

$$\text{Life (millions of stress cycles)} = \left(\frac{C}{k-u}\right)^3 - e \tag{5}$$

The value $e$ suggests a finite time below which no failure would be expected to occur. By letting $e$ = 0 and eliminating the concept of a fatigue limit for bearing steels, Eq. (5) can be rewritten as

$$L(\text{million of race revolutions}) = \left(\frac{CZd^2/5}{Q}\right)^3 \tag{6}$$

In Eq. (6), by letting $f_c = C/5$, and $P_{eq} = Q$, the 1924 version of the dynamic load capacity $C_D$ for a radial ball bearing would be

$$C_D = f_c Z d^2 \tag{7}$$

and Eq. (6) becomes

$$L_{10} = \left(\frac{C_D}{P_{eq}}\right)^3 \tag{8}$$

where $L_{10}$ is the life in millions of inner-race revolutions, at which 10 percent of a bearing population will have failed and 90 percent will have survived. This is also referred to as 10-percent life or $L_{10}$ life.

By 1945, Palmgren [5] empirically modified the dynamic load capacity $C_D$ for ball and roller bearings as follows:
For ball bearings

$$C_D = f_c \frac{i d^2 Z^{2/3} \cos\beta}{1 + 0.02d} \tag{9}$$

For roller bearings

$$C_D = f_c i d^2 l_t Z^{2/3} \cos\beta \tag{10}$$

where

| | |
|---|---|
| $f_c$ | material-geometry coefficient[2] |
| $i$ | number of rows of rolling elements (balls or rollers) |
| $d$ | ball or roller diameter |
| $l_t$ | roller length |
| $Z$ | number of rolling elements (balls or rollers) in a row $i$ |
| $\beta$ | bearing contact angle |

From Anderson [21], for a constant bearing load, the normal force between a rolling element and a race will be inversely proportional to the number of rolling elements. Therefore, for a constant number of stress cycles at a point, the capacity is proportional to the number of rolling elements. Alternately, the number of stress cycles per revolution is also proportional to the number of rolling elements, so that for a constant rolling-element load the capacity for point contact is inversely proportional to the cube root of the number of rolling elements. This comes from the inverse cubic relation between load and life for point contact. Then the dynamic load capacity varies with number of balls as

$$C_D \sim \frac{Z}{Z^{1/3}} = Z^{2/3} \tag{11}$$

[2] Post 1990, the coefficient $f_c$ is designated as $f_{cm}$ in the ANSI/ABMA/ISO standards [12 to 14].

Equation (11) is reflected in the dynamic load capacity of Eqs. (9) and (10).

According to Palmgren [5], the coefficient $f_c$ (in Eqs. (9) and (10)) is dependent, among other things, on the properties of the material, the degree of osculation (bearing race-ball conformity), and the reduction in capacity on account of uneven load distribution within multiple row bearings and bearings with long rollers. The magnitude of this coefficient can be determined only by numerous laboratory tests. It has one definite value for all sizes of a given bearing type.

In all of the above equations, the units of the input variables and the resultant units used by Palmgren have been omitted because they cannot be reasonably used or compared with engineering practice today. As a result, these equations should be considered only for their conceptual content and not for any quantitative calculations.

## $L_{10}$ life

The $L_{10}$ life, or the time that 90 percent of a group of bearings will exceed without failing by rolling-element fatigue, is the basis for calculating bearing life and reliability today. Accepting this criterion means that the bearing user is willing in principle to accept that 10 percent of a bearing group will fail before this time. In Eq. (8) the life calculated is the $L_{10}$ life.

The rationale for using the $L_{10}$ life was first laid down by Palmgren in 1924. He states [4], "The (material) constant $C$ (Eq. (4)) has been determined on the basis of a very great number of tests run under different types of loads. However, certain difficulties are involved in the determination of this constant as a result of service life demonstrated by the different configurations of the same bearing type under equal test conditions. Therefore, it is necessary to state whether an expression is desired for the minimum, (for the) maximum, or for an intermediate service life between these two extremes.…In order to obtain a good, cost effective result, it is necessary to accept that a certain small number of bearings will have a shorter service life than the calculated lifetime, and therefore the constants must be calculated so that 90 percent of all the bearings have a service life longer than that stated in the formula. The calculation procedure must be considered entirely satisfactory from both an engineering and a business point of view, if we are to keep in mind that the mean service life is much longer than the calculated service life and that those bearings that have a shorter life actually only require repairs by replacement of the part which is damaged first."

Palmgren is perhaps the first person to advocate a probabilistic approach to engineering design and reliability. Certainly, at that time, engineering practice dictated a deterministic approach to component design. This approach by Palmgren was decades ahead of its time. What he advocated is designing for finite life and

reliability at an acceptable risk. This concept was incorporated in the ANSI/ABMA and ISO standards [12 to 14].

**Linear damage rule**

Most bearings are operated under combinations of variable loading and speed. Palmgren recognized that the variation in both load and speed must be accounted for in order to predict bearing life. Palmgren reasoned: "In order to obtain a value for a calculation, the assumption might be conceivable that (for) a bearing which has a life of $n$ million revolutions under constant load at a certain rpm (speed), a portion $M/n$ of its durability will have been consumed. If the bearing is exposed to a certain load for a run of $M_1$ million revolutions where it has a life of $n_1$ million revolutions, and to a different load for a run of $M_2$ million revolutions where it will reach a life of $n_2$ million revolutions, and so on, we will obtain

$$\frac{M_1}{n_1} + \frac{M_2}{n_2} + \frac{M_3}{n_3} + \cdots = 1 \tag{12}$$

In the event of a cyclic variable load we obtain a convenient formula by introducing the number of intervals $p$ and designate $m$ as the revolutions in millions that are covered within a single interval. In that case we have

$$p\left(\frac{m_1}{n_1} + \frac{m_2}{n_2} + \frac{m_3}{n_3} + \ldots\right) = 1 \tag{13}$$

where $n$ still designates the total life in millions of revolutions under the load and rpm (speed) in question (and $M$ in Eq. (12) equal $pm$."

Equations (12) and (13) were independently proposed for conventional fatigue analysis by B. Langer [22] in 1937 and M. Miner [23] in 1945, 13 and 21 years after Palmgren, respectively. The equation has been subsequently referred to as the linear damage rule or the Palmgren-Langer-Miner rule. For convenience, the equation can be written as follows:

$$\frac{1}{L} = \frac{X_1}{L_1} + \frac{X_2}{L_2} + \frac{X_3}{L_3} + \ldots \frac{X_n}{L_n} \tag{14}$$

and

$$X_1 + X_2 + X_3 + \ldots X_n = 1 \tag{15}$$

where $L$ is the total life in stress cycles or race revolutions, $L_1 \ldots L_n$ is the life at a particular load and speed in stress cycles or race revolutions, and $X_1 \ldots X_n$ is the fraction of total running time at load and speed. The values of $M_1$, $M_2$, etc. in Eq. (12) equal $X_1L$, $X_2L$, etc. from Eq. (14). Equation (14) is the basis for most variable-load fatigue analysis and is used extensively in bearing life prediction.

## Weibull analysis

### Weibull distribution function

In 1939, W. Weibull [6,7] developed a method and an equation for statistically evaluating the fracture strength of materials based upon small population sizes. This method can be and has been applied to analyze, determine, and predict the cumulative statistical distribution of fatigue failure or any other phenomenon or physical characteristic that manifests a statistical distribution. The dispersion in life for a group of homogeneous test specimens can be expressed by

$$\ln \ln \frac{1}{S} = e \ln\left(\frac{L - L_\mu}{L_\beta - L_\mu}\right) \quad \text{where} \quad 0 < L < \infty;\ 0 < S < 1 \tag{16}$$

where $S$ is the probability of survival as a fraction ($0 \leq S \leq 1$); $e$ is the slope of the Weibull plot; $L$ is the life cycle (stress cycles); $L_\mu$ is the location parameter, or the time (cycles) below which no failure occurs; and $L_\beta$ is the characteristic life (stress cycles). The characteristic life is that time at which 63.2 percent of a population will fail, or 36.8 percent will survive.

The format of Eq. (16) is referred to as a three-parameter Weibull analysis. For most—if not all—failure phenomenon, there is a finite time period under operating conditions when no failure will occur. In other words, there is zero probability of failure, or a 100-percent probability of survival, for a period of time during which the probability density function is nonnegative. This value is represented by the location parameter $L_\mu$. Without a significantly large data base, this value is difficult to determine with reasonable engineering or statistical certainty. As a result, $L_\mu$ is usually assumed to be zero and Eq. (16) can be written as

$$\ln \ln \frac{1}{S} = e \ln \left( \frac{L}{L_\beta} \right) \quad \text{where } 0 < L < \infty;\ 0 < S < 1 \tag{17}$$

This format is referred to as the two-parameter Weibull distribution function. The estimated values of the Weibull slope $e$ and $L_\beta$ for the two-parameter Weibull analysis may not be equal to those of the three-parameter analysis. As a result, for a given survivability value $S$, the corresponding value of life $L$ will be similar but not necessarily the same in each analysis.

By plotting the ordinate scale as ln ln(1/$S$) and the abscissa scale as ln $L$, a Weibull cumulative distribution will plot as a straight line, which is called a "Weibull plot." Usually, the ordinate is graduated in statistical percent of specimens failed $F$ where $F = [(1 - S) \times 100]$. Figure 1(a) is a generic Weibull plot with some of the values of interest indicated. Figure 1(b) is a Weibull plot of actual bearing fatigue data. The derivation of the Weibull distribution function can be found in Appendix A.

The Weibull plot can be used to evaluate any phenomenon that results in a statistical distribution. The tangent of the resulting plot, called the "Weibull slope" (also called the "Weibull shape parameter" or "Weibull modulus") and designated by $e$, defines the statistical distribution. Weibull slopes of 1, 2, and 3.57 represent exponential, Rayleigh, and Gaussian (normal) distributions, respectively.

The scatter in the data is inversely proportional to the Weibull slope; that is, the lower the value of the Weibull slope, the larger the scatter in the data, and vice versa. The Weibull slope is also liable to statistical variation depending on the sample size (data base) making up the distribution [24]. The smaller the sample size, the greater the statistical variation in the slope.

A true fit of a two-parameter Weibull distribution function (Fig. 1) would imply a zero minimum life of $L_\mu = 0$ in Eq. (16). Tallian [25] analyzed a composite sample of 2500 rolling-element bearings and concluded that a good fit was obtained in the failure probability region between 10 and 60 percent. Outside this region, experimental life is longer than that obtained from the two-parameter Weibull plot prediction. In the early failure region, bearings were found to behave as shown in Fig. 2. From the Tallian data, it was found that the location parameter for the three-parameter Weibull distribution of Eq. (16) is 0.053 $L_{10}$, where $L_{10}$ is that value obtained from the two-parameter Weibull plot (Eq. (17) and Fig. 1) [15].

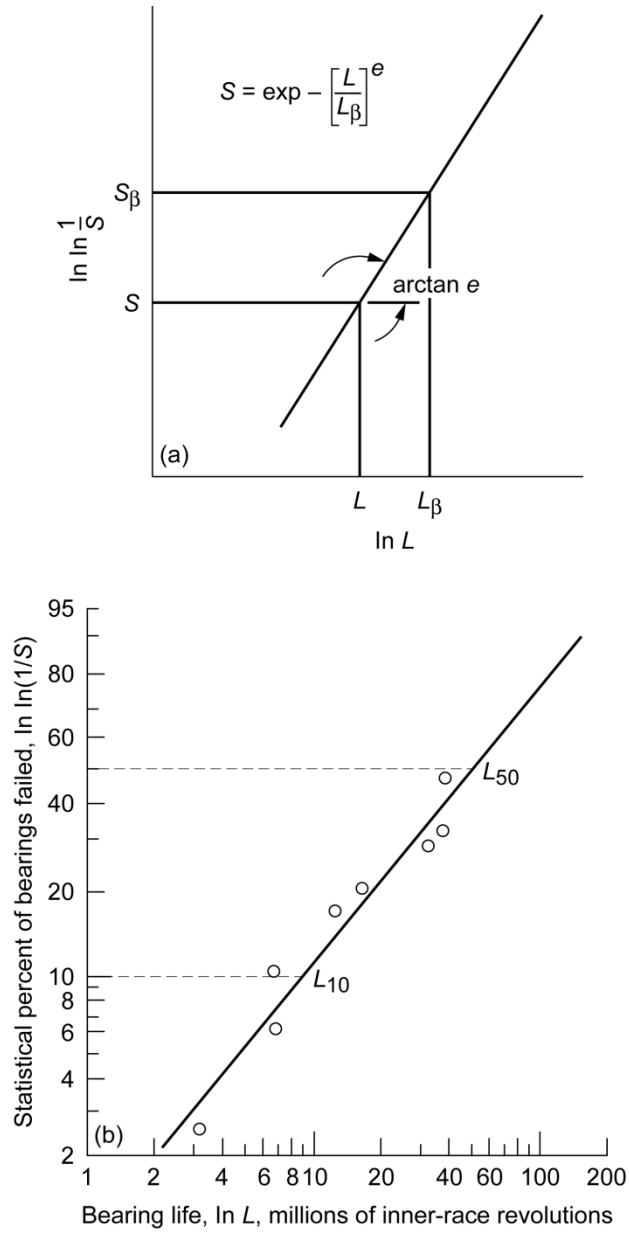


**Figure 1.** Weibull plot where (Weibull) slope or tangent of line is $e$; probability of survival, $S_\beta$, is 36.8 percent at which $L = L_\beta$, or $L = L_\beta = 1$. (a) Schematic. (b) Rolling-element bearing fatigue data.

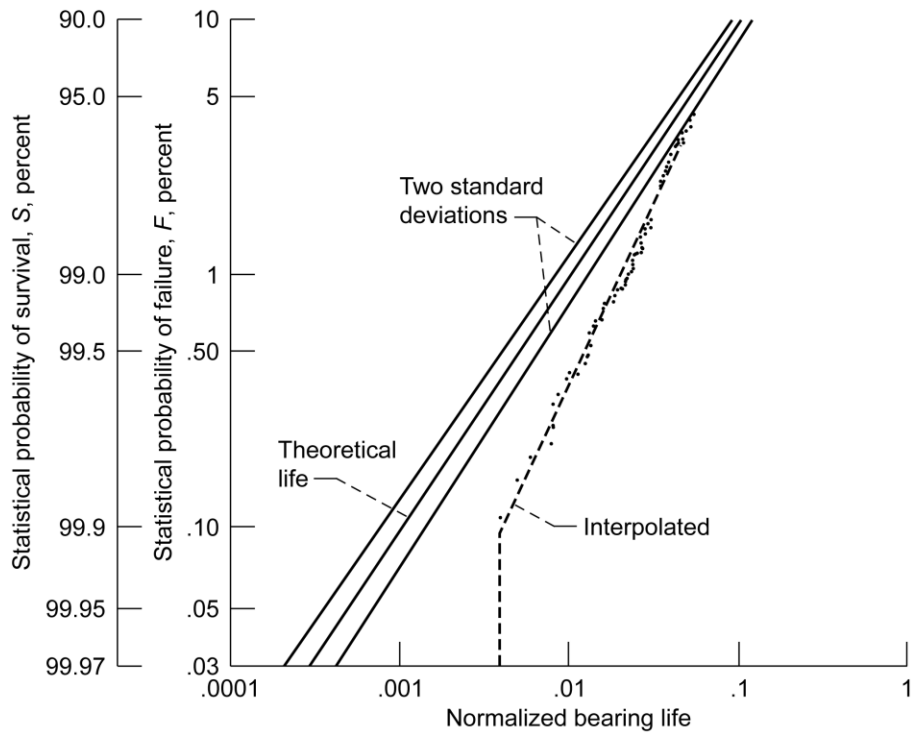


**Figure 2.** Two-parameter Weibull plot of bearing life distribution in early failure region [25].

## Weibull fracture strength model

Weibull [6,7,26,27] related the material strength to the volume of the material subjected to stress. If the solid were to be divided in an arbitrary manner into $n$ volume elements, the probability of survival for the entire solid can be obtained by multiplying the individual survivabilities together as follows

$$S = S_1 \cdot S_2 \cdot S_3 \cdots S_n \tag{18}$$

where the probability of failure $F$ is

$$F = 1 - S \tag{19}$$

Weibull further related the probability of survival $S$, the material strength σ, and the stressed volume $V$ according to the following relation

$$\ln \frac{1}{S} = \int_V f(X) dV \tag{20}$$

where

$$f(X) = \sigma^e \tag{21}$$

For a given probability of survival $S$,

$$\sigma \sim \left[\frac{1}{V}\right]^{1/e} \tag{22}$$

From Eq. (22), for the same probability of survival the components with the larger stressed volume will have lower strength (or shorter life).

# Bearing life models

## Weibull fatigue life model

In conversations E.V. Zaretsky had with W. Weibull on January 22, 1964, Weibull related that he suggested to his contemporaries A. Palmgren and G. Lundberg in Gothenberg, Sweden (circa 1944), to use his equation (Eq. (20)) to predict bearing (fatigue) life where

$$f(X) = \tau^c \eta^e \tag{23}$$

and where $\tau$ is the critical shear stress and $\eta$ is the number of stress cycles to failure.

In the past E.V. Zaretsky has credited this relation to Weibull. However, there appears to be no documentation of the above nor any publication of the application of Eq. (23) by Weibull in the open literature. However, in [28] Poplawski *et al.* applied Eq. (23) to Eq. (20) where

$$\eta \sim \left[\frac{1}{\tau}\right]^{c/e} \left[\frac{1}{V}\right]^{1/e} \tag{24}$$

The parameter $c/e$ is the stress-life exponent. This implies that the inverse relation of life with stress is a function of the life scatter (Weibull slope) or data dispersion.

Referring to Figs. 3 and 4 for point contact and line contact, respectively, the stressed volume [9] is defined as

Point contact: $V = a\, l_{\boldsymbol{L}} z$ (25a)

Line contact: $V = l_t l_{\boldsymbol{L}} z$ (25b)

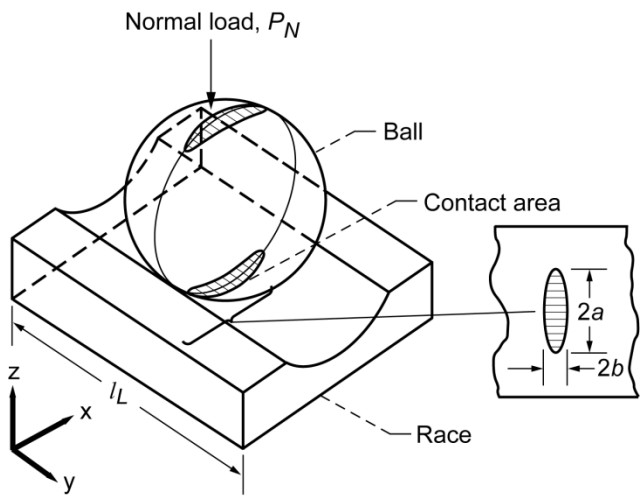


**Figure 3.** Ball-race model for point contact.

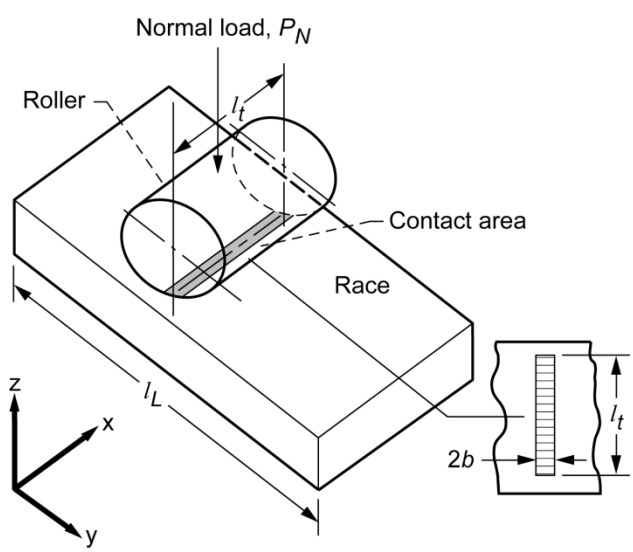


**Figure 4.** Roller-race model for line contact.

The depth $z$ to the critical shear stress $\tau$ below the Hertzian contact in the running track is shown in Fig. 5. The length of the running track is $l_L$, and $l_t$ is the roller width.

The critical shearing stress can be any one or a combination of the maximum shearing stress, $\tau_{\max}$, the maximum orthogonal shearing stress, $\tau_o$, the octahedral shearing stress $\tau_{oct}$, or the von Mises shearing stress $\tau_{VM}$. The von Mises shearing stress is a variation of the octahedral shearing stress.

From Hertz theory [11,29] for point contact (Fig. 3), $V$ and $\tau$ can be expressed as a function of the maximum Hertz (contact) stress, $S_{\max}$ [29], where

$$\tau \sim S_{\max} \tag{26a}$$

$$V \sim S_{\max}^2 \tag{26b}$$

Substituting Eqs. (26a) and (26b) in Eq. (24) and $L$ for $\eta$,

$$L \sim \left(\frac{1}{S_{\max}}\right)^{c/e} \left[\frac{1}{S_{\max}^2}\right]^{1/e} \sim \frac{1}{S_{\max}^n} \tag{27}$$

From [28], solving for the value of the exponent $n$ for point contact (ball in a raceway) from Eq. (27) gives

$$n = \frac{c+2}{e} \tag{28}$$

From Hertz theory for line contact (roller in a raceway, Fig. 4),

$$V \sim S_{\max} \tag{29}$$

Substituting Eqs. (26a) and (29) in Eq. (24) and $L$ for $\eta$,

$$L \sim \left[\frac{1}{S_{\max}}\right]^{c/e} \left[\frac{1}{S_{\max}}\right]^{1/e} \sim \frac{1}{S_{\max}^n} \tag{30}$$

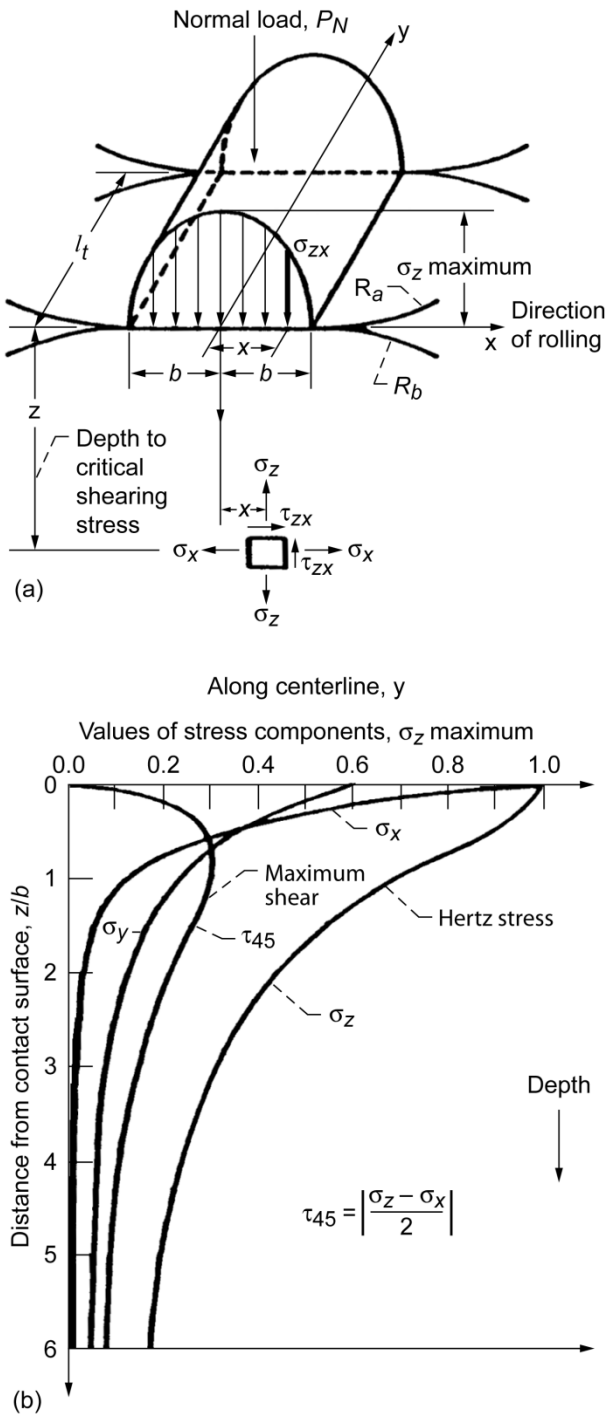


**Figure 5.** Subsurface stress field under line contact. (a) Hertz stress distribution for roller on raceway showing principal stresses at distance *z* below surface. (b) Distribution of principal and shearing stress as a function of depth *z* below surface.

Solving for the value of $n$ for line contact by substituting Eqs. (25a) and (28) into Eq. (26) gives

$$n = \frac{c+1}{e} \tag{31}$$

From Lundberg and Palmgren [9] for point contact, $c$ = 10.33 and $e$ = 1.11. Then from Eq. (28),

$$n = \frac{c+2}{e} = \frac{10.33+2}{1.11} = 11.12 \tag{32}$$

From Hertz theory [29] for point contact,

$$S_{\max} \sim P^{1/3} \tag{33}$$

From Eq. (27) for point contact,

$$\boldsymbol{L} \sim \frac{1}{S_{\max}^{n}} \sim \frac{1}{P_N^{p}} \tag{34a}$$

Combining Eqs. (33) and (34a) for point contact, and solving for $p$,

$$p = \frac{n}{3} = \frac{c+2}{3e} \tag{34b}$$

From Eq. (32) where $n$ = 11.12,

$$p = \frac{11.12}{3} = 3.7 \tag{34c}$$

For line contact from Eq. (31),

$$n = \frac{c+1}{e} = \frac{10.33+1}{1.11} = 10.21 \tag{35}$$

From Eq. (30) for line contact,

$$L \sim \frac{1}{S_{\max}^{n}} \sim \frac{1}{P_N^{p}} \tag{36a}$$

From Hertz theory [29] for line contact,

$$S_{\max} \sim P^{1/2} \tag{36b}$$

Combining Eqs. (36a) and (36b) and solving for $p$ for line contact,

$$p = \frac{n}{2} = \frac{c+1}{2e} = \frac{10.21}{2} = 5.1 \tag{36c}$$

In their 1952 publication [10], Lundberg and Palmgren assume $e$ for line contact equals 1.125, then from Eq. (35) $n$ = 10.1, and from Eq. (36c) $p$ = 5. From Weibull, the values of the stress-life and the load-life exponents are dependent on the Weibull slope $e$, which for rolling-element bearings can and usually varies between 1 and 2. As a result, the values can be only valid for a single value of the Weibull slope. As an example, if in Eq. (32) for point contact, a Weibull slope $e$ of 1.02 were selected, $n$ = 12 and $p$ = 4 from Eq. (34b). These values did not fit the bearing data base that existed in the 1940s.

## Lundberg-Palmgren model

In 1947 Lundberg and Palmgren [9] applied the Weibull analysis to the prediction of rolling-element bearing fatigue life. In order to account for the variation between the values of the Hertz stress-life exponent $n$ and the load-life exponent $p$ from those experimentally determined at the time, they introduced another variable, the depth to the critical shearing stress $z$ to the $h$ power where $f(x)$ in Eq. (20) can be expressed as

$$f(x) = \frac{\tau^{c}\eta^{e}}{z^{h}} \tag{37}$$

The rationale for introducing $z^h$ was that it took a finite time period for a crack to initiate at a distance from the depth of the critical shearing to the rolling surface. Lundberg and Palmgren assumed that the time for crack propagation was a function of $z^h$.

Equation (24) thus becomes

$$\eta \sim \left[\frac{1}{\tau}\right]^{c/e}\left[\frac{1}{V}\right]^{1/e}\left[z\right]^{h/e} \tag{38}$$

For their critical shearing stress, Lundberg and Palmgren chose the orthogonal shearing stress. From Hertz theory [29],

$$z \sim S_{\max} \tag{39}$$

For point contact, substituting Eqs. (26a), (26b), and (39) in Eq. (38) and $L$ for η,

$$L \sim \left[\frac{1}{S_{\max}}\right]^{c/e}\left[\frac{1}{S_{\max}^{2}}\right]^{1/e}\left[S_{\max}\right]^{h/e} \sim \frac{1}{S_{\max}^{n}} \tag{40}$$

From [28], solving for the value of the exponent $n$ for point contact (ball on a raceway) from Eq. (40) gives

$$n = \frac{c+2-h}{e} \tag{41a}$$

From Lundberg and Palmgren [9], using values of 1.11 for $e$, $c$ = 10.33, and $h$ = 2.33, from Eq. (41a) for point contact

$$n = \frac{10.33+2-2.33}{1.11} = 9 \tag{41b}$$

From Eq. (34b) for point contact, where $n$ = 9,

$$p = \frac{n}{3} = \frac{9}{3} = 3 \tag{41c}$$

For line contact, substituting Eqs. (26a), (29), and (39) in Eq. (38) and $L$ for η,

$$L \sim \left[\frac{1}{S_{\max}}\right]^{c/e}\left[\frac{1}{S_{\max}}\right]^{1/e}\left[\frac{1}{S_{\max}}\right]^{h/e} \sim \frac{1}{S_{\max}^{n}} \tag{42}$$

From Eq. (42) solving for $n$ for line contact,

$$n = \frac{c+1-h}{e} \tag{43a}$$

Using previous values of $c$ and $h$, and $e$ = 1.125 for line contact,

$$n = \frac{10.33+1-2.33}{1.125} = 8 \tag{43b}$$

From Eq. (36b) for line contact,

$$p = \frac{n}{2} = \frac{8}{2} = 4 \tag{43c}$$

These values of $n$ and $p$ for point and line contacts correlated to the then-existing rolling-element bearing database.

In their 1952 paper [10], Lundberg and Palmgren modified their value of the load-life exponent $p$ for roller bearings from 4 to 10/3. The rationale for doing so was that various roller bearing types had one contact that is line contact and other that is point contact. They state ". . . as a rule the contacts between the rollers and the raceways transforms from a point to a line contact for some certain load so that the life exponent varies from 3 to 4 for differing loading intervals within the same bearing." The ANSI/ABMA and ISO standards [12,14] incorporate $p$ = 10/3 for roller bearings. Computer codes for rolling-element bearings incorporate $p$ = 4.

**Strict series reliability**

Figures 6 and 7 show schematics of deep-groove and angular-contact ball bearings. Figure 8 is a schematic of a roller bearing. From Eqs. (20) and (30), the fatigue life $L$ of a bearing inner or outer race determined from the Lundberg-Palmgren theory [9] can be expressed as follows:

$$L = A\left(\frac{1}{\tau}\right)^{c/e}\left(\frac{1}{V}\right)^{1/e}\left(\frac{1}{N}\right)[z]^{h/e} \tag{44}$$

where $N$ is the number of stress cycles per inner-race revolution and $A$ is a material life factor based upon air-melt, pre-1940 AISI 52100 steel[3] and mineral oil lubricant.

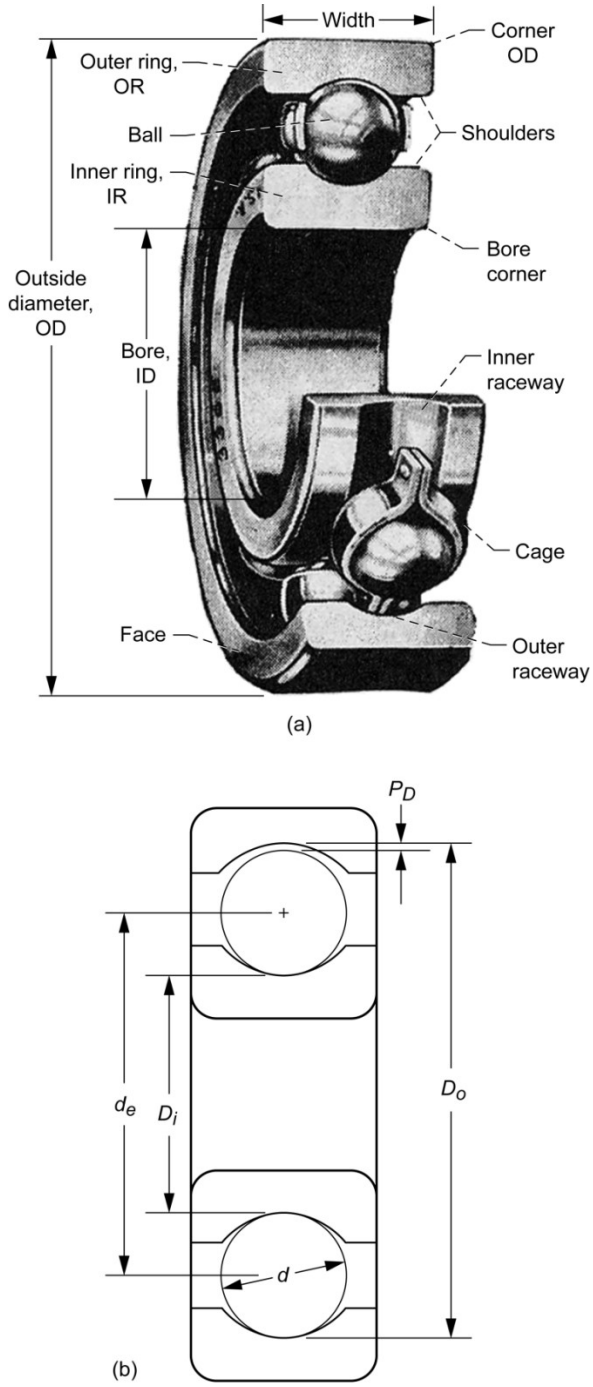


**Figure 6.** Deep-groove ball bearing. (a) Schematic. (b) Cross section without cage.

[3] Numbered AISI steel grades are standardized by the American Iron and Steel Institute (AISI).

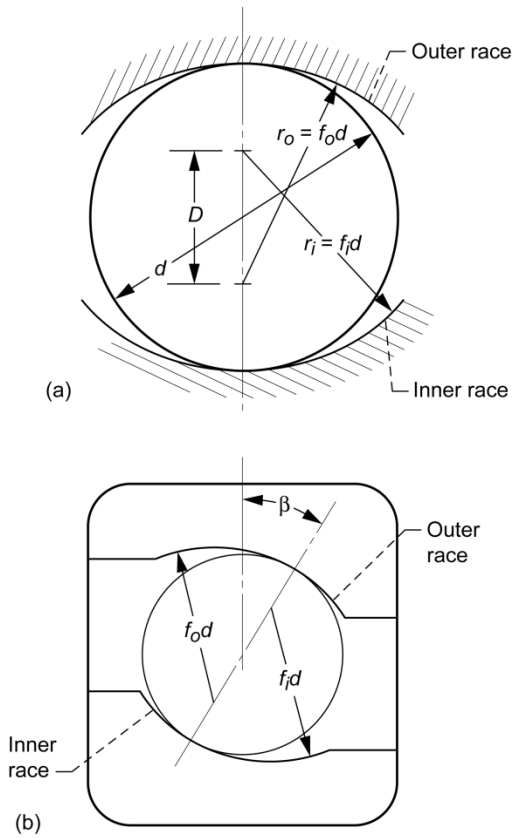


**Figure 7.** Ball-race conformity. (a) Deep-groove ball bearing. (b) Angular-contact ball bearing.

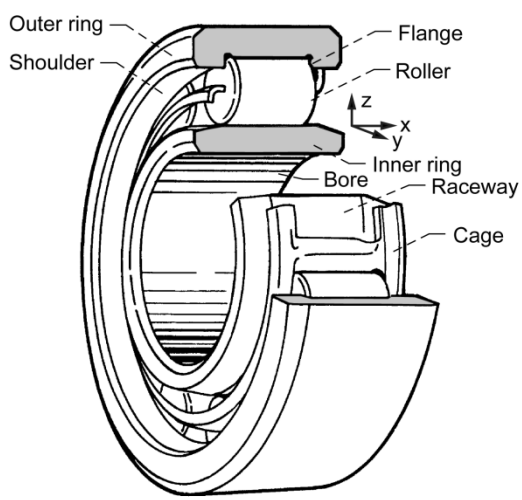


**Figure 8.** Schematic of cylindrical roller bearing with inner raceway. Bearing accommodates axial movement by not restraining rollers axially on inner raceway. Similar bearing with flanged inner ring allows axial roller movement on outer raceway.

In general, for ball and roller bearings, the running track lengths for Eqs. (25a) and (25b) for the inner and outer raceways are, respectively,

$$l_{\boldsymbol{L}_{ir}} = \pi D_i = \pi\left(d_e - d\cos\beta\right) \tag{45a}$$

and

$$l_{\boldsymbol{L}_{or}} = \pi D_o = \pi k\left(d_e + d\cos\beta\right) \tag{45b}$$

where $d_e$ is the bearing pitch diameter (see Fig. 6).

In Eq. (45b), $k$ is a correction factor that can account for variation of the stressed volume in the outer raceway. Equations (45a) and (45b) without the correction factor $k$ are used in the Lundberg-Palmgren theory [9] to develop the capacity of a single contact on a raceway, assuming that all the ball-raceway loads are the same. In Eq. (45b), for an angular-contact bearing under thrust load only, $k = 1$.

Under radial load and no misalignment, the stressed volume $V$ of a stationary outer race in a roller bearing or deep-groove ball bearing varies along the outer raceway in a load zone equal to or less than 180°. In the ANSI/ABMA and ISO standards [12,14] for radially loaded, rolling-element bearings, Eqs. (45a) and (45b) are adjusted for inner-race rotation and a fixed outer race with zero internal clearance, using system-life equations for multiple single contacts to calculate the bearing fatigue life. The outer raceway has a maximum load zone of 180°. An equivalent radial load $P_{eq}$ was developed by Lundberg and Palmgren [9] and is used in the standards [12,14]. The equivalent load $P_{eq}$ mimics a 180° ball-race load distribution assumed in the standards when pure axial loads are applied. It is also used throughout the referenced standards when combined axial and radial loads are applied in an angular-contact ball bearing.

Equations (45a) and (45b) are applicable for radially loaded roller bearing and deep-groove ball bearings where the rolling element-raceway contact diameters are at the pitch diameter plus or minus the roller/ball diameter, $\cos\beta = 1$, and $k < 1$. The maximum Hertz stress values are different at each ball or roller-race contact, at the inner and outer races, and vary along the arc in the zone of contact in a predictable manner. The width of the contact $2a$ for a ball bearing (Fig. 3) and the depth $z$ for both ball and roller bearings (Fig. 5) to the critical shearing stress $\tau$ are functions of the maximum Hertz stress and are different at the inner and outer race contacts.

From Jones [29], for a ball bearing with a rotating inner race and a stationary outer race, the number of stress cycles $N_{ir}$ and $N_{or}$ for a single inner-race rotation for single points on the inner- and outer-races, respectively, are

$$N_{ir} = \frac{Z}{2}\left(1 + \frac{d}{d_e}\cos\beta\right) \tag{46a}$$

$$N_{or} = \frac{Z}{2}\left(1 - \frac{d}{d_e}\cos\beta\right) \tag{46b}$$

From Eqs. (12) and (17) from Weibull [6,7], Lundberg and Palmgren [9] first derived the relationship between individual component life and system life. A bearing is a system of multiple components, each with a different life. As a result, the life of the system is different from the life of an individual component in the system. The $L_{10}$ bearing system life, where 90 percent of the population survives, can be expressed as

$$\frac{1}{L_{10}^{e}} = \frac{1}{L_{10ir}^{e}} + \frac{1}{L_{10or}^{e}} \tag{47}$$

where the life of the rolling elements, by inference, is incorporated into the life of each raceway tacitly assuming that all components have the same Weibull slope $e$ where the $L_{10}$ life of the bearing will be less than the $L_{10}$ life of the lowest lived component in the bearing, which is usually that of the inner race. This is referred to as a "strict series reliability" equation and is derived in Appendix B. In properly designed and operated rolling-element bearings, fatigue of the cage or separator should not occur and, therefore, is not considered in determining bearing life and reliability. From Eqs. (17) and (44), Lundberg and Palmgren [9] derived the following relation:

$$L_{10} = \left(\frac{C_D}{P_{eq}}\right)^{p} \tag{48}$$

Equation (48) is identical to Eq. (8) proposed by Palmgren [4] in 1924 if $p$ equal 3. From Lundberg-Palmgren [9], the load-life exponent $p$ equals 3 for ball

bearings and 4 for roller bearings. However, as previously discussed, Lundberg and Palmgren in 1952 [10] proposed $p = 10/3$ for roller bearings.

## Dynamic load capacity, $C_D$

Palmgren [4] proposed the concept of a dynamic load rating or capacity for a rolling-element bearing, defined as the load placed on a bearing that will theoretically result in a $L_{10}$ life of 1 million inner-race revolutions. He first characterized this concept as that shown in Eq. (6) that subsequently evolved as Eqs. (9) and (10).

From Anderson [21], according to the Hertz theory, the dynamic load capacity should be proportional to the square of the rolling-element diameter. From experimental data, Palmgren [30] found that capacity varied as $d^{1.8}$ for balls up to about 25 mm in diameter and $d^{1.4}$ for balls larger than 25 mm in diameter.

From Eq. (11), the dynamic load capacity varies with the number of rolling elements $Z$ to the 2/3 power ($Z^{2/3}$). However, this would only be correct for an inverse cubic relation between load and life.

From Anderson [21], multiple-row bearings with $i$ rows of balls may be considered as a combination of $i$ single-row bearings [21]. From strict series reliability (Appendix B) the following relation between the life of a multirow bearing and the lives of the $i$ individual rows is obtained assuming that all rows carry equal load:

$$\frac{1}{L^e} = \frac{1}{L_1^e} + \frac{1}{L_2^e} + \cdots + \frac{1}{L_i^e} \tag{49a}$$

Then

$$\frac{1}{L^e} = \frac{i}{L_i^e} \tag{49b}$$

If each row of the bearing is loaded with a load equal to the dynamic load capacity of one row $C_i$, then $L_i = 1$ (i.e., one million inner-race revolutions) and from Eq. (49b),

$$L^e = \frac{1}{i} \tag{50a}$$

or

$$\boldsymbol{L} = \frac{1}{i^{1/e}} \tag{50b}$$

The load $P_{eq}$ on the entire bearing is $iC_i$, where $P_{eq}$ is the equivalent bearing load. In this case,

$$P_{eq} = iC_i \tag{51}$$

From Eqs. (50b) and (51),

$$\left(\frac{C_D}{iC_i}\right)^n = \frac{1}{i^{1/e}} \tag{52a}$$

or

$$C_D = C_i \; i^{1-(1/ep)} \tag{52b}$$

For ball bearings, $p = 3$ and $e$ is approximately 1.1, so that the capacity of multirow bearings varies as $i^{0.7}$. For radial ball bearings, the normal force between a ball and a race varies as 1/cos β, so that the capacity is proportional to cos β, where β is the contact angle (see Fig. 7). The influence of the ball-race conformity, bearing type, and internal dimensions expressed by $f_{cm}/(\cos\beta)^{0.3}$, where $f_{cm}$ is the material and geometry coefficient. Therefore the capacity of a radial ball bearing varies as $(i\cos\beta)^{0.7}$.

For thrust ball bearings, the normal force between a ball and a race varies as 1/sin β, so that the capacity is proportional to sin β or to (cos β)(tan β). When the influences of the degree of conformity, of bearing type, and of internal dimensions are included, the capacity of a thrust ball bearing varies as $(i\cos\beta)^{0.7}(\tan\beta)$.

For roller bearings with line contact, the load-life exponent in the life equation is 4, so that the capacity varies as $Z^{3/4}$. From Eq. (52b) with $p = 4$, the capacity of a multirow-roller bearing is found to vary as $i^{0.78}$. Theoretically, the capacity of roller bearings should be proportional to $l_t d$. Experimental data [9] indicate that capacity varies as $l_t^{0.78} d^{1.07}$.

Formulas for the dynamic load capacity *CD* as developed by Palmgren [30] and Lundberg and Palmgren [9, 10] are dependent on

(1) Size of rolling elements, $d$ (ball or roller diameter) and $l_t$ (ball or roller length)
(2) Size of rolling elements, $d$ (ball or roller diameter) and $l_t$ (ball or roller length)
(3) Number of rolling elements per row, $Z$
(4) Number of rows of rolling elements, $i$
(5) Contact angle, β (see Fig. 7)
(6) Material and geometry coefficient, $f_{cm}$

They are incorporated into the ANSI/ABMA and ISO standards [12 to 14], are semiempirical, and are as follows:

For radial ball bearings with $d \leq 25$ mm,

$$C_D = f_{cm}(i \cos\beta)^{0.7} Z^{2/3} d^{1.8} \tag{53a}$$

For radial ball bearings with $d > 25$ mm,

$$C_D = f_{cm}(i \cos\beta)^{0.7} Z^{2/3} d^{1.4} \tag{53b}$$

For radial roller bearings,

$$C_D = f_{cm}(i\, l_t \cos\beta)^{7/9} Z^{3/4} d^{29/27} \tag{53c}$$

For thrust ball bearings with $\beta \neq 90°$,

$$C_D = f_{cm}(i \cos\beta)^{0.7} (\tan\beta) Z^{2/3} d^{1.8} \tag{53d}$$

For thrust roller bearings with $\beta \neq 90°$,

$$C_D = f_{cm}(i\, l_t \cos\beta)^{7/9} (\tan\beta) Z^{3/4} d^{29/27} \tag{53e}$$

For thrust ball bearings with $\beta = 90°$,

$$C_D = f_{cm}\, i^{0.7} Z^{2/3} d^{1.8} \tag{53f}$$

For thrust roller bearings with β = 90°,

$$C_D = f_{cm}\left(i\, l_t\right)^{7/9} Z^{3/4} d^{29/27} \tag{53g}$$

The material and geometry coefficient $f_{cm}$ (originally designated $fc$ by Lundberg and Palmgren [9]) in turn depends on the bearing type, material, and processing and the conformity between the rolling elements and the races. Representative values of $f_{cm}$ are given in Table 1 from the ANSI/ABMA standards [13,14]. It should be noted that the coefficient $f_{cm}$ and the various exponents of Eqs. (53a) through (53g) were chosen by Lundberg and Palmgren [9] and Palmgren [30] to match their bearing data base at the time of their writing. However, the values of $f_{cm}$ have been updated periodically in the ANSI/ABMA and ISO standards [18,31].

**Table 1.** Representative values of rolling-element bearing geometry and material coefficient $f_{cm}$ in ANSI/ABMA Standards 9 and 11 ([13], [14]) for representative rolling-element bearing sizes [18].

| Bearing envelope size, $\frac{d \cos \beta}{d_e}$ | Bearing geometry and material coefficient,[a] $f_{cm}$[b] | |
|---|---|---|
| | Deep-groove and angular-contact ball bearings[c] | Cylindrical (radial) roller bearing |
| 0.05 | 6070 (4610) | 81.51 (7329) |
| .10 | 72.16 (5480) | 92.62 (8322) |
| .16 | 77.56 (5890) | 97.35 (8747) |
| .22 | 77.56 (5890) | 97.02 (8767) |
| .28 | 74.27 (5640) | 93.02 (8767) |
| .34 | 69.26 (5260) | ------- |
| .40 | 62.94 (4780) | ------- |

[a]Values of $f_{cm}$ are for use with newtons and millimeters; those in parentheses are for use with pounds and inches.
[b]Prior to 1990, $f_{cm}$ was designated as $f_c$.
[c]Inner- and outer-race conformities are equal to 0.52.

Substituting the bearing geometry and the Hertzian contact stresses for a given normal load $P_N$ into Eqs. (44) through (47), the dynamic load capacity $C_D$ can be calculated from Eq. (48). Since $P_N$ is the normal load on the maximum-loaded rolling element, it is required that the equivalent load $P_{eq}$ be calculated. Once $C_D$ is determined, $f_{cm}$ can be calculated for the appropriate bearing type from Eq. (53).

The equivalent load $P_{eq}$ can be obtained from Eq. (3) where values of $X$ and $Y$ for different bearing types are given in the ANSI/ABMA standards [13,14]. The dynamic load capacity $C_D$ in the standards should be $C_r$ (Eqs. (53a) to (53c)) for a radial bearing or $C_a$ (Eqs. (53d) to (53g)) for a thrust bearing.

Lives determined using Eq. (53) are based on the "first evidence of fatigue." This can be a small spall or surface pit that may not significantly impair the function of the bearing. The actual useful bearing life can be much longer. It should be also noted that in these Eqs. (53) where derived exponents differed from those obtained experimentally, those exponents obtained experimentally were substituted by Lundberg and Palmgren [9,10] for those that they analytically derived.

## Ioannides-Harris model

Ioannides and Harris [32], using Weibull [6,7] and Lundberg and Palmgren [9,10] introduced a fatigue-limiting shear stress $\tau_u$ where from Eq. (37),

$$f(X) = \frac{(\tau - \tau_u)^c \eta^e}{z^h} \tag{54}$$

The equation is identical to that of Lundberg and Palmgren (Eq. 37) except for the introduction of a fatigue-limiting stress where

$$\eta \sim \left[\frac{1}{\tau - \tau_u}\right]^{c/e} \left[\frac{1}{V}\right]^{1/e} [z]^{h/e} \tag{55}$$

Equation (55) can be expressed as a function of $S_{\max}$ where

$$L \sim \left(\frac{1}{\tau - \tau_u}\right)^{c/e} \left[\frac{1}{V}\right]^{1/e} [z]^{h/e} \sim \frac{1}{S_{\max}^{n(\tau_u)}} \tag{56}$$

Ioannides and Harris [32] use the same values of Lundberg and Palmgren for $e$, $c$, and $h$. If $\tau_u$ equals 0, then the values of the Hertz stress-life exponent $n$ are identical to those of Lundberg and Palmgren (Eqs. (41b) and (43b)). However, for values of $\tau_u > 0$, $n$ is also a function of $(\tau - \tau_u)$. For their critical shearing stress, Ioannides and Harris chose the von Mises stress.

From the above, Eq. (48) can be rewritten to include a "fatigue-limiting" load $P_u$:

$$L_{10} = \left( \frac{C_D}{P_{eq} - P_u} \right)^p \tag{57a}$$

where

$$P_u = f(\tau_u) \tag{57b}$$

When $P_{eq} \leq P_u$, bearing life is infinite and no failure would be expected. When $P_u$ = 0, the life is the same as that for Lundberg and Palmgren.

The concept of a fatigue limit for rolling-element bearings was first proposed by Palmgren in 1924 (Eq. (5)) [4]. It was apparently abandoned by him first in 1945 [5] and then again with Lundberg in 1947 [9]. In 1985, Ioannides and Harris [32] applied Palmgren's concept of a fatigue limit to the Lundberg-Palmgren equations in the form shown in Eq. (54). The ostensible reason Ioannides and Harris used the fatigue limit was to replace the material and processing life factors [18] that are used as life modifiers in conjunction with the bearing lives calculated from the Lundberg-Palmgren equations.

There are two problems associated with the use of a fatigue limit for rolling-element bearing. The first problem is that the form of Eq. (55) may not reflect the presence of a fatigue limit but the presence of a compressive residual stress [18]. The second problem is that there are no data in the open literature that would justify the use of a fatigue limit for through-hardened bearing steels such as AISI 52100 and AISI M–50. In fact, a paper presented by Tosha *et al*. [33], reporting the results of rotating beam fatigue experiments for through-hardened AISI 52100 steel at very low stress levels, shows conclusively that a fatigue limit does not exist for this bearing steel.

Recent publications by the ASME [34] and the ISO [35,36] for calculating the life of rolling-element bearings include a fatigue limit and the effects of ball-race conformity on bearing fatigue life. These methods do not, however, include the effect of ball failure on bearing life. The ISO method is based on the work reported by Ioannides, Bergling, and Gabelli [37]. The ASME method as contained in their ASMELIFE software [34] uses the von Mises stress as the critical shearing stress with a fatigue limit value of 684 MPa (99,180 psi). This corresponds to a Hertz surface contact stress of 1140 MPa (165,300 psi). The ISO 281:2007 [36] method uses a fatigue limit stress of 900 MPa (130,500 psi), which corresponds to a Hertz contact stress of 1500 MPa (217,500 psi) [31].

The concepts of a fatigue limit load (bearing load under which the fatigue stress limit is just reached in the most heavily loaded raceway contact) introduced in the

new ISO rating methods [36] is proportional to the fatigue limit load raised to the 3rd power for ball bearings (point contact). These differing values of load would result in a 128-percent higher load below which no fatigue failure would be expected to occur [31] using ISO 281:2007 [36] than ASMELIFE [34].

The effect of using different values of fatigue limit or no fatigue limit on rolling-element fatigue life prediction is shown in Table 2. This table summarizes the qualitative results obtained for maximum Hertz stresses of 1379, 1724, and 2068 MPa (200, 250, and 300 ksi) for point contact using Eq. (38) for Lundberg-Palmgren without a fatigue limit and Eq. (55) for fatigue limits of 684 MPa (99,180 psi) (from ASMELIFE) and 900 MPa (130,500 psi) (from ISO 281:2007). The results are normalized to a maximum Hertz stress of 1379 MPa (200 ksi) with no fatigue limit where the quotient of Eq. (55) divided by Eq. (38) is taken to the $c/e$ power of 9.3 (taken from Lundberg and Palmgren). The effect of stressed volume was also factored into these calculations [31]:

$$L_{IH} \approx L\left[\frac{\tau}{\left(\tau - \tau_u\right)}\right]^{c/e} \tag{58}$$

where $L_{IH}$ is the life with the fatigue limit $\tau_u$, $L$ is the life without a fatigue limit $\tau_u$ and $\tau$ is the critical shearing stress.

**Table 2.** Effect of fatigue limit $\tau$ on rolling-element fatigue life [31].

| Fatigue limit,[a] $\tau_u$, MPa (ksi) | Relative life[b,c] (Eq. (58)) | | |
|---|---|---|---|
| | Maximum Hertz stress, MPa (ksi) | | |
| | 1379 (200) | 1724 (250) | 2068 (300) |
| 0 (0), Lundberg-Palmgren [9] | 1 | 0.134 | 0.026 |
| 684 (99.2), ASMELIFE [34] | $11.9\times10^6$ | 3152 | 44.6 |
| 900 (130.5), ISO 281: 2007 [36] | $\infty$ | $23.3\times10^6$ | 4258 |

[a] The von Mises stress.
[b] Includes effect of stressed volume.
[c] Normalized to life at maximum Hertz stress of 1379 MPa (200 ksi) with no fatigue limit.

## Zaretsky model

Both the Weibull and Lundberg-Palmgren models relate the critical shear stress-life exponent $c$ to the Weibull slope $e$. The parameter $c/e$ thus becomes, in

essence, the effective critical shear stress-life exponent, implying that the critical shear stress-life exponent depends on bearing life scatter or dispersion of the data. A search of the literature for a wide variety of materials and for nonrolling-element fatigue reveals that most stress-life exponents vary from 6 to 12. The exponent appears to be independent of scatter or dispersion in the data. Hence, Zaretsky [38] has rewritten the Weibull equation to reflect that observation by making the exponent $c$ independent of the Weibull slope $e$, where

$$f(X) = \tau^{ce}\eta^{e} \tag{59}$$

From Eqs. (5) and (59),

$$\eta \sim \left[\frac{1}{\tau}\right]^{c}\left[\frac{1}{V}\right]^{1/e} \tag{60}$$

For critical shearing stress $\tau$, Zaretsky chose the maximum shearing stress, $\tau_{45}$.

Lundberg and Palmgren [9] assumed that once initiated, the time a crack takes to propagate to the surface and form a fatigue spall is a function of the depth to the critical shear stress $z$. Hence, by implication, bearing fatigue life is crack propagation time dependent. However, rolling-element fatigue life can be categorized as "high-cycle fatigue." Crack propagation time is an extremely small fraction of the total life or running time of the bearing. The Lundberg-Palmgren relation implies that the opposite is true. To decouple the dependence of bearing life on crack propagation rate, Zaretsky [38,39] dispensed with the Lundberg-Palmgren relation of $L \sim z^{h/e}$ in Eq. (60). (It should be noted that at the time (1947) Lundberg and Palmgren published their theory [9], the concepts of "high-cycle" and "low-cycle" fatigue were only then beginning to be formulated.)

Equation (60) can be written as

$$L \sim \left[\frac{1}{\tau}\right]^{c}\left[\frac{1}{V}\right]^{1/e} \sim \frac{1}{S_{\max}^{n}} \tag{61}$$

From [28], solving for the value of the Hertz stress-life exponent $n$, for point contact from Eq. (61) gives

$$n = c + \frac{2}{e} \tag{62a}$$

and for line contact,

$$n = c + \frac{1}{e} \tag{62b}$$

If it is assumed that $c = 9$ and $e = 1.11$, $n = 10.8$ for point contact and $n = 9.9$ for line contact. If it is further assumed that $c = 10$ and $e = 1.0$, $n = 12$ for point contact and $n = 11$ for line contact.

What differentiates Eq. (61) and those of Weibull (Eq. 24), Lundberg and Palmgren (Eq. (38)) and Ioannides and Harris (Eq. (56)) is that the relation between shearing stress and life is independent of the Weibull slope, $e$, or the distribution of the failure data. However, in all four models, there is a dependency of the Hertz stress-life exponent, $n$, on the Weibull slope. The magnitude of the variation is least with the Zaretsky model.

Although Zaretsky [38,39] does not propose a fatigue-limiting stress, he does not exclude that concept either. However, his approach is entirely different from that of Ioannides and Harris [32]. For critical stresses less than the fatigue-limiting stress, the life for the elemental stressed volume is assumed to be infinite. Thus, the stressed volume of the component would be affected where $L \sim 1/V^{1/e}$. As an example, a reduction in stressed volume of 50 percent results in an increase in life by a factor of 1.9.

## Ball and roller set life

Lundberg and Palmgren [9] do not directly calculate the life of the rolling-element (ball or roller) set of the bearing. However, through benchmarking of the equations with bearing life data by use of a material-geometry factor $f_{cm}$, the life of the rolling-element set is implicitly included in the life calculation of Eqs. (53a) to (53g).

The rationale for not including the rolling-element set in Eq. (47) appears in the 1945 edition of A. Palmgren's book [5] wherein he states that, "…the fatigue phenomenon which determines the life (of the bearing) usually develops on the raceway of one ring or the other. Thus, the rolling elements are not the weakest parts of the bearing …". The database that Palmgren used to benchmark his and later the Lundberg-Palmgren equations were obtained under radially loaded conditions. Under these conditions, the life of the rolling elements as a system (set) will be equal to or greater than that of the outer race. As a result, failure of the rolling elements in determining bearing life was not initially considered by Palmgren. Had it been, Eq. (47) would have been written as follows:

$$\left(\frac{1}{L_{10}}\right)^e = \left(\frac{1}{L_{ir}}\right)^e + \left(\frac{1}{L_{re}}\right)^e + \left(\frac{1}{L_{or}}\right)^e \tag{63}$$

where the Weibull slope $e$ is the same for each of the components as well as for the bearing as a system.

Comparing Eq. (63) with Eq. (47), the value of the $L_{10}$ bearing life will be the same. However, the values of the $L_{ir}$ and $L_{or}$ between the two equations will not be the same, but the ratio of $L_{or}/L_{ir}$ will remain unchanged.

The fraction of failures due to the failure of a bearing component is expressed by Johnson [24] as

$$\text{Fraction of inner-race failures} = \left[\frac{L_{10}}{L_{ir}}\right]^e \tag{64a}$$

$$\text{Fraction of rolling-element failures} = \left[\frac{L_{10}}{L_{re}}\right]^e \tag{64b}$$

$$\text{Fraction of outer-race failures} = \left[\frac{L_{sys}}{L_{or}}\right]^e \tag{64c}$$

From Eqs. (64a) to (64c), if the life of the bearing and the fractions of the total failures represented by the inner race, the outer race and the rolling element set are known, the life of each of these components can be calculated. Hence, by observation, it is possible to determine the life of each of the bearing components with respect to the life of the bearing.

Equations (64a) to (64c) were verified using radially loaded and thrust-loaded 50-mm-bore ball bearings. Three hundred and forty virtual bearing sets totaling 31,400 bearings were randomly assembled and tested by Monte Carlo (random) number generation [40]. From the Monte Carlo simulation, the percentage of each component failed was determined and compared to those predicted from Eqs. (64a) to (64c). These results are shown in Table 3. There is excellent agreement between these techniques [40].

**Table 3.** Comparison of bearing failure distributions based upon Weibull-based Monte Carlo method and those calculated from equations (64a) to (64c) for 50-mm-bore deep-groove and angular-contact ball bearings [40].

| Ball bearing type | Component | Percent failure | |
|---|---|---|---|
| | | Weibull-based Monte Carlo results | Results from Eqs. (64a) to (64c) |
| Deep groove | Inner race | 70.1 | 69.9 |
| | Rolling element | 14.8 | 15.0 |
| | Outer race | 15.1 | 15.0 |
| Angular contact | Inner race | 45.4 | 45.1 |
| | Rolling element | 45.2 | 45.1 |
| | Outer race | 9.4 | 9.7 |

Figure 9 summarizes rolling-element fatigue life data for ABEC 7 204-size angular-contact ball bearings[4] made from AISI 52100 steel [41]. The bearings had a free contact angle of 10°. Operating conditions were an inner-ring speed of 10,000 rpm, an outer-ring temperature of 79 °C (175 °F), and a thrust load of 1108 N (249 lb). The thrust load produced maximum Hertz stresses of 3172 MPa (460 ksi) on the inner race and 2613 MPa (379 ksi) on the outer race. From a Weibull analysis of the data, the bearing $L_{10}$ life was 20.5 million inner-race revolutions, or approximately 34.2 hr of operation [41].

Seven of the twelve bearings failed from rolling-element fatigue. Two of the failed bearings had fatigue spalls on a ball and an inner race. Two bearings had inner-race fatigue spalls. Two bearings had fatigue spalls on a ball, and one bearing had an outer-race fatigue spall. Counting each component that failed as an individual failure independent of the bearing, there were four inner-race failures, four ball failures, and one outer-race failure for a total of nine failed components. Inner-race failures were responsible for 44.4 percent of the failures; ball failures, 44.4 percent; and outer-race failures, 11.2 percent. Using each of these percentages in Eqs. (64a) to (64c) together with the experimental $L_{10}$ life, the lives of the inner and outer races and the ball set were calculated. For purposes of the calculation, the Weibull slope $e$ was assumed to be 1.11, the same as Lundberg and Palmgren [9]. The resultant component $L_{10}$ lives were 53 million inner-race revolutions (88.3 hr) for both the inner race and ball set and 183.3 million inner-race revolutions (305.5 hr) for the outer race.

[4]The ABEC scale is a system for rating the manufacturing tolerances of precision bearings developed by the Annular Bearing Engineering Committee (ABEC) of the ABMA.

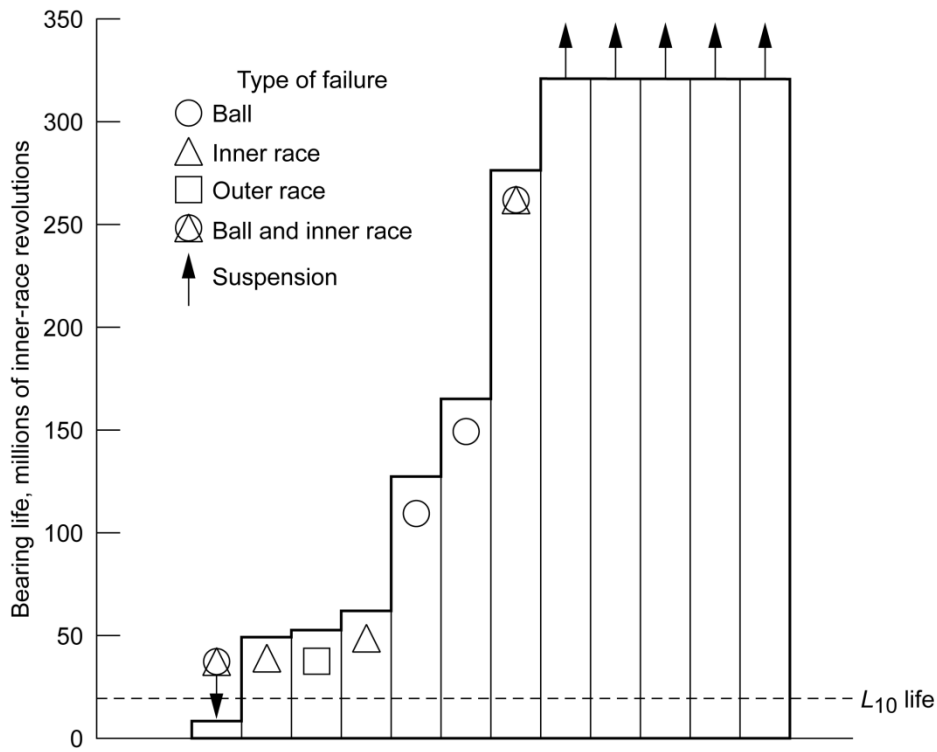


**Figure 9.** Rolling-element fatigue lives of AISI 52100 204-size angular-contact ball bearings. Contact angle is 10°; outer-race temperature, 79 °C (175 °F); thrust load, 1108 N (249 lb); inner-ring speed, 10,000 rpm; lubricant, MIL-L-7808; $L_{10}$ life, $20.5\times10^6$ inner-ring revolutions (34.2 hr); and failure index, 7 out of 12 [41].

For nearly all rolling-element bearings the number of inner-race failures is greater than those of the outer race. Accordingly, from Eqs. (64a) and (64c), the life of the outer race will be greater than that of the inner race. Zaretsky [18] noted that for radially loaded bearings (ball or roller), the percentage of failures of the rolling-element set was generally equal to and/or less than that of the outer race. For thrust-loaded ball or roller bearings, Zaretsky [18] further noted that the percent for the rolling-element set was equal to or less than that for the inner race but more than for the outer race. In order to account for material and processing variations, Zaretsky developed what is now referred to as Zaretsky's Rule [18]:

For radially loaded ball and roller bearings, the life of the rolling element set is equal to or greater than the life of the outer race. Let the life of the rolling element set (as a system) be equal to that of the outer race.

From Eq. (63)

$$\left(\frac{1}{L_{10}}\right)^e = \left(\frac{1}{L_{ir}}\right)^e + 2\left(\frac{1}{L_{or}}\right)^e \tag{65}$$

where $L_{re} = L_{or}$.

For thrust-loaded ball and roller bearings, the life of the rolling-element set is equal to or greater than the life of the inner race but less than that of the outer race. Let the life of the rolling-element set (as a system) be equal to that of the inner race.

From Eq. (63),

$$\left(\frac{1}{L_{10}}\right)^e = 2\left(\frac{1}{L_{ir}}\right)^e + \left(\frac{1}{L_{or}}\right)^e \tag{66}$$

where $L_{re} = L_{ir}$.

Examples of using Eqs. (65) and (66) are given in [18]. As previously stated, the resulting values for $L_{ir}$ and $L_{or}$ from these equations are not the same as those from Eq. (47). They will be higher.

H. Takata [42], using a modified approach to the Lundberg-Palmgren theory [9], derived the basic dynamic load capacity of the rolling-element bearing set in addition to those for the inner and outer races for radial and thrust-loaded ball and roller bearings. For radially loaded ball bearings, Takata assumes random ball rotation. For thrust-loaded ball bearings, he assumes a single or fixed running track on each ball. According to Takata, the basic dynamic load capacity $C_D$ of a bearing system can be expressed as

$$C_D = \left(C_{ir}^{-w} + C_{re}^{-w} + C_{or}^{-w}\right)^{-1/w} \tag{67}$$

where $C_D$ is calculated from Eqs. (53a) and (53b) (from Lundberg-Palmgren [9]), and the exponent $w$ is equal to 10/3 for ball bearings. Takata [42] provides equations for calculating the dynamic load capacity of the rolling-element (ball) set, $C_{re}$. The resulting values for $C_{ir}$ and $C_{or}$ will be higher than those from the Lundberg-Palmgren equations [9].

Takata [42] performed a single ball-set life calculation within his paper for a 30-mm-bore deep-groove ball bearing. From this calculation he concluded that for this bearing

$$C_{ir} < C_{re} < C_{or} \tag{68a}$$

This would imply that

$$L_{ir} < L_{re} < L_{or} \tag{68b}$$

However, Takata [42] did not validate his example or his equations to determine ball- or roller-set life with a bearing life data base.

**Ball-race conformity effects**

ANSI/ABMA and ISO standards based on the Lundberg-Palmgren bearing life model [9] are normalized for ball bearings having inner- and outer-race conformities of 52 percent (0.52) and made from pre-1940 bearing steel. As discussed previously, the Lundberg-Palmgren model incorporates an inverse 9th-power relation between Hertz stress and fatigue life for ball bearings. Except for differences in applied loading, deep-groove and angular-contact ball bearings are treated identically. The effect of race conformity on ball set life independent of race life is not incorporated into the Lundberg-Palmgren model. An analysis by Zaretsky, Poplawski, and Root [31,43] considered the life of the ball set independently from race life, resulting in different life relations for deep-groove and angular-contact ball bearings. Both a 9th- and a 12th-power relation between Hertz stress and life were considered by them.

Rolling-element bearing computer models are capable of handling various race conformities in combination with Lundberg-Palmgren theory, but they universally do not include the influence of ball-set life on overall bearing life. Computer programs acknowledging the influence of ball-set life are typically used for more rigorous analysis of bearing systems but are not commonly used in the general bearing design community.

The conformities at the inner and outer races affect the resultant Hertz stresses and the lives of their respective raceways. The determination of life factors $LF_i$ and $LF_o$ based on the conformities at the inner and outer races, respectively, can be calculated by normalizing the equations for Hertz stress for the inner and outer races to a conformity of 0.52 (the value of 0.52 was chosen as a typical reference value). Stresses are evaluated for the same race diameter as a function of conformity. Based on Eq. (27), the ratio of the stress at a 0.52 conformity to the value at the same normal load $P_N$ at another ball-race conformity, where $n = 9$ or 12, gives the appropriate life factor

$$LF = \left( \frac{S_{\max_{0.52}}}{S_{\max}} \right)^n \tag{69a}$$

For the inner race,

$$LF_i = \left[ \frac{\left( \frac{2}{d_e - d} + \frac{4}{d} - \frac{1}{0.52d} \right)^{2/3} (\mu\nu)_i}{\left( \frac{2}{d_e - d} + \frac{4}{d} - \frac{1}{f_i d} \right)^{2/3} (\mu\nu)_{0.52}} \right]^n \tag{69b}$$

and for the outer race,

$$LF_o = \left[ \frac{\left( -\frac{2}{d_e + d} + \frac{4}{d} - \frac{1}{0.52d} \right)^{2/3} (\mu\nu)_o}{\left( -\frac{2}{d_e + d} + \frac{4}{d} - \frac{1}{f_o d} \right)^{2/3} (\mu\nu)_{0.52}} \right]^n \tag{69c}$$

The values of $(\mu\nu)_{0.52}$ are different for the inner and outer races.

For various ball bearing series (see Fig. 10), values of these life factors for conformities ranging from 0.505 to 0.570, subject to round-off error, are given in Table 4 for inner and outer races, for $n$ = 9 and 12.

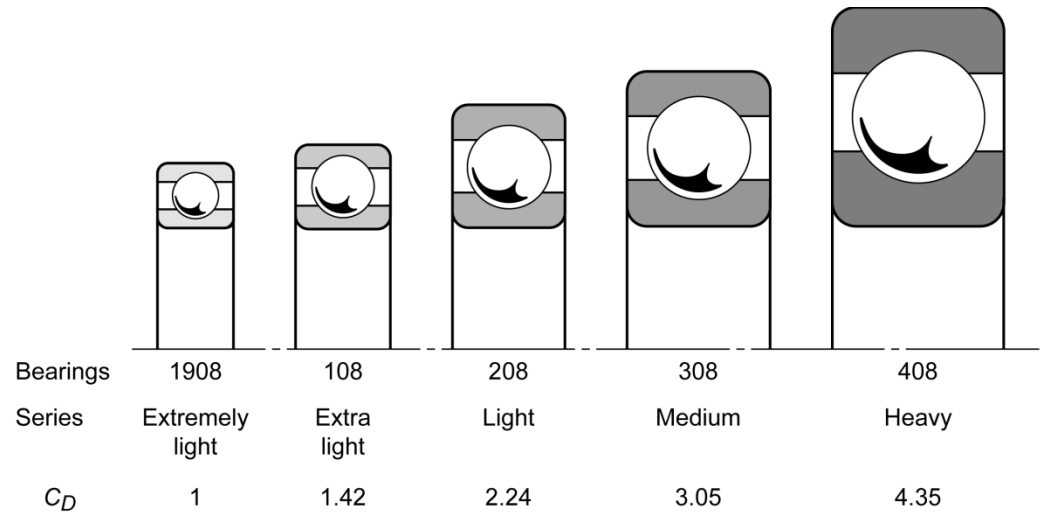


**Figure 10.** Effect of bearing series on relative sizes and dynamic capacities, $C_D$, of 40-mm bore deep-groove ball bearings [31].

From [31] and [43], the ratio of the outer- to the inner-race life can be approximated as

$$X = \frac{L_o}{L_i} \approx \left( \frac{S_{\max_i}}{S_{\max_o}} \right)^n \tag{70}$$

Referring to Figs. 7 and 8 and Hertzian contact theory [29] (see Appendix C),

$$X = \frac{L_o}{L_i} \approx \left[ \frac{\left( \dfrac{2\cos\beta}{d_e - d\cos\beta} + \dfrac{4}{d} - \dfrac{1}{f_i d} \right)^{2/3} (\mu\nu)_o}{\left( -\dfrac{2\cos\beta}{d_e + d\cos\beta} + \dfrac{4}{d} - \dfrac{1}{f_o d} \right)^{2/3} (\mu\nu)_i} \right]^n \tag{71}$$

Values of $\mu\nu$ for representative ball bearing series can be obtained from Table 4. Assuming $\cos\beta = 1$ and $f_i = f_o = 0.52$, values of $L_o/L_i$ were calculated from Eq. (71) for $n = 9$ and 12 and are summarized in Table 5. It should be noted that in the development of these relationships it was assumed that the contact angle $\beta$ does not change with speed and load [31,43].

**Table 4.** Effect of race conformity and Hertz stress-life exponent $n$ on ball bearing life as function of ball bearing series[a] [43].

| Conformity, $f$ | Ball bearing series | | | | | |
|---|---|---|---|---|---|---|
| | Extremely light, $\frac{d\cos\beta}{d_e} = 0.15$ | | | | | |
| | Inner race | | | Outer race | | |
| | $(\mu\nu)_i$ | Life factor, $LF_i$ | | $(\mu\nu)_o$ | Life factor, $LF_o$ | |
| | | $n = 9$ | $n = 12$ | | $n = 9$ | $n = 12$ |
| 0.505 | 2.013 | 14.7 | 36.05 | 1.826 | 11.84 | 27.00 |
| 0.510 | 1.776 | 4.53 | 7.51 | 1.673 | 3.61 | 5.53 |
| 0.515 | 1.641 | 2.12 | 2.73 | 1.551 | 1.71 | 2.05 |
| 0.520 | 1.517 | 1.00 | 1.00 | 1.471 | 1.00 | 1.00 |
| 0.525 | 1.503 | 0.88 | 0.84 | 1.415 | 0.66 | 0.57 |
| 0.530 | 1.452 | 0.62 | 0.53 | 1.369 | 0.46 | 0.36 |
| 0.535 | 1.409 | 0.45 | 0.35 | 1.335 | 0.35 | 0.25 |
| 0.540 | 1.376 | 0.35 | 0.25 | 1.304 | 0.27 | 0.17 |
| 0.545 | 1.361 | 0.30 | 0.20 | 1.282 | 0.22 | 0.13 |
| 0.550 | 1.328 | 0.23 | 0.14 | 1.262 | 0.18 | 0.10 |
| 0.555 | 1.306 | 0.19 | 0.11 | 1.244 | 0.15 | 0.08 |
| 0.560 | 1.296 | 0.17 | 0.10 | 1.227 | 0.13 | 0.06 |
| 0.565 | 1.278 | 0.15 | 0.08 | 1.211 | 0.11 | 0.05 |
| 0.570 | 1.262 | 0.13 | 0.06 | 1.196 | 0.09 | 0.04 |
| | Extra light, $\frac{d\cos\beta}{d_e} = 0.18$ | | | | | |
| 0.505 | 2.048 | 12.58 | 29.27 | 1.887 | 11.88 | 27.10 |
| 0.510 | 1.784 | 3.47 | 5.25 | 1.662 | 3.54 | 5.40 |
| 0.515 | 1.654 | 1.68 | 1.99 | 1.541 | 1.68 | 2.00 |
| 0.520 | 1.570 | 1.00 | 1.00 | 1.465 | 1.00 | 1.00 |
| 0.525 | 1.505 | 0.66 | 0.57 | 1.407 | 0.65 | 0.57 |
| 0.530 | 1.458 | 0.47 | 0.37 | 1.364 | 0.47 | 0.36 |
| 0.535 | 1.441 | 0.41 | 0.30 | 1.345 | 0.39 | 0.28 |
| 0.540 | 1.398 | 0.30 | 0.20 | 1.303 | 0.28 | 0.18 |
| 0.545 | 1.366 | 0.23 | 0.14 | 1.276 | 0.22 | 0.13 |
| 0.550 | 1.336 | 0.18 | 0.10 | 1.254 | 0.17 | 0.10 |
| 0.555 | 1.307 | 0.15 | 0.08 | 1.234 | 0.14 | 0.08 |
| 0.560 | 1.301 | 0.13 | 0.07 | 1.212 | 0.12 | 0.06 |
| 0.565 | 1.283 | 0.11 | 0.06 | 1.204 | 0.10 | 0.05 |
| 0.570 | 1.267 | 0.10 | 0.05 | 1.192 | 0.09 | 0.04 |
| | Light, $\frac{d\cos\beta}{d_e} = 0.23$ | | | | | |
| 0.505 | 2.062 | 12.32 | 28.38 | 1.870 | 11.83 | 26.94 |
| 0.510 | 1.843 | 4.28 | 6.95 | 1.652 | 3.61 | 5.54 |
| 0.515 | 1.658 | 1.58 | 1.84 | 1.549 | 1.89 | 2.34 |
| 0.520 | 1.583 | 1.00 | 1.00 | 1.454 | 1.00 | 1.00 |
| 0.525 | 1.520 | 0.67 | 0.58 | 1.397 | 0.66 | 0.57 |
| 0.530 | 1.471 | 0.48 | 0.37 | 1.354 | 0.47 | 0.36 |
| 0.535 | 1.431 | 0.36 | 0.25 | 1.333 | 0.38 | 0.28 |
| 0.540 | 1.401 | 0.28 | 0.19 | 1.292 | 0.27 | 0.18 |
| 0.545 | 1.374 | 0.22 | 0.14 | 1.267 | 0.21 | 0.13 |
| 0.550 | 1.347 | 0.19 | 0.11 | 1.235 | 0.16 | 0.09 |
| 0.555 | 1.324 | 0.15 | 0.08 | 1.227 | 0.14 | 0.08 |
| 0.560 | 1.312 | 0.14 | 0.07 | 1.211 | 0.12 | 0.06 |
| 0.565 | 1.298 | 0.12 | 0.06 | 1.198 | 0.10 | 0.05 |
| 0.570 | 1.280 | 0.10 | 0.05 | 1.180 | 0.09 | 0.04 |

**Table 4.** Continued

| Conformity, $f$ | Ball bearing series | | | | | |
|---|---|---|---|---|---|---|
| | Medium, $\frac{d\cos\beta}{d_e} = 0.25$ | | | | | |
| | Inner race | | | Outer race | | |
| | $(\mu\nu)_i$ | Life factor, $LF_i$ | | $(\mu\nu)_o$ | Life factor, $LF_o$ | |
| | | $n = 9$ | $n = 12$ | | $n = 9$ | $n = 12$ |
| 0.505 | 2.067 | 11.78 | 26.82 | 1.878 | 12.34 | 28.53 |
| 0.510 | 1.893 | 5.11 | 8.81 | 1.623 | 3.09 | 4.50 |
| 0.515 | 1.684 | 1.71 | 2.04 | 1.524 | 1.64 | 1.93 |
| 0.520 | 1.594 | 1.00 | 1.00 | 1.454 | 1.00 | 1.00 |
| 0.525 | 1.548 | 0.74 | 0.67 | 1.393 | 0.64 | 0.55 |
| 0.530 | 1.483 | 0.48 | 0.38 | 1.350 | 0.45 | 0.35 |
| 0.535 | 1.442 | 0.36 | 0.26 | 1.314 | 0.33 | 0.23 |
| 0.540 | 1.409 | 0.28 | 0.19 | 1.285 | 0.26 | 0.16 |
| 0.545 | 1.382 | 0.23 | 0.14 | 1.253 | 0.19 | 0.11 |
| 0.550 | 1.360 | 0.19 | 0.11 | 1.234 | 0.16 | 0.09 |
| 0.555 | 1.338 | 0.16 | 0.09 | 1.214 | 0.13 | 0.07 |
| 0.560 | 1.318 | 0.14 | 0.07 | 1.206 | 0.12 | 0.06 |
| 0.565 | 1.304 | 0.12 | 0.06 | 1.186 | 0.09 | 0.04 |
| 0.570 | 1.289 | 0.10 | 0.05 | 1.190 | 0.09 | 0.04 |
| | Heavy, $\frac{d\cos\beta}{d_e} = 0.28$ | | | | | |
| 0.505 | 2.056 | 11.87 | 27.08 | 1.874 | 13.02 | 30.62 |
| 0.510 | 1.784 | 3.18 | 4.17 | 1.637 | 3.58 | 5.47 |
| 0.515 | 1.668 | 1.62 | 1.97 | 1.519 | 1.70 | 2.03 |
| 0.520 | 1.583 | 1.00 | 1.00 | 1.443 | 1.00 | 1.00 |
| 0.525 | 1.547 | 0.78 | 0.72 | 1.387 | 0.66 | 0.57 |
| 0.530 | 1.472 | 0.48 | 0.38 | 1.345 | 0.47 | 0.36 |
| 0.535 | 1.435 | 0.37 | 0.27 | 1.310 | 0.34 | 0.24 |
| 0.540 | 1.400 | 0.29 | 0.19 | 1.282 | 0.27 | 0.17 |
| 0.545 | 1.373 | 0.23 | 0.14 | 1.260 | 0.22 | 0.13 |
| 0.550 | 1.346 | 0.19 | 0.11 | 1.231 | 0.17 | 0.09 |
| 0.555 | 1.327 | 0.16 | 0.09 | 1.217 | 0.14 | 0.07 |
| 0.560 | 1.310 | 0.14 | 0.07 | 1.206 | 0.12 | 0.06 |
| 0.565 | 1.292 | 0.12 | 0.06 | 1.191 | 0.10 | 0.05 |
| 0.570 | 1.283 | 0.11 | 0.05 | 1.180 | 0.09 | 0.04 |

[a]All values of $LF_i$ and $LF_o$ are normalized to 1.00 for conformity $f$ of 0.520.

**Table 5.** Representative ratios of outer- to inner-race life, $L_o/L_i$ for representative ball bearing series as a function of Hertz stress-life exponent, $n$, at inner- and outer-race conformities of 0.52 (from Eq. (70)).

| Ball bearing series | $\frac{d\cos\beta}{d_e}$ | Outer- to inner-race life ratio, $X = L_o/L_i$ | |
|---|---|---|---|
| | | Hertz stress-life exponent, $n$ | |
| | | 9 | 12 |
| Extremely light | 0.15 | 4.35 | 7.11 |
| Extra light | 0.18 | 4.39 | 7.18 |
| Light | 0.23 | 6.61 | 12.40 |
| Medium | 0.25 | 8.36 | 16.96 |
| Heavy | 0.28 | 12.04 | 27.60 |

## Deep-groove ball bearings

Zaretsky's Rule for radially loaded deep-groove ball bearings (Eq. (65)), the life of the rolling element set is equal to or greater than the life of the outer race. Therefore, $L_{re} = L_o$ with $X = L_o/L_i$, Eq. (65) can be rewritten as

$$L_{10} = \left( \frac{X^e L_i^e}{X^e + 2} \right)^{1/e} \tag{72}$$

Applying life factors based on the effect of conformity to the respective lives of the inner and outer races, Eq. (72) becomes

$$L_{10_m} = \frac{(LF_i)(LF_o)XL_i}{\left[(LF_o)^e X^e + 2(LF_i)^e\right]^{1/e}} \tag{73}$$

Dividing Eq. (73) by (72) provides the bearing life factor $LF_c$ for the radially loaded deep-groove ball bearing based on conformity:

$$LF_c = \left[ \frac{(LF_i)^e (LF_o)^e (X + 2)}{(LF_o)^e X^e + 2(LF_i)^e} \right]^{1/e} \tag{74}$$

## Angular-contact ball bearings

From Zaretsky's Rule for thrust-loaded ball bearings (Eq. (66)), the life of the rolling element set is equal to or greater than the life of the inner race but less than that of the outer race with $L_{re} = L_i$ and $X = L_o/L_i$. Equation (66) can be written as follows:

$$L_{10} = \left( \frac{X^e L_i^e}{2X^e + 1} \right)^{1/e} \tag{75}$$

Applying life factors based on the effect of conformity on the respective lives of the inner and outer races, Eq. (75) becomes

$$L_{10_m} = \frac{(LF_i)(LF_o)XL_i}{\left[2(LF_o)^e X^e + (LF_i)^e\right]^{1/e}} \tag{76}$$

Dividing Eq. (76) by (75) provides the bearing life factor $LF_c$ for the thrust-loaded, angular-contact ball bearing recognizing conformity:

$$LF_c = \left[\frac{(LF_i)^e (LF_o)^e \left(2X^e + 1\right)}{2(LF_o)^e X^e + (LF_i)^e}\right]^{1/e} \tag{77}$$

Representative life factors $LF_c$ from Eqs. (22), (27), and (31) were determined with the Lundberg-Palmgren theory and Zaretsky's Rule based on four combinations of inner- and outer-race conformities and for three representative series. These results are summarized in Table 6, for the two Hertz stress-life exponents $n$ = 9 and 12 [43].

From the above, the ANSI/ABMA and ISO life calculations can be modified based upon ball-race conformity as follows:

$$L_{10} = LF_c \left(\frac{C_D}{P_{eq}}\right)^p \tag{78}$$

The bearing fatigue lives in actual application will usually be equal to or greater than those calculated using the ANSI/ABMA and ISO standards that incorporate the Lundberg-Palmgren model. The relative fatigue life of an individual race is more sensitive to changes in race conformity for a Hertz stress-life exponent $n$ of 12 than where $n$ = 9. However, when the effects are combined to predict actual bearing life for a specified set of conditions and bearing geometry, the predicted life of the bearing will be greater for a value of $n$ = 12 ($p$ = 4) than $n$ = 9 ($p$ = 3) [43].

**Table 6.** Life factors based on combinations of ball-race conformities for Hertz stress-life exponent $n$ = 9 and 12 normalized to inner- and outer-race conformities of 0.52 [43].

| Ball bearing series | Ball-race conformity | | Bearing life factor for conformity,[a] $LF_c$ | | | | |
|---|---|---|---|---|---|---|---|
| | | | Lundberg-Palmgren[b] | Deep-groove ball bearing | | Angular-contact ball bearing | |
| | Inner race, IR | Outer race, OR | | From Eq. (72) | Change from Lundberg-Palmgren, % | From Eq. (77) | Change from Lundberg-Palmgren, % |
| Hertz stress-life exponent $n$ = 9 and $L_{10} = \left(\frac{C_D}{P_{eq}}\right)^3$ | | | | | | | |
| Extremely light, $\frac{d\cos\beta}{d_e} = 0.15$ | 0.505 | 0.52 | 4.16 | 3.15 | –24.30 | 7.40 | –77.83 |
| | 0.57 | 0.52 | 0.15 | 0.15 | -------- | 0.14 | –6.59 |
| | 0.52 | 0.505 | 1.16 | 1.19 | 2.59 | 1.09 | –6.23 |
| | 0.52 | 0.57 | 0.35 | 0.22 | –37.11 | 0.45 | 29.83 |
| Light, $\frac{d\cos\beta}{d_e} = 0.23$ | 0.505 | 0.52 | 5.10 | 3.05 | –40.28 | 6.97 | 36.76 |
| | 0.57 | 0.52 | 0.11 | 0.10 | –9.09 | 0.11 | ------- |
| | 0.52 | 0.505 | 1.10 | 1.04 | –5.68 | 7.05 | –4.42 |
| | 0.52 | 0.57 | 0.49 | 0.27 | –39.04 | 0.59 | 35.15 |
| Heavy, $\frac{d\cos\beta}{d_e} = 0.28$ | 0.505 | 0.52 | 6.77 | 4.66 | –32.24 | 8.51 | 25.73 |
| | 0.57 | 0.52 | 0.12 | 0.10 | –18.53 | 0.09 | –26.03 |
| | 0.52 | 0.505 | 1.05 | 0.89 | –15.08 | 1.03 | –2.22 |
| | 0.52 | 0.57 | 0.59 | 0.31 | –46.87 | 0.73 | 24.15 |
| Hertz stress-life exponent $n$ = 12 and $L_{10} = \left(\frac{C_D}{P_{eq}}\right)^4$ | | | | | | | |
| Extremely light, $\frac{d\cos\beta}{d_e} = 0.15$ | 0.505 | 0.52 | $6.83\left(\frac{C_D}{P_{eq}}\right)$ | $3.65\left(\frac{C_D}{P_{eq}}\right)$ | –46.56 | $10.79\left(\frac{C_D}{P_{eq}}\right)$ | 57.98 |
| | 0.57 | 0.52 | $0.07\left(\frac{C_D}{P_{eq}}\right)$ | $0.06\left(\frac{C_D}{P_{eq}}\right)$ | –14.29 | $0.06\left(\frac{C_D}{P_{eq}}\right)$ | –14.29 |
| | 0.52 | 0.505 | $1.10\left(\frac{C_D}{P_{eq}}\right)$ | $1.02\left(\frac{C_D}{P_{eq}}\right)$ | –7.27 | $1.05\left(\frac{C_D}{P_{eq}}\right)$ | –4.55 |
| | 0.52 | 0.57 | $0.26\left(\frac{C_D}{P_{eq}}\right)$ | $0.14\left(\frac{C_D}{P_{eq}}\right)$ | –46.15 | $0.39\left(\frac{C_D}{P_{eq}}\right)$ | 50.00 |
| Light, $\frac{d\cos\beta}{d_e} = 0.23$ | 0.505 | 0.52 | $9.67\left(\frac{C_D}{P_{eq}}\right)$ | $5.03\left(\frac{C_D}{P_{eq}}\right)$ | –47.98 | $14.03\left(\frac{C_D}{P_{eq}}\right)$ | 45.09 |
| | 0.57 | 0.52 | $0.05\left(\frac{C_D}{P_{eq}}\right)$ | $0.04\left(\frac{C_D}{P_{eq}}\right)$ | –20.00 | $0.05\left(\frac{C_D}{P_{eq}}\right)$ | ------- |
| | 0.52 | 0.505 | $1.05\left(\frac{C_D}{P_{eq}}\right)$ | $0.89\left(\frac{C_D}{P_{eq}}\right)$ | –15.24 | $1.03\left(\frac{C_D}{P_{eq}}\right)$ | –1.90 |
| | 0.52 | 0.57 | $0.37\left(\frac{C_D}{P_{eq}}\right)$ | $0.20\left(\frac{C_D}{P_{eq}}\right)$ | –45.95 | $0.53\left(\frac{C_D}{P_{eq}}\right)$ | 43.24 |
| Heavy, $\frac{d\cos\beta}{d_e} = 0.28$ | 0.505 | 0.52 | $14.97\left(\frac{C_D}{P_{eq}}\right)$ | $7.81\left(\frac{C_D}{P_{eq}}\right)$ | –47.83 | $19.13\left(\frac{C_D}{P_{eq}}\right)$ | 27.79 |
| | 0.57 | 0.52 | $0.05\left(\frac{C_D}{P_{eq}}\right)$ | $0.04\left(\frac{C_D}{P_{eq}}\right)$ | –20.00 | $0.05\left(\frac{C_D}{P_{eq}}\right)$ | ------- |
| | 0.52 | 0.505 | $1.02\left(\frac{C_D}{P_{eq}}\right)$ | $0.77\left(\frac{C_D}{P_{eq}}\right)$ | –24.51 | $1.01\left(\frac{C_D}{P_{eq}}\right)$ | –0.01 |
| | 0.52 | 0.57 | $0.57\left(\frac{C_D}{P_{eq}}\right)$ | $0.30\left(\frac{C_D}{P_{eq}}\right)$ | –47.37 | $0.72\left(\frac{C_D}{P_{eq}}\right)$ | 26.32 |

[a]All life factors are benchmarked to $L_{10} = \left(\frac{C_D}{P_{eq}}\right)^3$ and inner- and outer-race conformities of 0.52.

[b]For deep-groove and angular-contact ball bearings.

# Stress effects

## Hertz Stress-Life Relation

There is an issue of what the value of the Hertz stress-life relation and, hence, the value of the load-life exponent $p$ should be for purposes of analysis. The generally accepted relation between load and life in a rolling-element bearing is that life varies with the inverse cubic power of load for ball bearings (point contact) and with the inverse 4th power of load for roller bearings (line contact). Work reported by Parker and Zaretsky [44] suggests that for air-melted steels the exponent $n$ is approximately 9 for point contact. However, for the cleaner post-1960 vacuum-processed steels, $n = 12$ for point contact. A definitive data base does not exist for line contact (roller bearings).

For ball bearings, the Hertz stress-life relation where life is inversely proportional to the maximum Hertz stress to the 9th power and the cubic root of load, has been generally accepted by ball bearing manufacturers and users. There is at least one exception where a manufacturer had indicated based on its unpublished data base that the life of ball bearings varies inversely with the 4th power of load (or 12th power of Hertz stress). Nevertheless, the inverse cubic load-life relation has been included in the ANSI/ABMA standards for ball bearings [13].

Varying the Hertz stress-life exponent $n$ can significantly affect life predictions for bearings. Using $n = 9$ results in a more conservative estimate of bearing life than using $n = 12$. Also, the ratio of the predicted lives at the two values of the Hertz stress-life exponent $n$ is a function of load and is directly related to $C_D/P_{eq}$. Hence, in the normal operating load envelope, life may be underpredicted by a factor of 20 when using the ANSI/ABMA standards or a 9th power Hertz stress-life exponent $n$. A proper stress-life exponent then becomes more than of mere academic interest, since a design engineer requires a reliable analytic tool to predict bearing life and performance.

Fatigue tests of ball bearings by several investigators tended to verify this inverse cubic relation. Styri [45] presented data for two types of ball bearings. For one group of 6207-size, deep-groove ball bearings under various radial loads from 3.5 to 17.3 kN (775 to 3880 lbf), life was inversely proportional to load to the 3.3 power. Another group of 1207-size double-row self-aligning bearings was tested such that the maximum Hertz stress at the outer-race-ball contact varied from 4.0 to 5.6 GPa (580 to 810 ksi). Here it was found that life varied inversely with the 9th power of stress (or the 3rd power of load). Cordiano *et al.* [46] reported load-life data for 217-size, thrust-loaded ball bearings. The resultant Hertz stress-life exponents were 8.1, 9.6, and 12.6 for three lubricants, a water-glycol base, a

phosphate ester base, and a phosphate ester, respectively. McKelvey and Moyer [47] reported that, with four groups of AISI 4620, carburized-steel, crowned rollers (elliptical contact), fatigue life varied inversely with maximum Hertz stress to a range of the 8th to 9th power. Maximum Hertz stress in these tests varied from 1.8 to 3.3 GPa (262 to 478 ksi). Townsend *et al*. [48] surface fatigue tested three groups of case-carburized, consumable-electrode-vacuum-arc-remelted AISI 9310 8.89-cm- (3.5-in.-) pitch-diameter spur gears at maximum Hertz stresses of 1.5, 1.7, and 1.9 GPa (222, 248, and 272 ksi). The gears were run at 10,000 rpm and 77 °C (170 °F). The lubricant was superrefined naphthenic mineral oil with an additive package. The $L_{10}$ life varied inversely with stress to the 8.4 power, but the $L_{50}$ life varied inversely with stress to the 10.2 power. The average Hertz stress-life exponent $n$ was 9.3.

Several other investigators [49 to 57] have reported data with bench-type, rolling-element fatigue testers, rather than with full-scale bearings or gears. Data are summarized in Table 7. The $L_{10}$ lives as a function of maximum Hertz stress for these data are shown in Fig. 11. From the table the maximum Hertz stress for these data ranged from 3.7 to 9.0 GPa (526 to 1300 ksi). With the exception of Greenert's work [54] the stress-life exponents ranged from 8.4 to 12.4. The data are all for AISI 52100 and AISI M–50 steels (except for the data reported by Barwell and Scott [49], who do not state the type of steel). At least two sets of data were for air-melted steel, three were for vacuum-degassed steel, and one was for vacuum-arc-remelted steel. The other references do not state the melting process.

**Table 7.** Published bench-type rig rolling-element fatigue data related to stress-life effects [44].

| Number from Fig. 11 | Reference | Material | | Lubricant | Load range, kg | Maximum Hertz stress range, GPa, (ksi) | Load-life exponent | Stress-life exponent | Test type |
|---|---|---|---|---|---|---|---|---|---|
| | | Type | Melting process | | | | | | |
| 1 | Barwell and Scott [49] | ——— | (a) | Mineral oil | 200 to 600 | [b]4.5 to 6.6 ([b]660 to 950) | 2.8 | 8.4 | Four ball |
| 2 | Butler and Carter [50] | AISI 52100 | Air melt | SAE 10 mineral oil | ---------- | 4.1 to 5.2 (600 to 750) | 3.5 | 10.4 | Spin rig |
| 3 | Butler and Carter [50] | MV–1 (AISI M-50) | Air melt | SAE 10 mineral oil | ---------- | 4.1 to 5.2 (600 to 750) | 3.2 | 9.7 | Spin rig |
| 4 | Baughman [51] | MV–1 (AISI M-50) | (a) | MIL–L–7808 | ---------- | 4.4 to 5.4 (640 to 777) | 3.2 | 9.7 | Rolling-contact rig |
| 5 | Scott [52] | EN–31 (AISI 52100) | (a) | Diester | 400 to 600 | [b]5.7 to 6.6 (830 to 950) | 3.6 | 10.8 | Four ball |
| 6 | Utsmi and Okomoto [53] | AISI 52100 | (a) | #60 Spindle oil | ---------- | 3.7 to 5.1 (526 to 730) | [c]2.8 | [c]8.5 | Crowned disk |
| 7 | Greenert [54] | AISI 52100 | (a) | Navy 2190 TEP lubricating oil | ---------- | 5.8 to 6.1 (840 to 890) | [c]5 to 6.3 | [c]15 to 19 | Toroids |
| 8 | Valori *et al.* [55] | AISI 52100 | Vacuum-arc remelted | Mineral oil | ---------- | 4.2 to 5.5 (610 to 800) | [d]4.1 | [d]12.4 | Four ball |
| 9 | Schatzberg and Felsen [56] | AISI 52100 | Vacuum degassed | Squalene | ---------- | 6.4 to 9.0 (925 to 1300) | 3.8 | 11.5 | Four ball |
| 10 | Schatzberg and Felsen [56] | AISI 52100 | Vacuum degassed | Squalene + 100 ppm $H_2O$ | ---------- | 6.4 to 9.0 (925 to 1300) | 3.9 | 11.7 | Four ball |
| 11 | Parker and Zaretsky [44] | AISI 52100 | Vacuum degassed | Paraffinic mineral oil | ---------- | 4.5 to 6.0 (6.50 to 8.57) | 4 | 12 | Five ball |

[a]Melting process not reported.
[b]Approximate stress range, not reported by authors of reference.
[c]Estimated, not reported by authors of reference.
[d]Reanalyzed by Zaretsky and Parker [57].

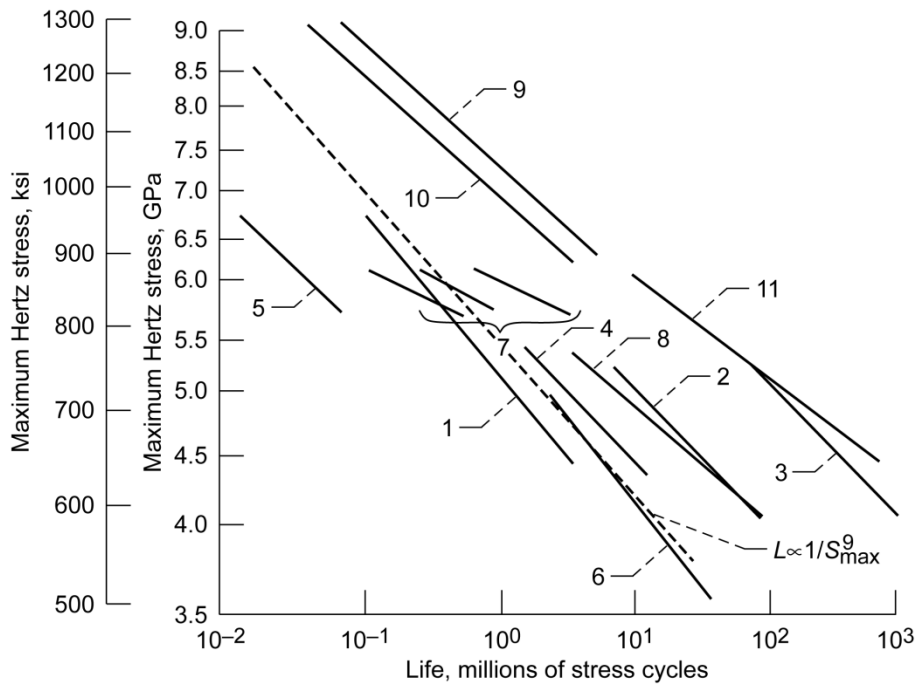


**Figure 11.** Summary of published stress-life relation data for Hertzian contacts failing from rolling-element fatigue. Refer to Table 7 [44].

The Hertz stress-life exponents from Greenert [54], ranging from 15 to 19, are much higher than those from other published data. This lack of correlation is unexplained. However, there is a probability that compressive residual stresses present in the steel could account for the resultant high values of the Hertz stress-life exponents.

Lorosch [58] fatigue tested three groups of vacuum-degassed 7205B-size AISI 52100 inner races at maximum Hertz stresses of 2.6, 2.8, and 3.5 GPa (370, 406, and 500 ksi), respectively. Each group consisted of 20 races, for a total of 60. (It is assumed that all 60 races came from a single heat of material and were of the same hardness, but Lorosch does not state so in his paper.) After the test runs Lorosch examined cross sections of the races. He observed that only at the lowest stress, 2.6 GPa (370 ksi), did no measurable plastic deformation occur. At the two higher stresses plastic deformations of different magnitudes were measured. Lorosch divided the races at the two higher stresses into groups according to these magnitudes. Group A included the races with the smaller deformations, and group B included the races with the larger deformations. The resultant stress-life exponent of groups A and B was 12. However, when E.V. Zaretsky [28] reconstituted the data for groups A and B into a single group, designated group AB, the stress-life exponent varied from 12 to 27 depending on the stress range over which the exponent was calculated. Lorosch [58] did not calculate the stress

reduction resulting from plastic deformation of the races, nor did he report on component hardness, hardness differential between the balls and races, or residual stresses induced during operation—all of which would also have affected his results. From these tests Lorosch concluded that "under low loads and with elastohydrodynamic lubrication there is no material fatigue, thus indicating that under such conditions bearing life is practically unlimited."

Zwirlein and Schlicht [59], in a companion paper published concurrently with that of Lorosch [58] and using the same 7205B-size bearing inner race data, state that "contact pressures less than 2.6 GPa (370 ksi) do not lead to the formation of pitting within a foreseeable period. This corresponds to 'true endurance'." This observation would support the assumption by Ioannides and Harris [32] of the existence of a "fatigue limit for bearing steels." However, this observation is not supported by rolling-element fatigue data in the open literature for stress levels under 2.6 GPa (370 ksi) – such as those reported in [60–64], which exhibited classical rolling-element fatigue. In rotating machinery nearly all rolling-element bearings operate at a maximum Hertz stress less than 2.1 GPa (300 ksi). Therefore, if Lorosch [58] and Zwirlein and Schlicht [59] were correct, no bearing in rotating machinery applications would fail by classical rolling-element fatigue.

To the author's knowledge there are no reported laboratory-generated, full-scale bearing rolling-element fatigue data at stresses significantly below 2.1 GPa (300 ksi) that would either establish or refute the presumption of a "fatigue limit." However, Townsend *et al*. [65] reported rolling-element and bending fatigue tests for four sets of spur gears made from through-hardened, vacuum-induction-melted, consumable-electrode-vacuum-arc-remelted (VIM–VAR) AISI M–50 steel and case-carburized, vacuum-arc-remelted (VAR) AISI 9310 steel. These gears were tested at a maximum Hertz stress of 1.7 GPa (248 ksi) and a maximum bending stress at the tooth root of 0.27 GPa (39 ksi). This results in a maximum shearing stress at the tooth root of 0.14 GPa (20 ksi). The AISI 9310 gears were "standard" machined as was one set of the AISI M–50 gears. A second set of AISI M–50 gears was "standard" near-net-shape forged using a controlled-energy-flow forming technique (CEFF). The third set of AISI M–50 gears was ausforged in a CEFF machine [65].

The results of these tests are shown in Fig. 12 [65]. The entire set of standard machined, case carburized VAR AISI 9310 gears failed by classical rolling-element fatigue at or near the gear tooth pitch diameter. There was no tooth-bending fatigue failure with the AISI 9310 gears. The entire set of standard machined AISI M–50 gears failed by bending fatigue. The standard forged and ausforged AISI M–50 gears failed by classical rolling-element fatigue and had approximately 5 times the $L_{10}$ life of the AISI 9310 gears. The standard machined

AISI M–50 gears had an $L_{10}$ bending fatigue life of about 40 percent that of the AISI 9310 gear surface fatigue life.

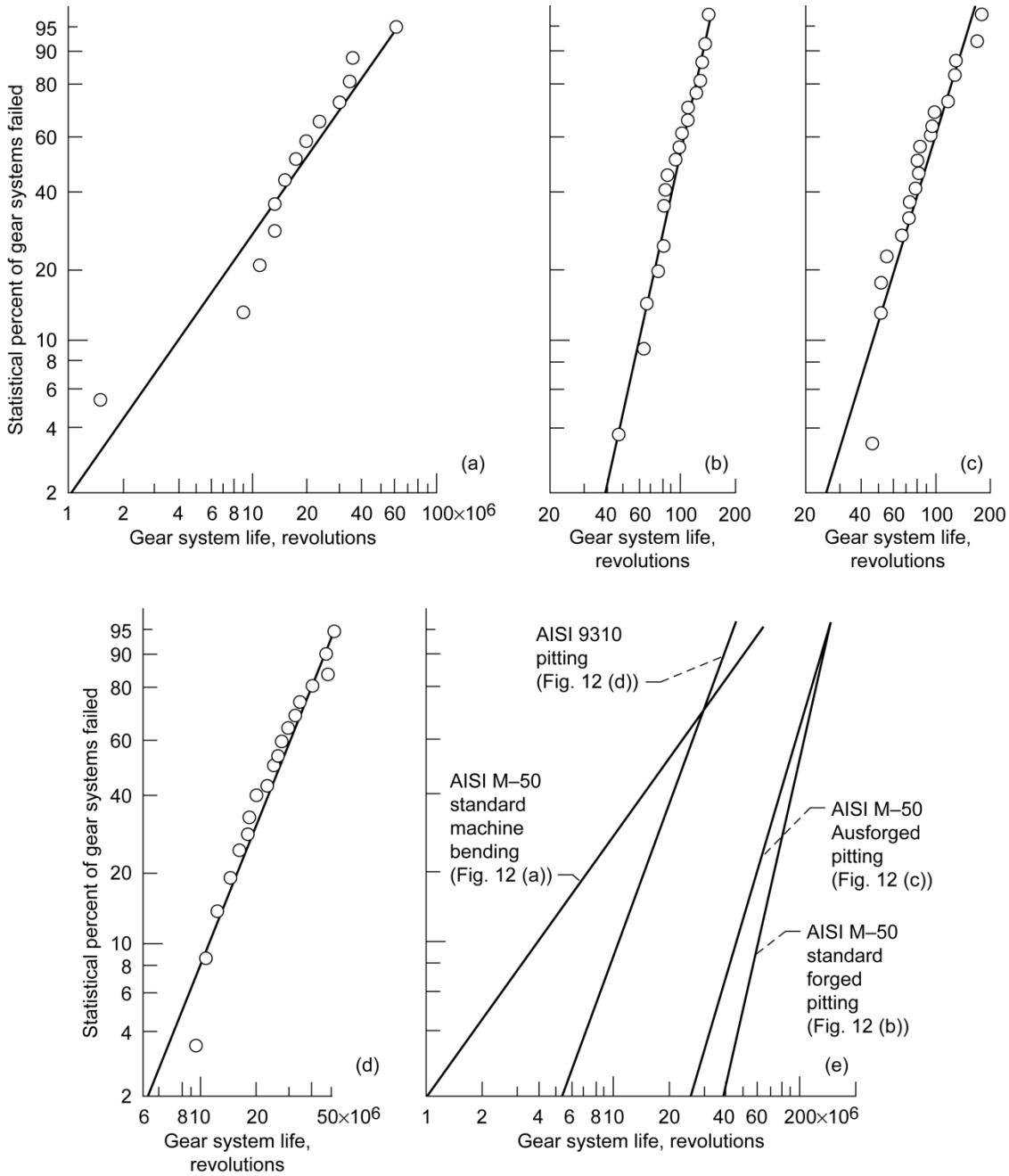


**Figure 12.** Fatigue lives of spur gear systems made of VIM-VAR AISI M-50 and VAR AISI 9310 [65]. Maximum Hertz stress, 1.71 GPa (248 ksi); maximum bending stress at tooth root, 0.27 GPa (39 ksi); speed, 10,000 rpm; temperature 350 K (170 °F); lubricant, super-refined naphthenic mineral oil. (a) Standard machined AISI M-50 bending fatigue. (b) Standard forged M-50 pitting fatigue. (c) Ausforged M-50 pitting fatigue. (d) AISI 9310 pitting fatigue. (e) Summary of gear life.

What is significant about these tests [65] is that bending fatigue is reported for through hardened bearing steel (AISI M–50) at shearing stresses of 0.14 GPa (20 ksi). These results suggest that if a fatigue limit exists for AISI M–50 it would be less than 0.14 GPa (20 ksi).

While it can be reasonably argued that the resultant stresses may be higher than that reported because of gear tooth dynamic loads, tooth bending fatigue was not experienced with the standard machined case-carburized AISI 9310 gears under the same conditions.

The standard forged and the ausforged AISI M–50 gears did not fail from bending fatigue but did fail from classical rolling-element (surface) fatigue. These results further suggest that if there is a fatigue limit for through-hardened bearing steels it would be less than at a maximum Hertz stress of 1.7 GPa (248 ksi).

As previously discussed, a paper presented by Tosha *et al*. [33] reporting the results of rotating beam fatigue experiments for through-hardened AISI 52100 steel at very low stress levels, shows conclusively that a fatigue limit does not exist for this bearing steel.

The explanation for the trend in the Lorosch [58] and Zwirlein and Schlicht [59] data is the inducement of compressive residual stresses in the AISI 52100 steel caused by the transformation of retained austenite into martensite during rolling-element cycling. These compressive residual stresses were reported by Zwirlein and Schlicht. Compressive residual stresses reduce the effective magnitude of the maximum shear stresses caused by Hertzian loading. This lower stress results in longer bearing life and deviation from the Hertz stress-life exponent $n$ of 9 or 12 to a significantly higher value. Lorosch [58] and Zwirlein and Schlicht [59] extrapolated their data, leading them to conclude the existence of a fatigue-limiting stress rather than concluding that induced compressive residual stresses had increased bearing life.

Lorosch [58] performed another series of rolling-element fatigue experiments with 20 inner races, designated group C, from the same heat as groups A and B. He used a Rockwell hardness tester to make 0.1-mm-diameter indentations at four evenly spaced locations around the center of the race circumference. He divided group C into 10-bearing sets, which were tested at 2.6 and 2.8 GPa (370 and 406 ksi), respectively. The $L_{10}$ lives for group C were significantly reduced from the group AB lives. These tests exhibited a 9.5 stress-life exponent. Because these indentations are analogous to wear debris denting during bearing operation, the results suggest that surface damage is another factor affecting the stress-life exponent.

## Residual and hoop stresses

Residual stresses can be induced in a material by heat treating, rolling, shot peening, diamond burnishing, and severe grinding. Each of these methods (except heat treating) is a separate mechanical process that is performed after heat treating [15,18]. Figure 13 shows representative residual stresses as a function of depth below the surface for three heat-treated bearing steels [15,18]. Carburized-grade steels generally have high compressive residual stresses in their cases, as shown for the carburized AISI 9310 and carburized AMS 6278 (VIM–VAR M50 NiL) steels in Fig. 13. Residual stresses are virtually nonexistent in unrun through-hardened steels but are induced at the surface by grinding to a depth of approximately 25 μm (0.001 in.) below the original surface. They can also be induced during operation or stressing of the bearing race surface [15,18].

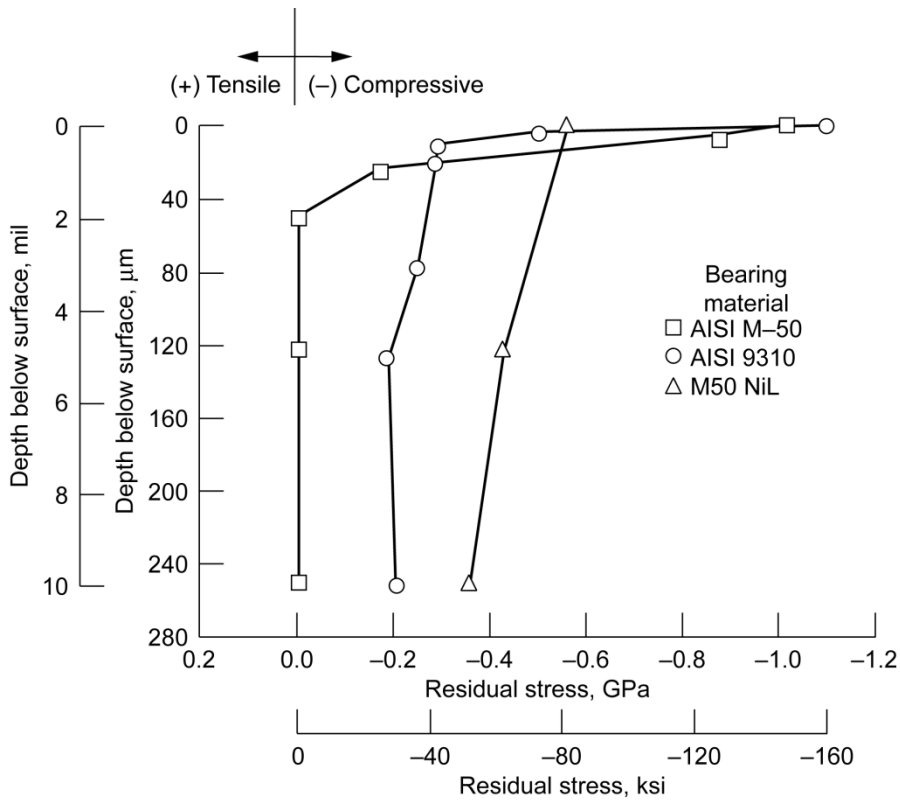


**Figure 13.** Representative principal residual stress as a function of depth below surface for heat-treated AISI M-50, AISI 9310, and M50 NiL (AMS 6278) [18].

Koistinen [66] reported a method of producing compressive residual stresses in the surface of AISI 52100 steel by austenitizing it in an atmosphere containing ammonia. Stickels and Janotik [67] also induced compressive residual stresses in

the surfaces of AISI 52100 steel rolling-element specimens by austenitizing them in a carbide atmosphere, even though the austenitizing temperature was below that needed to dissolve all primary carbides. The compressive residual stress extended to 300 μm (0.012 in.) below the surface and had a maximum value of 600 MPa (87 ksi). The carburized case (surface layer) contained a larger volume fraction of primary carbides and more retained austenite and was slightly harder than the core [15,18].

Pioneering research on the effect of residual stress on rolling-element fatigue life conducted by the staff of the General Motors Research Laboratories [68 to 71] found that compressive residual stresses induced beneath the surface of ball bearing race grooves prolong rolling-element fatigue life. According to [70], ball bearing lives were doubled when metallurgically induced ("prenitrided") compressive residual stress was present in the inner races. Scott *et al*. [71] found that compressive residual stresses induced by unidentified "mechanical processing" extend the fatigue life of ball bearings.

Naisong *et al*. [72] conducted rolling-element fatigue tests in the rolling-contact fatigue tester with AISI 52100 steel specimens that had compressive residual stress induced by treatment in a carburizing atmosphere. The tests, conducted at a maximum Hertz stress of 5 GPa (729 ksi), resulted in a depth to the maximum shear stress of 0.15 mm (0.006 in.). The treated material with the induced compressive residual stresses had approximately 1.6 times the life of untreated AISI 52100 in spite of having more carbides at or near the surface.

From Naisong *et al*. [72] it is apparent that the distribution of the induced compressive residual stresses is a function of the carbon potential. For ball and roller bearings the zone of maximum resolved shear stresses due to Hertzian loading occurs from 0.10 to 0.25 mm (0.004 to 0.010 in.) below the surface. With a carbon potential of 0.9 wt% carbon in iron, effective compressive residual stresses were available to a depth of 0.30 mm (0.012 in.). This depth was sufficient to have a beneficial effect. For carbon potentials less than 0.7 wt% carbon, high tensile residual stresses were present at depths to 0.20 mm (0.008 in.). Hence, without taking due care it is also possible to reduce the fatigue life by using the carburizing process to induce residual stresses [15,18].

The results of this research indicated that a compressive residual stress at the depth of the zone of maximum resolved shear stresses does prolong rolling-element fatigue life. Jones [73], Carter [74], Akoaka [75], and Zaretsky *et al*. [76] suggested that the maximum shear stress $\tau_{max}$ is the most significant stress in the rolling-element fatigue process. Zaretsky *et al*. [77] developed an analysis that superimposes the residual stresses upon the principal subsurface stress, lowering the maximum shear stress. A similar analysis was reported by Foord *et al*. [78] and then by Cioclov [79] in a discussion to Foord *et al*. The theoretical effect of

compressive residual stresses due to heat treatment on rolling-element fatigue is shown in Table 8.

**Table 8.** Theoretical effect of compressive residual stresses due to heat treatment on rolling-element fatigue life [18].

| Material | Compressive residual stress, GPa (ksi) | Maximum Hertz stress, GPa (ksi) | | | |
|---|---|---|---|---|---|
| | | 1.4 (200) | 1.9 (275) | 2.4 (350) | 4.8 (700) |
| | | Relative life[a] | | | |
| AISI M–50 | 0 | 1 | $5.7\times10^{-2}$ | $6.5\times10^{-3}$ | $1\times10^{-5}$ |
| AISI 9310 | 0.2 (29) | 12.1 | $32.4\times10^{-2}$ | $24.8\times10^{-3}$ | $2\times10^{-5}$ |
| AMS 6278 (VIM–VAR M50 NiL) | 0.4 (58) | 381 | $280\times10^{-2}$ | $119.1\times10^{-3}$ | $5\times10^{-5}$ |

[a]Relative life normalized to AISI M–50 at a maximum Hertz stress of 1.4 GPa (200 ksi) and no subsurface residual stress. These relative lives are not life factors. This table shows the potential effect of both applied stress and subsurface residual compressive stress on theoretical life.

The analysis of Zaretsky *et al.* [77], illustrated in Fig. 14, shows the principal stresses in the tangential (rolling) direction $S_t$ and in the normal direction $S_n$ for a Hertzian contact. The maximum shear stress is

$$\tau_{\max} = \frac{1}{2}\left(S_n - S_t\right) \tag{79}$$

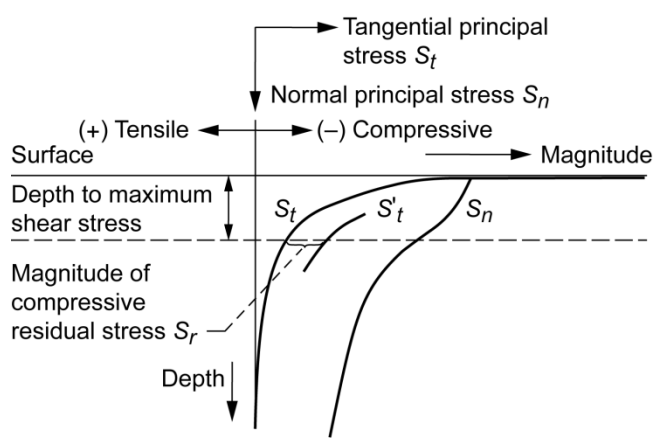


**Figure 14.** Effect of superimposing compressive residual stress on tangential principal stress in direction of rolling under Hertzian contact [15].

Superimposing the value of the compressive residual stress on the tangential principal stress gives the modified principal tangential stress

$$S_t' = S_t + S_r \tag{80}$$

By combining Eqs. (79) and (80), the maximum shear stress due to the effect of residual stresses $(\tau_{max})_r$ can be determined:

$$(\tau_{max})_r = \frac{1}{2}(S_n - S_t') = \frac{1}{2}[S_n - (S_t + S_r)] = -\tau_{max} - \frac{1}{2}(-S_r) \tag{81}$$

The negative sign before $S_r$ designates a compressive residual stress. A positive sign before $S_r$ would designate a tensile residual stress [77]. Hence, the residual stress can either increase or decrease the maximum shear stress. Accordingly, a compressive residual stress would reduce the maximum shear stress and increase the fatigue life according to the inverse relation of life and stress to the $c/e$ power,

$$L \sim \left[\frac{1}{(\tau_{max})_r}\right]^{c/e} \tag{82a}$$

for Lundberg and Palmgren, where $c/e = 9.3$, or

$$L \sim \left[\frac{1}{(\tau_{max})_r}\right]^{c} \tag{82b}$$

for Zaretsky, where $9 \le c \le 10$.

For rolling-element bearings the beneficial effect of the compressive residual stresses is offset by the presence of tensile (hoop) stresses in the bearing inner race.

These hoop stresses are induced and affected primarily by the press fit of the inner race over the shaft, centrifugal loading, and thermal effects between the race and the shaft. Coe and Zaretsky [80] analyzed the effect of hoop stresses on rolling-element fatigue. Czyzewski [81] showed that, in the absence of compressive residual stress, hoop stresses are generally tensile, are designated by a + sign, and can negatively affect fatigue life. As with the compressive residual stresses, hoop stresses alter the critical subsurface shear stress and affect the life of the bearing inner race. Equation (81) can be rewritten to account for the effect of both residual and tensile (hoop) stresses as

$$(\tau_{max})_{rh} = -\tau_{max} - \frac{1}{2}(\pm S_r \pm S_h) \tag{83}$$

Again the positive or negative sign indicates a tensile or compressive stress, respectively. Equation (82) can be written to reflect the effect of both the compressive and tensile stresses on life as

$$L \sim \left[ \frac{1}{(\tau_{\max})_{rh}} \right]^{c/e} \tag{84a}$$

for Lundberg and Palmgren, where $c/e = 9.3$, or

$$L \sim \left[ \frac{1}{(\tau_{\max})_{rh}} \right]^{c} \tag{84b}$$

for Zaretsky, where $9 \le c \le 10$.

Since life $L \sim \left(\frac{1}{\tau}\right)^{c/e}$ or $\left(\frac{1}{\tau}\right)^{c}$, Eqs. (48) and (84) have been combined to modify the predicted bearing life [18]:

$$L_{10} = \left[ \frac{\tau_{\max}}{(\tau_{\max})_{rh}} \right]^{c/e} \left[ \frac{C_D}{P_{eq}} \right]^{p} \tag{85a}$$

From Lundberg and Palmgren [9], $c/e = 9.3$ and $p = 3$ for ball bearings and $p = 4$ for roller bearings. From Zaretsky,

$$L_{10} = \left[ \frac{\tau_{\max}}{(\tau_{\max})_{rh}} \right]^{c} \left[ \frac{C_D}{P_{eq}} \right]^{p} \tag{85b}$$

where $p = 4$ for ball bearings, $p = 5$ for roller bearings, and $9 \le c \le 10$. From Hertz theory [29], $\tau_{\max} \approx 0.32 S_{\max}$ for ball bearings and $0.3 S_{\max}$ for roller bearings.

## Comparison of bearing life models

The Ioannides-Harris model without a fatigue limit is identical to Lundberg-Palmgren model. The Weibull model is similar to that of Zaretsky if the exponents are chosen to be identical. Comparison of the Lundberg-Palmgren model and the Zaretsky model with the ANSI/ABMA and ISO standards is shown in Fig. 15 for

ball and cylindrical roller bearings. The theoretical lives were normalized to a maximum Hertz stress of 4.14 GPa (600 ksi) and subsequently normalized to the calculated ANSI/ABMA and ISO standards at each stress level. For the Ioannides-Harris comparison shown in Fig. 15, a fatigue-limiting stress of 276 MPa (40 ksi) was assumed. For ball bearings, the ANSI/ABMA and ISO standards and the Lundberg-Palmgren model give identical results. For roller bearings, the results are not identical [82].

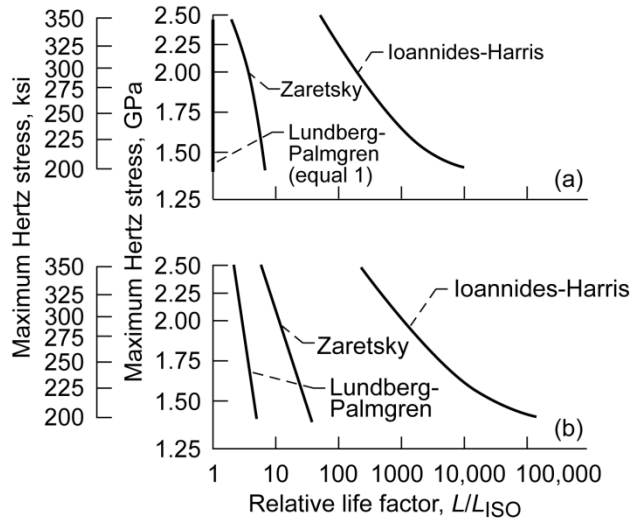


**Figure 15.** Comparison of life models for rolling-element bearings with ANSI/ABMA and ISO standard without a fatigue limit. Fatigue-limiting shear stress for $\tau_{45}$ assumed for Ioannides-Harris model, 276 MPa (40 ksi) [82]. (a) Ball bearings. (b) Cylindrical roller bearings.

The ANSI/ABMA and ISO standards use a load-life exponent $p$ of 10/3 (3.33) for line contact (roller bearings). This results in a value of $n$ equal to 6.6 and can account in part for lower life predictions than those experienced in the field. From Lundberg and Palmgren [9], the load-life exponent $p$ for line contact should be 4. However, Lundberg and Palmgren's justification for a $p$ of 10/3 was that a roller bearing can experience "mixed contact"; that is, one raceway can experience line contact and the other raceway point contact [10]. This may be true in limited number of roller bearing designs, but it is certainly not consistent with the vast majority of cylindrical roller and tapered roller bearings designed and used today.

Both the load-life and stress-life relations of Weibull, Lundberg and Palmgren, and Ioannides and Harris reflect a strong dependence on the Weibull slope. The existing rolling-element fatigue data reported by Parker and Zaretsky [44] reflect slopes in the range of 1 to 2 and some cases higher or lower. If the slope were factored into these equations, then the stress-life (load-life) exponent significantly

decreases with increases in Weibull slope, whereby the relation no longer matches reality.

The Zaretsky model that decouples the dependence of the critical shear stress-life relation and the Weibull slope shows only a slight variation of the maximum Hertz stress-life exponent *n* with Weibull slope *e*.

These results would indicate that for 9th- and 8th-power Hertz stress-life exponents for ball and roller bearings, respectively, the Lundberg-Palmgren model best predicts life. However, for 12th- and 10th-power relations reflected by modern bearing steels, the Zaretsky model based on the Weibull equation is superior [82].

Under the range of stresses examined, the use of a fatigue limit would suggest that (for most operating conditions under which a rolling-element bearing will operate) the bearing will not fail from classical rolling-element fatigue. Realistically, this does not occur. The use of a fatigue limit will significantly overpredict life over a range of normal operating Hertz stresses. (The use of ISO 281:2007 [36] in these calculations would result in a bearing life approaching infinity.) Since the predicted lives of rolling-element bearings are high, the problem can become one of undersizing a bearing for a particular application [31].

## Comparing life data with predictions

### Bearing life variation

Vlcek *et al*. [83] randomly assembled and tested 340 virtual bearing sets totaling 31,400 radially loaded and thrust-loaded rolling-element bearings. It was assumed that each bearing was assembled from three separate bins of components, with one bin containing 1000 inner rings; one with 1000 rolling element sets, and one with 1000 outer rings. The median ranks of the individual components were assigned and then virtual bearing assemblies were created using a Monte Carlo technique. The corresponding lives of the bearing components were determined using Eq. (17). The weakest link theory was applied; that is, it was assumed that the life of the shortest-lived component of the system was the life of the system. A linear curve fit of these system lives results in a Weibull plot. Weibull parameters from the plot and Eq. (17) can be used to determine lives at any percentage of survivability.

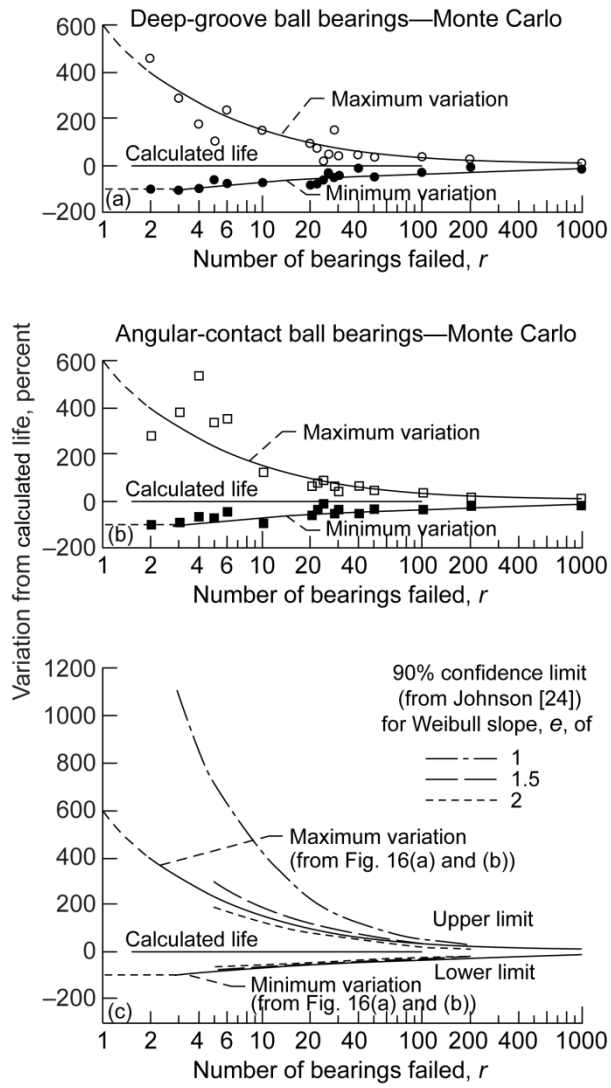


**Figure 16.** Maximum and minimum variation of $L_{10}$ lives as percent of calculated $L_{10}$ for groups of $r$ bearings and 90% confidence limits based on Weibull slope and number of bearings failed $r$ [83]. (a) 50-mm-bore deep-groove ball bearing. (b) 50-mm-bore angular-contact ball bearing. (c) 90% confidence limits.

Vlcek *et al*. [83] determined the $L_{10}$ maximum limit and $L_{10}$ minimum limit for the number of bearings failed, $r$, using a Weibull-based Monte Carlo method. By fitting the resultant lives for different size populations of failed bearings (Fig. 16), equations were determined for both of these limits:

$$\text{Maximum variation } L_{10} \text{ life} = \text{calculated } L_{10} \text{ life } (1+6r^{-0.6}) \tag{86a}$$

$$\text{Minimum variation } L_{10} \text{ life} = \text{calculated } L_{10} \text{ life } (1-1.5r^{-0.33}) \text{ where } r > 3 \tag{86b}$$

Minimum $L_{10}$ life = 0 where $r \leq 3$ (86c)

These curves compared favorably with the 90-percent confidence limits of Johnson [24] at a Weibull slope of 1.5 (Fig. 16) [83].

Rules can be implied from these results to compare and distinguish resultant lives of similar bearings from two or more sources and/or made using different manufacturing methods. The following rules are suggested to determine if the bearings are acceptable for their intended application and if there are significant differences between two groups of bearings.

1. If the $L_{10}$ lives of both bearing sets are between the maximum and minimum $L_{10}$ life variations, there can be no conclusion that there is a significant difference between the two sets of bearings regardless of the ratio of the $L_{10}$ lives. The bearing sets are acceptable for their intended application (Fig. 17(a)).
2. If the $L_{10}$ life of one set of bearings is greater than the maximum variation and the second set is less than the minimum value, there exists a significant difference between the bearing sets. Only one bearing set is acceptable for its intended application (Fig. 17(b)).
3. If the $L_{10}$ lives of both sets of bearings exceed the maximum variation, the bearing life differences may or may not be significant and should be evaluated based upon calculation of confidence numbers according to the method of Johnson [24]. Both sets of bearings are acceptable for their intended application (Fig. 17(c)).
4. If the $L_{10}$ lives of both sets of bearings are less than the minimum variation, the bearing life differences may or may not be significant. However, neither set of bearings is acceptable for its intended application (Fig. 17(d)).
5. If the $L_{10}$ life of one set of bearings exceeds the maximum variation and the other set is between the maximum and minimum variation, the bearing life differences may or may not be significant and should be evaluated based upon calculation of confidence numbers according to the method of Johnson [24]. Both sets of bearings are acceptable for their intended application (Fig. 17(e)).
6. If the $L_{10}$ life of one set of bearings is less than the minimum variation and the other set is between the maximum and minimum variation, there exists a significant difference between the bearing sets. Only one set of bearings is acceptable for its intended application (Fig. 17(f)).

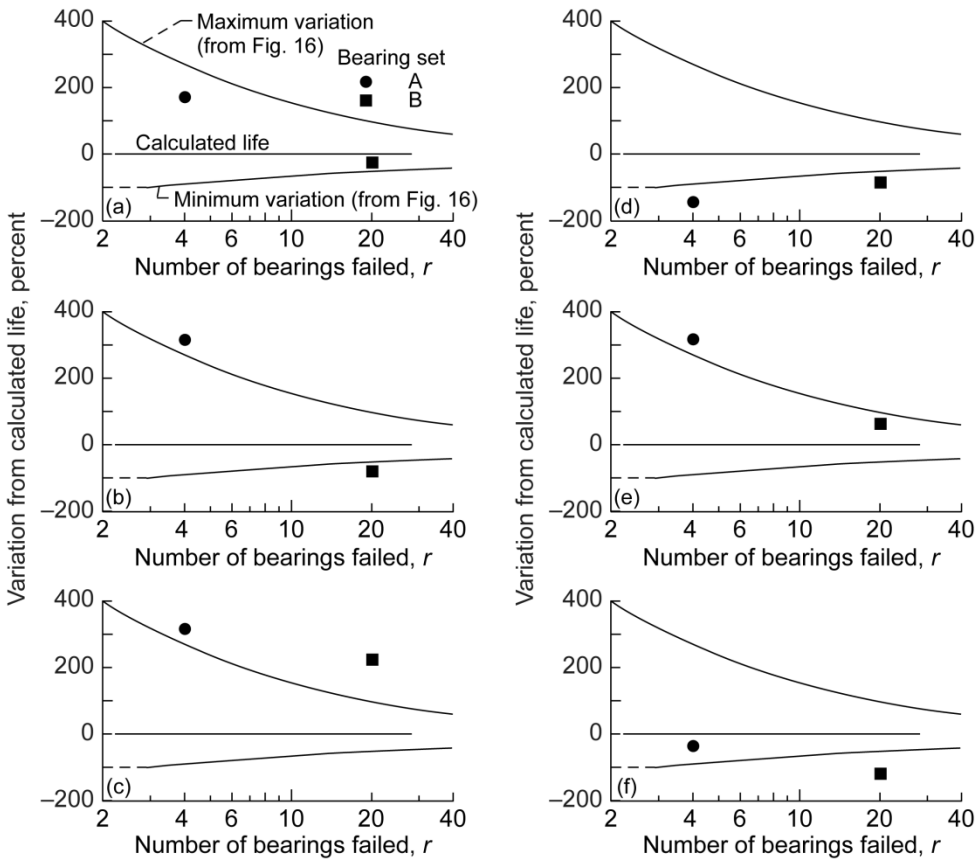


**Figure 17.** Rules for comparing bearing life results to calculated life [83]. (a) Bearing sets A and B are acceptable. (b) Bearing set A is acceptable. Bearing set B is not acceptable. (c) Bearing sets A and B are acceptable. (d) Bearing sets A and B are not acceptable. (e) Bearing sets A and B are acceptable. (f) Bearing set A is acceptable. Bearing set B is not acceptable.

Harris [84] and Harris and McCool [85] analyzed endurance data for 62 rolling-element bearing sets. These data were obtained from four bearing manufacturers, two helicopter manufacturers, three aircraft engine manufacturers, and U.S. Government agency-sponsored technical reports. The data sets comprised deep-groove radial ball bearings, angular-contact ball bearings, and cylindrical roller bearings for a total of 7935 bearings. Of these, 5321 bearings comprised one sample size for a single cylindrical roller bearing, leaving 2614 bearings distributed among the remaining bearing types and sizes. Among the 62 rolling-element bearing endurance sets, 11 had one or no failure and could not be used for the analysis. These data are summarized in [83] and plotted in Fig. 18. A discussion of the Harris data can be found in [28] and [43].

Of these data, 39 percent fall between the maximum and minimum life variations suggesting that the statistical variations of these lives are within that

predicted. Four bearing sets representing 8 percent of the bearing sets had lives less than what was predicted. Thirty bearing sets, or 59 percent of the bearing sets, exceeded the maximum life variation of the Monte Carlo study of Vlcek *et al*. [83]. Eight of these bearing sets or 16 percent exceeded the 90-percent confidence upper limit of Johnson [24]. However, only one bearing set representing 2 percent of the bearing sets fall below the lower life limit. Therefore, it can be reasonably concluded that 98 percent of the bearing sets have acceptable life results using the Lundberg-Palmgren equations with the life adjustment factors from [18] to predict bearing life.

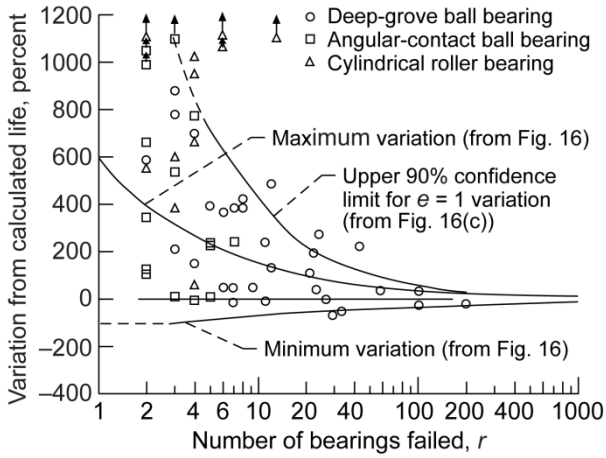


**Figure 18.** Variation between actual and calculated $L_{10}$ bearing lives for 51 sets of deep-groove and angular-contact ball bearings and cylindrical roller bearings from [84] and [85] compared with Monte Carlo variations and 90% confidence limit [83].

The life calculations for the data of Fig. 18 have material and steel processing life factors from [18] incorporated in them. Table 9 summarizes these life factors for each of the materials. The data of Fig. 18 are broken down and plotted in parts (a) of Figs. 19 through 22 based on the steel type and processing. These data were adjusted for a load-life exponent $p$ of 4 for ball bearings and 5 for roller bearings and are shown in parts (b) of Figs. 19 through 22. The adjusted life results correlated with those of the Monte Carlo tests shown in Fig. 16. Based upon these material and processing life factors and load-life exponents, each bearing data set appears consistent with the other.

Lundberg and Palmgren [9] assumed the value of the Weibull slope $e$ in Eq. (17) to be 1.11 for ball bearings [9] and 1.125 for roller bearings [10]. These values were necessary in their analysis because it approximated those values exhibited by their experimental data, and it made the end result of their life prediction analysis correlate with their bearing life database at that time. Experience has shown that

most rolling bearing life data exhibit Weibull slopes between 1 and 2. For the analysis in [83] a Weibull slope of 1.11 was assumed for all of the components for each bearing. This should theoretically result in a bearing Weibull slope of 1.11 as shown in Fig. 23 for the deep-groove and angular-contact ball bearings.

**Table 9.** Life factors for bearing steels and processing [18].

| Material and process | Life factor | | |
|---|---|---|---|
| | Material | Process | Resultant |
| CVD[a] AISI 52100 | 3 | 1.5 | 4.5 |
| CVD[a] AISI 8620 | 1.5 | 1.5 | 2.25 |
| VAR[b] AISI M–50 | 2 | 3 | 6 |
| VIM–VAR[c] AISI M–50 | 2 | 6 | 12 |
| VIM–VAR[c] M50 NiL | 4 | 6 | 24 |

[a]Carbon vacuum degassing.
[b]Vacuum arc remelting.
[c]Vacuum induction melting and vacuum arc remelting.

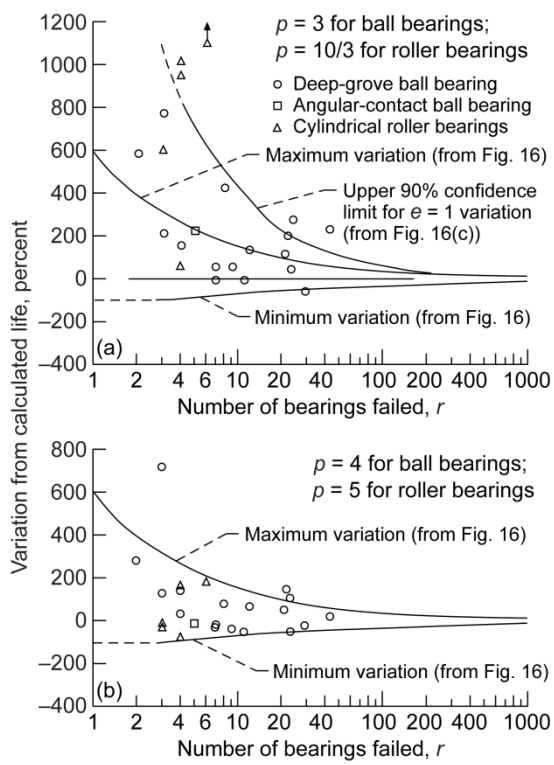


**Figure 19.** Effect of CVD AISI 52100 steel and load-life exponent on bearing life [83]. (a) Load-life exponent $p$ is 3 for ball bearings and 10/3 for cylindrical roller bearings (from Fig. 18). (b) Load-life exponent $p$ is 4 for ball bearings and 5 for cylindrical roller bearings.

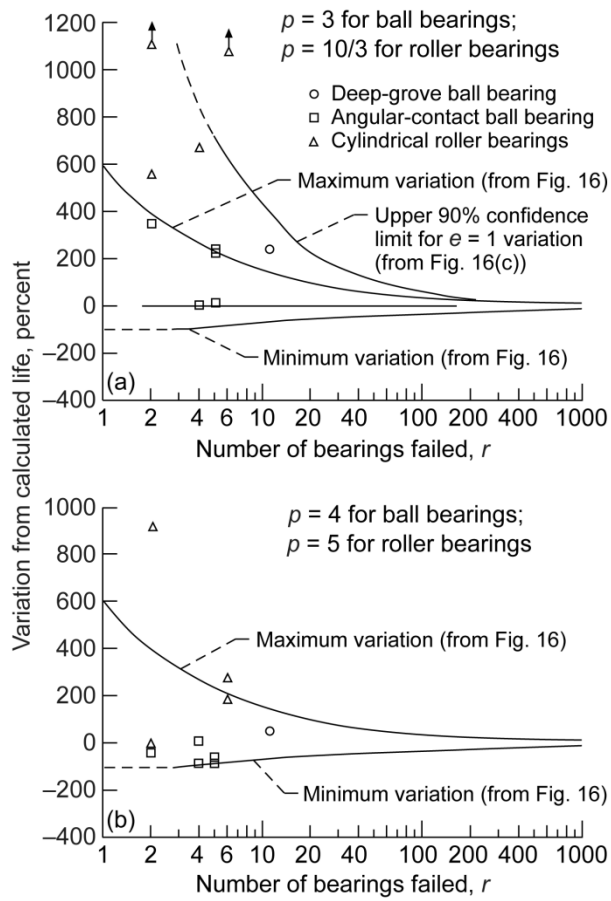


**Figure 20.** Effect of VAR AISI M-50 steel and load-life exponent on bearing life [83]. (a) Load-life exponent $p$ is 3 for ball bearings and 10/3 for cylindrical roller bearings (from Fig. 18). (b) Load-life exponent $p$ is 4 for ball bearings and 5 for cylindrical roller bearings.

## Weibull slope variation

Johnson [24] analyzed the probable variation of the Weibull slope as a function of the number of bearings tested to failure. Based on the Johnson analysis, in 90 percent of all possible cases the resultant Weibull slope will be within the limits shown in Fig. 23 based upon a Weibull slope of 1.11. Based on Johnson, the approximate relation for the number of bearings failed $r$ and the limits of the value of Weibull slope $e$ equal to 1.11 are as follows:

$$\text{Maximum Weibull slope} = 1.11 + 1.31\, r^{-0.5} \tag{87a}$$

$$\text{Minimum Weibull slope} = 1.11 - 1.31\, r^{-0.5} \tag{87b}$$

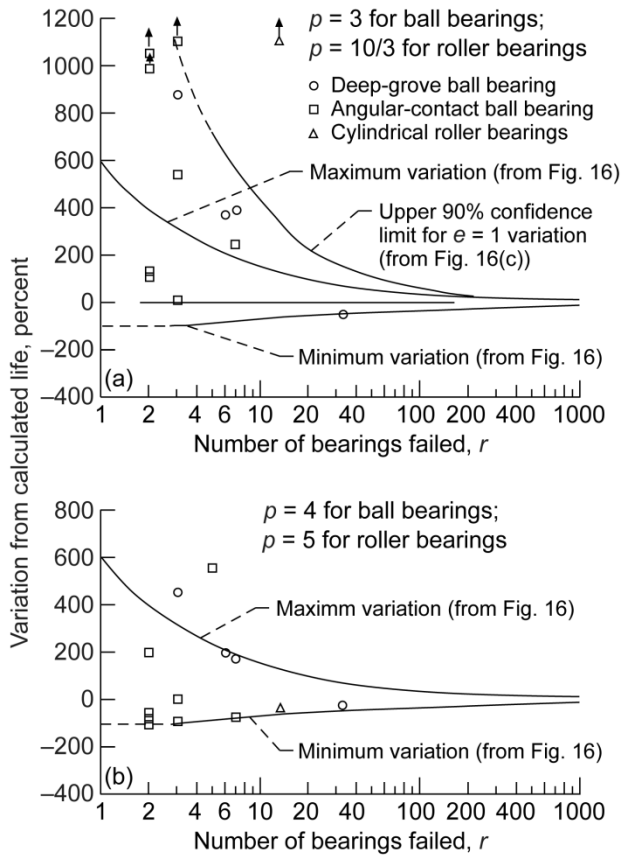


**Figure 21.** Effect of VIM-VAR AISI M-50 steel and load-life exponent on bearing life [83]. (a) Load-life exponent $p$ is 3 for ball bearings and 10/3 for cylindrical roller bearings (from Fig. 18). (b) Load-life exponent $p$ is 4 for ball bearings and 5 for cylindrical roller bearings.

The results of the extremes in the Weibull slopes for each group of the 10 bearing trials of $r$ bearings are compared with the Johnson analysis in Fig. 23(a). (Note that the Weibull slopes for the data summarized in Fig. 18 for the maximum and minimum bearing lives are not necessarily the same as the maximum and minimum values of the Weibull slopes for each of trials of $r$ bearings.) For the data shown in Fig. 18 the relation between the number of bearings tested and the limits of the Weibull slope are as follows:

$$\text{Maximum Weibull slope} = 1.2 + 5(\ln r)^{-3} \tag{88a}$$

$$\text{Minimum Weibull slope} = 1.11 - 0.95r^{-0.33} \tag{88b}$$

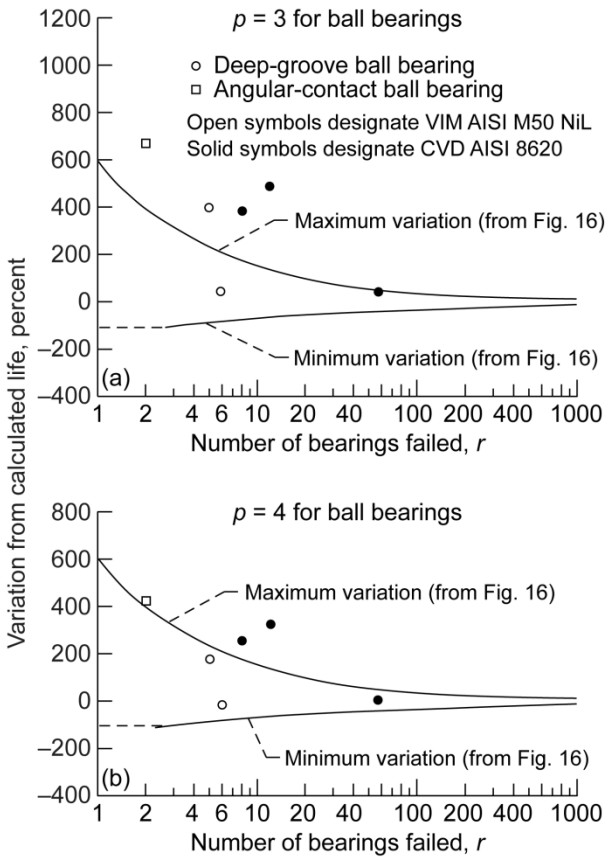


**Figure 22.** Effect of VIM-VAR AISI M50 NiL and CVD AISI 8620 steels and load-life exponent on bearing life [83]. (a) Load-life exponent $p$ is 3 for ball bearings (from Fig. 18). (b) Load-life exponent $p$ is 4 for ball bearings.

Where the number of bearings failed is 10 or greater, there is a reasonably good correlation between the limits of the slopes generated from the Johnson analysis [24] and those from the Monte Carlo bearing tests shown in Fig. 23(a). Where the number of failed bearings is below 10, there are differences between the extremes in Weibull slope between the Monte Carlo bearing tests and those of Johnson, especially at the upper limits for the Weibull slopes [83].

## Case study

### Turboprop gearbox

The commercial turboprop gearbox used for this analysis (Fig. 24) consists of 2 stages with a single mesh spur reduction followed by a 5-planet planetary gearbox consisting of 11 rolling-element bearings and 9 spur gears [86]. The first stage consists of the input pinion gear meshing with the main drive gear. The second

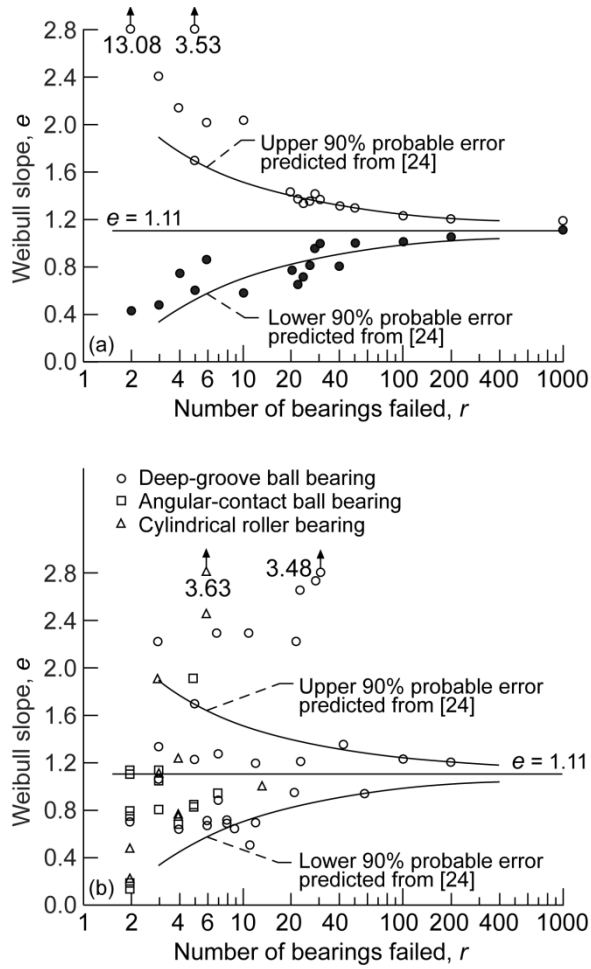


**Figure 23.** Variation of Weibull slope *e* compared with predicted 90% probable error. (a) Extremes of Weibull slope from Monte Carlo testing for each group of 10 bearing trials of *r* bearings (data from [83]). (b) Weibull slopes from 51 sets of ball and roller bearings (data from [84] and [85]).

stage is provided by the fixed-ring planetary gear driven by a floating sun gear as input with a five-planet carrier as output. At cruise conditions, the input pinion speed is constant at 13,820 rpm, producing a carrier output speed of 1021 rpm. A list of the component parts of the gearbox is given in Table 10.

A typical mission profile for this commercial gearbox is given in Table 11, which presents the duration as a percentage and the propeller shaft power for each flight condition. This profile includes loads for (a) takeoff, (b) climb, (c) cruise, and (d) descent. The cruise segment of the profile consumes 68 percent of the flight time with a little less than half of the power required for the takeoff, which lasts for less than 3 percent of the flight time [87].

The cause for removal can be assumed to be one or more bearings or gears that had fatigue or damage resulting in wear and/or vibration detected by magnetic chip

detectors and/or vibration pickups. The gearbox is removed from service before secondary damage occurs and is inspected. After the failed part or parts are replaced, the gearbox is put back into service [87].

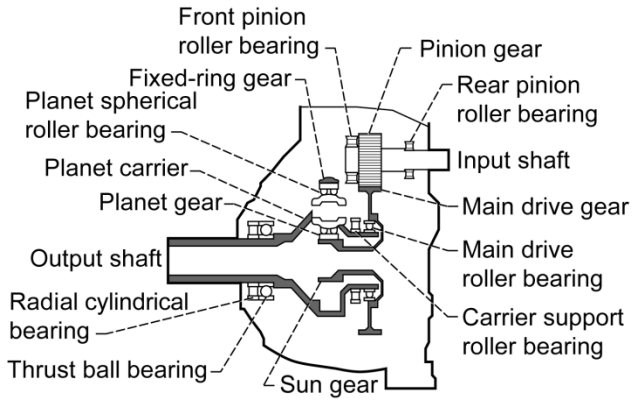


**Figure 24.** Commercial turboprop gearbox [87].

**Table 10.** Predicted turboprop gearbox component lives from Lundberg-Palmgren analysis with life factors and strict-series system reliability [87].

| Component description (see Fig. 24) | Predicted life, hr | | Weibull slope, $e$ |
|---|---|---|---|
| | $L_{10}$ | $L_{50}$ | |
| Rolling-element bearings | | | |
| Cylindrical roller bearings | | | |
| Front pinion | 20,890 | 111,476 | 1.125 |
| Rear pinion | 21,312 | 113,728 | ↓ |
| Main drive | 26,459 | 141,194 | |
| Carrier support | 312,881 | 1,669,635 | |
| Propeller radial | 68,194 | 363,905 | |
| Propeller thrust ball bearing | 33,065 | 180,484 | 1.11 |
| Planet double-row spherical roller bearing set, five bearings | 844 | 4,503 | 1.125 |
| Bearing system life | 774 | 4,132 | 1.125 |
| Gears | | | |
| Pinion | 53,477 | 131,552 | 2.5 |
| Ring | 4,540,212 | 11,168,760 | ↓ |
| Sun | 19,033 | 46,821 | |
| Main drive | 108,148 | 266,040 | |
| Planet gear set, five gears | 28,092 | 69,105 | |
| Gear system life | 16,680 | 44,032 | 2.5 |
| Gearbox life | 774 | 4,132 | 1.125 |

**Table 11.** Mission profile of commercial turboprop gearbox [87].

| Mission segment | Percent time of segment | Propeller shaft power, kW (hp) |
|---|---|---|
| Takeoff | 2.84 | 3132 (4200) |
| Climb | 17.02 | 2461 (3300) |
| Cruise | 68.08 | 1516 (2033) |
| Descent | 12.06 | 945 (1267) |
| Equivalent | 100.00 | 1833 (2457) |

Individual failure occurrences are not predictable but are probabilistic. No two gearboxes run under the same conditions fail necessarily from the same cause and/or at the same time. At a given probability of survival, the life of the gearbox system will always be less than that of the lowest lived element in it.

Historical field data for 64 gearboxes were collected. The first part of these data covered the time from their field installation and first field operation to their removal for cause (failure) and refurbishment [87].

## Analysis

### Bearing life analysis

Equations based on the Lundberg-Palmgren model with life modifying factors [18] were used to calculate bearing lives in Table 10 and shown in Fig. 25(a). Equation (48) can be rewritten to include the bearing life modifying factors [18] as follows:

$$L = a_1 a_2 a_3 L_{10} = a_1 a_2 a_3 \left[ \frac{C_D}{P_{eq}} \right]^p \tag{89}$$

where $a_1$ is a reliability factor, $a_2$ is a materials and processing factor, and $a_3$ is an operating conditions factor such as lubrication [18]. Table 12 contains a list of representative variables affecting bearing life that contribute to these factors [18]. For the purpose of the bearing life analysis summarized in Table 10, for ball bearings $p \leq 3$, and for roller bearings $p = 4$ [87].

The $L_{10}$ life of a single double-row spherical bearing is 3529 hr. The system $L_{10}$ life for the five-bearing planetary set is 774 hr. For all the bearings in the gearbox, the bearing system $L_{10}$ life is also predicted to be 774 hr [87].

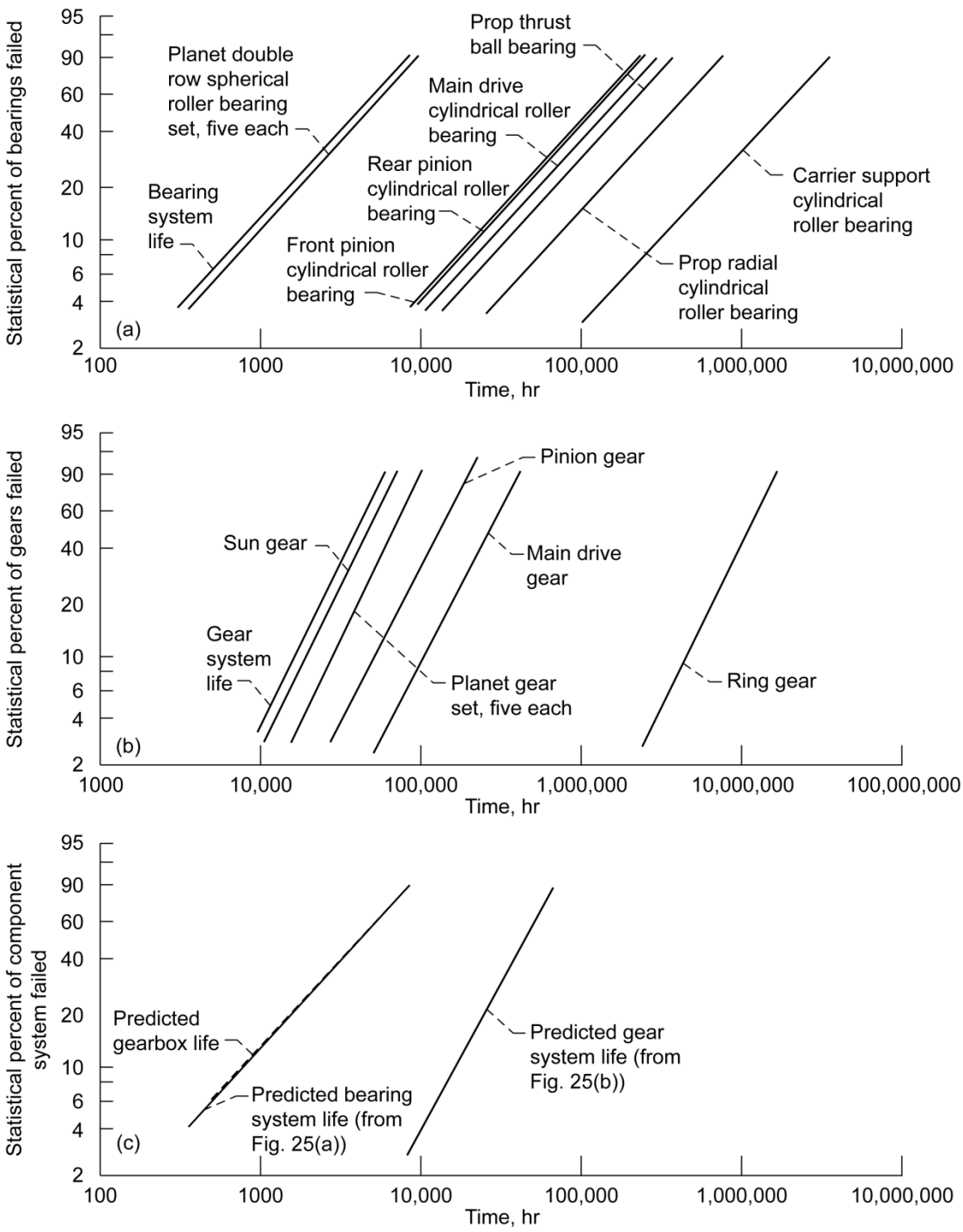


**Figure 25.** Weibull plots of predicted lives for commercial turboprop gearbox and its respective bearing gear components using Lundberg-Palmgren life theory [87]. (a) Bearing component lives. (b) Gear component lives. (c) Gearbox life and component lives.

**Table 12.** Representative variables affecting bearing life and reliability [18].

| Life adjustment factor | Variable |
|---|---|
| Reliability, $a_1$ | Probability of failure |
| Materials and processing, $a_2$ | Bearing steel<br>Material hardness<br>Residual stress<br>Melting process<br>Metal working |
| Operating conditions, $a_3$ | Load<br>Misalignment<br>Housing clearance<br>Axially loaded cylindrical bearings<br>Rotordynamics<br>Hoop stresses<br>Speed<br>Temperature<br>Steel<br>Lubrication<br>Lubricant film thickness<br>Surface finish<br>Water<br>Oil<br>Filtration |

## Gear life analysis

Between 1975 and 1981, Coy, Townsend, and Zaretsky [88 to 90] published a series of papers developing a methodology for calculating the life of spur and helical gears based upon the Lundberg-Palmgren theory and methodology for rolling-element bearings. Townsend, Coy, and Zaretsky [48] reported that for AISI 9310 spur gears, the Weibull slope $e$ is 2.5. Based on Eq. (20), for all gears except a planet gear, the gear life can be written as

$$L_{10_G} = \frac{N^{-1/e_G}\left(\eta_{10_t}\right)}{k} \tag{90}$$

For a planet gear, the life is

$$L_{10_G} = \frac{N^{-1/e_G}\left(\eta_{10_{t1}}^{-e_G} + \eta_{10_{t2}}^{-e_G}\right)^{-1/e_G}}{k} \tag{91}$$

The $L_{10}$ life in millions of stress cycles of a single gear tooth can be written as

$$\eta_{10_t} = a_2 a_3 \left( \frac{C_t}{P_t} \right)^{p_G} \tag{92}$$

where

$$C_t = B f^{0.907} \rho^{-1.165} l^{-0.093} \tag{93}$$

and

$$\rho = \left( \frac{1}{r_1} + \frac{1}{r_2} \right) \frac{1}{\sin \varphi} \tag{94}$$

The value for $\eta_{10_t}$ can be determined by using Eq. (92) where for bearings $C_t$ is the basic load capacity of the gear tooth, $P_t$ is the normal tooth load, $p_G$ is the load-life exponent usually taken as 4.3 for gears based on experimental data for AISI 9310 steel, and $a_2$ and $a_3$ are life adjustment factors similar to those for rolling-element bearings. The value for $C_t$ can be determined by using Eq. (93), where $B$ is a material constant that is based on experimental data and is approximately equal to $1.39\times10^8$ when calculating $C_t$ in SI units (Newtons and meters) and is 21,800 in English units (pounds and inches) for AISI 9310 steel spur gears. Also, $f$ is the tooth width, and $\rho$ is the curvature sum at the start of single-tooth contact.

The $L_{10_G}$ life of the gear (all teeth) in millions of input shaft revolutions at which 90 percent will survive can be determined from Eq. (90) or (91) where $N$ is the total number of teeth on the gear, $e_G$ is the Weibull slope for the gear and is assumed to be 2.5 (from [48]), and $k$ is the number of load (stress) cycles on a gear tooth per input shaft revolution.

For all gears except the planet gears, each tooth will see a load on only one side of its face for a given direction of input shaft rotation. However, each tooth on a planet gear will see contact on both sides of its face for a given direction of input shaft rotation. One side of its face will contact a tooth on the sun gear, and the other side of its face will contact a tooth on the ring gear. This results in reverse bending of the gear teeth on the planetary gears. Since the gears are operated at bending stresses less than those that may cause bending fatigue in carburized gear steels, this effect is ignored. However, for purposes of contact fatigue, Eq. (91) takes into account that both sides of the gear tooth are stressed, where $\eta_{10_{t1}}$ is the $L_{10}$ life in millions of stress cycles of a planet tooth meshing with the

sun gear, and $\eta_{10_{t2}}$ is the $L_{10}$ life in millions of stress cycles of a planet tooth meshing with the ring gear.

The calculated gear lives are summarized in Table 10 and shown in the Weibull plots of Fig. 25(b). The gear system predicted $L_{10}$ life is 16,680 hr [87].

## Gearbox system life

The $L_{10}$ lives of the individual bearings and gears that make up a rotating machine are calculated for each condition of their operating profiles. For each component, the resulting lives from each of the operating conditions are combined using the linear damage (Palmgren-Langer-Miner) rule, Eq. (14).

The resultant lives of each of the gearbox components are then combined to determine the calculated system $L_{10}$ life using the two-parameter Weibull distribution function (Eq. (17)) for the bearings and gears comprising the system and strict-series system reliability (Eq. (49a)) as follows:

$$\frac{1}{L_{sys}^{e}} = \sum_{i=1}^{n} \frac{1}{L_{n}^{e}} = \left( \frac{1}{L_{1}^{e}} + \frac{1}{L_{2}^{e}} + \ldots \frac{1}{L_{n}^{e}} \right) \tag{95a}$$

The resultant system lives previously discussed for the bearings and gears are shown in Figs. 25(a) and (b), respectively, and summarized in Table 10.

The system Weibull slope using strict-series reliability (Eq. (95a)) where each component or combinations of multiple bearings and gears have different Weibull slopes is not intuitively obvious. If at each time sequence the probability of survival of each component is multiplied together, the system reliability at that time and, hence, the probability of failure can be determined. When these values are plotted on Weibull paper, a Weibull slope (shape parameter) can be determined for the system life distribution using a least squares fit. When this is done, it is found that the system Weibull slope approximates that of the lowest lived component in the system. For the gearbox, where the subscripts $B$ and $G$ relate the $L_{10}$ life to a bearing or a gear, respectively,

$$\frac{1}{L_{sys}^{e}} = \left( \frac{1}{L_{B_1}^{eB}} + \frac{1}{L_{B_2}^{eB}} + \ldots \frac{1}{L_{B_n}^{eB}} \right) + \left( \frac{1}{L_{G_1}^{eG}} + \frac{1}{L_{G_2}^{eG}} + \ldots \frac{1}{L_{G_n}^{eG}} \right) \tag{95b}$$

The lowest lived components in the gearbox are the roller bearings. As a result, the Weibull slope assumed for the planetary gear spherical roller bearings is

assumed to be the Weibull slope $e$ of the entire gearbox system in Eq. (95b). The individual system and combined system lives are shown in the Weibull plots of Fig. 25(c) and summarized in Table 10. The predicted $L_{10}$ life of the gearbox is 774 hr [87].

## Gearbox field data

The application of the Lundberg-Palmgren model [9] to predict gearbox life and reliability needs to be benchmarked and verified under a varied load and operating profile. The cost and time to laboratory test a statistically significant number of gearboxes to determine their life and reliability is prohibitive. A practical solution to this problem is to benchmark the analysis to field data. Fortunately, these data were available for the commercial turboprop gearbox used in this study.

No two gearboxes are expected to operate in exactly the same manner. Flight variables include operating temperature and load. Small variations in operational load can result in significant changes in life. Hence, the accuracy of the calculations is dependent on how close the defined mission profile is to actual flight operation.

The condition of the gearboxes is monitored, and they are removed from service upon the detection of a perceived component failure. At the time of removal, the gearboxes are functional. The removal precludes secondary damage; that is, the damage is limited to the failed component.

Field data were collected for 64 new commercial turboprop gearboxes. From these field data, the resultant time to removal of each gearbox is presented in the Weibull plot of Fig. 26. The failure index was 59 out of 64. That is, 59 out of the 64 gearboxes removed from service were considered failed. For these data, there was no breakdown of the cause for removal or the percent of each component that had failed. The resultant $L_{10}$ life from the field data was 5627 hr and the Weibull slope $e$ was 2.189. Using the Lundberg-Palmgren method (above), the predicted $L_{10}$ life was 774 hr and the Weibull slope $e$ was 1.125. The field data suggest that the $L_{10}$ life of the gearbox was underpredicted by a factor of 7.56 [87].

## Reevaluation of bearing load-life exponent *p*

Although errors in the assumed operating profile of the gearbox may account for the difference between actual and predicted life, it is suggested that using the Lundberg-Palmgren equations results in a life prediction that is too low for the bearings.

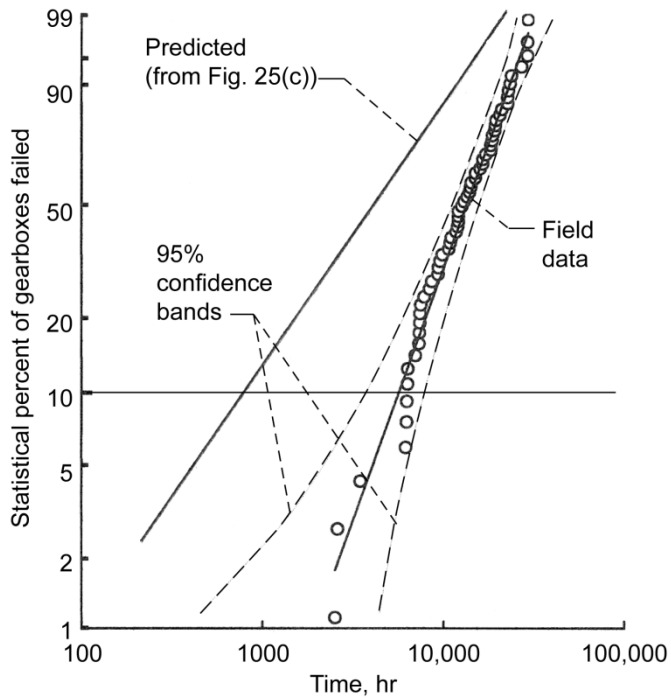


**Figure 26.** Weibull plot of field data for lives of turboprop gearboxes compared with predicted lives using Lundberg-Palmgren life model. Failure index, 59 out of 64 [87].

With reference to Eq. (48), in their 1952 publication [10], Lundberg and Palmgren proposed a load-life exponent $p$ = 10/3 for roller bearings, where one raceway has point contact and the other raceway has line contact. The 10/3 load-life exponent has been incorporated in the ANSI/ABMA and ISO standards first published in 1953 [12 to 14]. Their assumption of point and line contact may have been correct for many types of roller bearings in use at that time. However, it is no longer the case for most roller bearings manufactured today, and most certainly not for cylindrical roller bearings. The analysis employed for the bearing life calculations used a value of $p$ = 3 for ball bearings and $p$ = 4 for roller bearings. Poplawski, Peters, and Zaretsky [91,92] suggest the use of $p$ = 4 for ball bearings and $p$ = 5 for roller bearings [87].

From Eq. (95b), assuming that the bearing system, which is the shortest lived component in the gearbox and has the same Weibull slope as that of the gearbox system (i.e., $e$ = 2.189),

$$\frac{1}{L_{sys}^{e_s}} = \frac{1}{L_B^{e_B}} + \frac{1}{L_G^{e_G}} \tag{96a}$$

and substituting in the known values

$$\frac{1}{(5627)^{2.189}} = \frac{1}{L_B^{2.189}} + \frac{1}{(16,680)^{2.5}} \tag{96b}$$

and solving for the bearing system life, results in a value of

$$L_B = 5627\text{hr} \tag{96c}$$

From Lundberg-Palmgren [9], the predicted bearing system life is

$$L_B \sim \left(\frac{C_D}{P_{eq}}\right)^4 \sim 774 \text{ hr} \tag{97a}$$

then,

$$\left(\frac{C_D}{P_{eq}}\right) \sim 5.27 \tag{97b}$$

Calculating a revised value for the load-life exponent $p$ for the gearbox bearings based on the actual bearing system life of 5627 hr,

$$\left(\frac{C_D}{P_{eq}}\right)^p \sim (5.27)^p \sim 5627 \text{ hr} \tag{98a}$$

Solving for load-life exponent $p$,

$$p = 5.2 \tag{98b}$$

Referring to Eq. (43c), for line contact (roller bearing) the Hertz stress-life exponent $n = 2p$. From Eq. (98b), $n = 10.4$ for line contact for the turboprop gearbox data. Referring to the Zaretsky model for line contact, Eq. (62b), the shear stress-life exponent is

$$c = n - \frac{1}{e} \tag{99a}$$

and where $n = 10.4$ and $e = 2.189$,

$$c = 10.4 - \frac{1}{2.189} = 9.943 \tag{99b}$$

Using the value of $c$ from Eq. (99b) in Eq. (62a) for point contact where $e$ is assumed to equal 1.11, then

$$n = c + \frac{2}{e} = 9.943 + \frac{2}{1.11}$$

$$= 11.74 \tag{100a}$$

and for point contact,

$$p = \frac{n}{3} = \frac{11.74}{3} = 3.91 \tag{100b}$$

The apparent load-life exponent $p$ for the roller bearings is equal to 5.2 and correlates with the Zaretsky model. Were the roller bearing lives to be recalculated using a load-life exponent $p$ = 5.2, the predicted $L_{10}$ life of the gearbox would be equal to the actual life obtained in the field, 5627 hr. It should be noted that if an exponent $p$ = 5 were used, the predicted $L_{10}$ life of the gearbox would be 4065 hr. This result suggests a strong reliance of the predicted bearing life upon the load-life exponent $p$. The values of the load-life exponent $p$ for roller bearings equal to 10/3 from the ANSI/ABMA and ISO standards [12,14] and 4 from computer codes may provide predicted roller bearing lives that are too conservative for design purposes. The use of the ANSI/ABMA and ISO standards load-life exponent of 10/3 to predict roller bearing life is not reflective of modern roller bearings. It will underpredict bearing lives.

## Appendix A – Derivation of Weibull distribution function

According to Weibull [6,7] and as presented in [93] (also see [91]), any distribution function can be written as

$$F(X) = 1 - \exp - [f(X)] \tag{A1}$$

where $F(X)$ is the probability of an event (failure) occurring and $f(X)$ is a function

of an operating variable $X$. Conversely, from Eq. (A1) the probability of an event not occurring (survival) can be written as

$$1 - F(X) = \exp - [f(X)] \tag{A2a}$$

or

$$1 - F = \exp - [f(X)] \tag{A2b}$$

where $F = F(X)$ and $(1 - F) = S$, the probability of survival.

If there are $n$ independent components, each with a probability of the event (failure) not occurring $(1 - F)$, the probability of the event not occurring in the combined total of all components can be expressed from Eq. (A2b) as

$$1 - F^n = \exp - [nf(X)] \tag{A3}$$

Equation (A3) gives the appropriate mathematical expression for the principle of the weakest link in a chain or, more generally, for the size effect on failures in solids. The application of Eq. (A3) is illustrated by a chain consisting of several links. Testing finds the probability of failure $F$ at any load $X$ applied to a "single" link. To find the probability of failure $F_n$ of a chain consisting of $n$ links, one must assume that if one link has failed the whole chain fails. That is, if any single part of a component fails, the whole component has failed. Accordingly, the probability of nonfailure of the chain $(1–F_n)$, is equal to the probability of the simultaneous nonfailure of all the links. Thus,

$$1 - F_n = (1 - F)^n \tag{A4a}$$

or

$$S_n = S^n \tag{A4b}$$

Where the probabilities of failure (or survival) of each link are not necessarily equal (i.e., $S_1 \neq S_2 \neq S_3 \neq \ldots$), Eq. (A4b) can be expressed as

$$S_n = S_1 \cdot S_2 \cdot S_3 \cdot \ldots \tag{A4c}$$

This is the same as Eq. (18) of the main text.

From Eq. (A3) for a uniform distribution of stresses σ throughout a volume $V$,

$$F_v = 1 - \exp - \left[ V f(\sigma) \right] \tag{A5a}$$

or

$$S = 1 - F_v = \exp - \left[ V f(\sigma) \right] \tag{A5b}$$

Equation (A5b) can be expressed as follows:

$$\ln \ln \left[ \frac{1}{S} \right] = \ln f(\sigma) + \ln V \tag{A6}$$

It follows that if ln ln (1/$S$) is plotted as the ordinate and ln$f$(σ) as the abscissa in a system of rectangular coordinates, a variation of volume $V$ of the test specimen will imply only a parallel displacement but no deformation of the distribution function. Weibull [6] assumed the form

$$f(\sigma) = \left[ \frac{\sigma - \sigma_u}{\sigma_\beta - \sigma_u} \right]^e \tag{A7}$$

Where $e$ is the Weibull slope, σ is a stress at a given probability of failure, $\sigma_u$ is a location parameter below which stress no failure will occur, and $\sigma_\beta$ is the characteristic stress at which 63.2 percent of the population will fail, Eq. (A6) becomes

$$\ln \ln \left[ \frac{1}{S} \right] = e \ln(\sigma - \sigma_u) - e \ln(\sigma_\beta - \sigma_u) + \ln V \tag{A8}$$

If the location parameter $\sigma_u$ is assumed to be zero, and $V$ is normalized whereby ln $V$ is zero, Eq. (A8) can be written as

$$\ln \ln \left[ \frac{1}{S} \right] = e \ln \left[ \frac{\sigma}{\sigma_\beta} \right] \quad \text{where } 0 < \sigma < \infty \text{ and } 0 < S < 1 \tag{A9}$$

Equation (A9) is identical to Eq. (17) of the main text.

The form of Eq. (A9) where $\sigma_u$ is assumed to be zero is referred to as "two-parameter Weibull." Where $\sigma_u$ is not assumed to be zero, the form of the equation is referred to as "three-parameter Weibull."

## Appendix B – Derivation of strict series reliability

As discussed and presented in [91] and [93], G. Lundberg and A. Palmgren [9] in 1947, using the Weibull equation for rolling-element bearing life analysis, first derived the relationship between individual component lives and system life. The following derivation is based on but is not identical to the Lundberg-Palmgren analysis.

Referring to Fig. 1(a), from Eq. (A9) in Appendix A, the Weibull equation can be written as

$$\ln \ln\left[\frac{1}{S_{\text{sys}}}\right] = e \ln\left[\frac{L}{L_\beta}\right] \tag{B1}$$

where $L$ is the number of cycles to failure at a given system reliability $S_{\text{sys}}$, and $L_\beta$ is the characteristic life at which 63.2 percent of the population has failed.

Figure 27 is a sketch of multiple Weibull plots where each Weibull plot represents a cumulative distribution of each component in the system. The system Weibull plot represents the combined Weibull plots 1, 2, 3, and so forth. All plots are assumed to have the same Weibull slope $e$ [91]. The slope $e$ can be defined as follows:

$$e = \frac{\ln \ln\left[\frac{1}{S_{\text{sys}}}\right] - \ln \ln\left[\frac{1}{S_{\text{ref}}}\right]}{\ln L - \ln L_{\text{ref}}} \tag{B2a}$$

or

$$\frac{\ln\left[\dfrac{1}{S_{\text{sys}}}\right]}{\ln\left[\dfrac{1}{S_{\text{ref}}}\right]} = \left[\frac{L}{L_{\text{ref}}}\right]^{e} \tag{B2b}$$

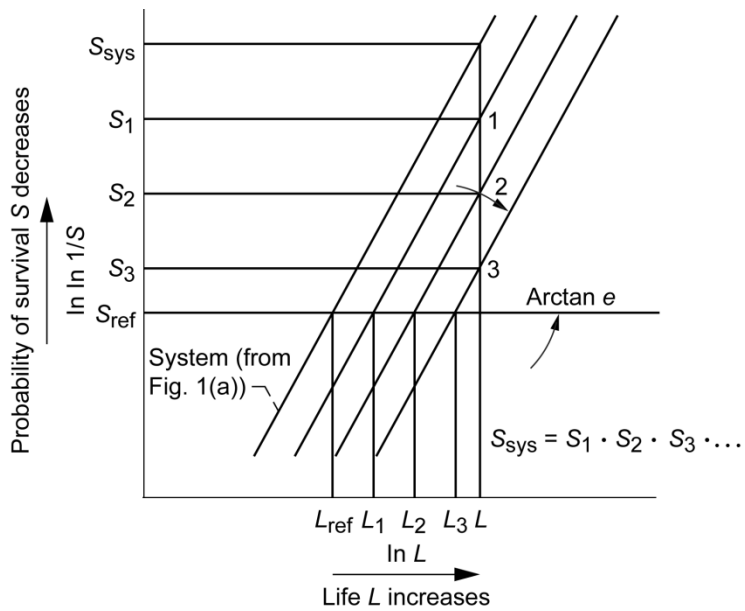


**Figure 27.** Sketch of multiple Weibull plots where each numbered plot represents cumulative distribution of each component in system and system Weibull plot represents combined distribution of plots 1, 2, 3, etc. (all plots are assumed to have same Weibull slope *e*) [91].

From Eqs. (B1) and (B2b),

$$\ln\left[\frac{1}{S_{\text{sys}}}\right] = \left[\ln\frac{1}{S_{\text{ref}}}\right]\left[\frac{L}{L_{\text{ref}}}\right]^{e} = \left[\frac{L}{L_{\beta}}\right]^{e} \tag{B3}$$

and

$$S_{\text{sys}} = \exp - \left[\frac{L}{L_{\beta}}\right]^{e} \tag{B4}$$

where $S_{sys} = S$ in Eq. (B1). For a given time or life $L$, each component or stressed volume in a system will have a different reliability $S$. From Eq. (A4c) for a series reliability system

$$S_{sys} = S_1 \cdot S_2 \cdot S_3 \cdot \ldots \tag{B5}$$

Combining Eqs. (B4) and (B5) gives

$$\exp - \left[ \frac{L}{L_\beta} \right]^e = \exp - \left[ \frac{L}{L_{\beta 1}} \right]^e \times \exp - \left[ \frac{L}{L_{\beta 3}} \right]^e \times \ldots \tag{B6a}$$

$$\exp - \left[ \frac{L}{L_\beta} \right]^e = \exp - \left\{ \left[ \frac{L}{L_{\beta 1}} \right]^e + \left[ \frac{L}{L_{\beta 2}} \right]^e + \left[ \frac{L}{L_{\beta 3}} \right]^e + \ldots \right\} \tag{B6b}$$

It is assumed that the Weibull slope $e$ is the same for all components. From Eq. (B6b)

$$- \left[ \frac{L}{L_\beta} \right]^e = - \left\{ \left[ \frac{L}{L_{\beta 1}} \right]^e + \left[ \frac{L}{L_{\beta 2}} \right]^e + \left[ \frac{L}{L_{\beta 3}} \right]^e + \ldots \right\} \tag{B7a}$$

Factoring out $L$ from Eq. (B7a) gives

$$\left[ \frac{1}{L_\beta} \right]^e = \left[ \frac{1}{L_{\beta 1}} \right]^e + \left[ \frac{1}{L_{\beta 2}} \right]^e + \left[ \frac{1}{L_{\beta 3}} \right]^e + \ldots \tag{B7b}$$

From Eq. (B3) the characteristic lives $L_{\beta 1}$, $L_{\beta 2}$, $L_{\beta 3}$, etc., can be replaced with the respective lives $L_1$, $L_2$, $L_3$, etc., at $S_{ref}$ (or the lives of each component that have the same probability of survival $S_{ref}$) as follows:

$$\left[ \ln \frac{1}{S_{ref}} \right] \left[ \frac{1}{L_{ref}} \right]^e = \left[ \ln \frac{1}{S_{ref}} \right] \left[ \frac{1}{L_1} \right]^e + \left[ \ln \frac{1}{S_{ref}} \right] \left[ \frac{1}{L_2} \right]^e + \left[ \ln \frac{1}{S_{ref}} \right] \left[ \frac{1}{L_3} \right]^e + \ldots \tag{B8}$$

where, in general, from Eq. (B3)

$$\left[\frac{1}{L_\beta}\right]^e = \left[\ln\frac{1}{S_{\text{ref}}}\right]\left[\frac{1}{L_{\text{ref}}}\right]^e \tag{B9a}$$

and

$$\left[\frac{1}{L_{\beta 1}}\right]^e = \left[\ln\frac{1}{S_{\text{ref}}}\right]\left[\frac{1}{L_1}\right]^e, \text{etc.} \tag{B9b}$$

Factoring out ln $(1/S_{\text{ref}})$ from Eq. (B8) gives

$$\left[\frac{1}{L_{\text{ref}}}\right] = \left\{\left[\frac{1}{L_1}\right]^e + \left[\frac{1}{L_2}\right]^e + \left[\frac{1}{L_3}\right]^e + \ldots\right\}^{1/e} \tag{B10}$$

or rewriting Eq. (B10) results in

$$\left[\frac{1}{L}\right]^e = \sum_{i=1}^{n}\left[\frac{1}{L_i}\right]^e \tag{B11}$$

Equation (B11) is identical to Eqs. (47) and (49a) of the text.

# Appendix C – Contact (Hertz) stress

The contact (Hertz) stresses at the respective races of a bearing are a function of the bearing geometry, the normal load at the contact, and the elastic properties of the bearing materials. Jones [29] relates the Hertz contact theory for the stresses of nonconforming bodies in contact for both ball and roller bearings. From Jones, the following relations for the maximum Hertz stresses $S_{\max}$ at the inner and outer races of ball bearings can be derived:

1. For deep-groove ball bearings with a radial load only,

$$S_{\max_{or}} = \frac{K\left[\frac{2}{D_{or}} + \frac{4}{d} - \frac{1}{f_{or}d}\right]^{2/3} P_{\max}^{1/3}}{\mu v} \tag{C1a}$$

for the outer race, and

$$S_{\max_{ir}} = \frac{K\left[\frac{2}{D_{ir}} + \frac{4}{d} - \frac{1}{f_{ir}d}\right]^{2/3} P_{\max}^{1/3}}{\mu v} \tag{C1b}$$

for the inner race, where

$$P_{\max} = W_r \frac{5}{Z} \tag{C2}$$

2. For angular-contact ball bearings with a thrust load only,

$$S_{\max_{or}} = \frac{K\left[\frac{2\cos\beta}{d_e + d\cos\beta} + \frac{4}{d} - \frac{1}{f_{or}d}\right]^{2/3} P_N^{1/3}}{\mu v} \tag{C3a}$$

for the outer race, and

$$S_{\max_{ir}} = \frac{K\left[\frac{2\cos\beta}{d_e - d\cos\beta} + \frac{4}{d} - \frac{1}{f_{ir}d}\right]^{2/3} P_N^{1/3}}{\mu v} \tag{C3b}$$

for the inner race, where

$$P_N = \frac{Wt}{Z}\frac{1}{\sin\beta} \tag{C4}$$

3. For roller bearings with a radial load only

$$S_{\max_{or}} = K\sqrt{\frac{P_{\max}}{\ell}\left(\frac{-2}{D_{or}}+\frac{2}{d}\right)} \tag{C5a}$$

for the outer race, and

$$S_{\max_{ir}} = K\sqrt{\frac{P_{\max}}{\ell}\left(\frac{2}{D_{ir}}+\frac{2}{d}\right)} \tag{C5b}$$

for the inner race, where

$$P_{\max} = W_r\,\frac{4}{Z} \tag{C6}$$

for

| | |
|---|---|
| $D_{or}$ | outer-race diameter |
| $D_{ir}$ | inner-race diameter |
| $d$ | ball diameter |
| $d_e$ | pitch diameter |
| $f_{or}, f_{ir}$ | outer- and inner-race conformity, respectively |
| $W_r$ | radial load |
| $P_{\max}$ | normal load on maximum loaded ball |
| $\mu$, $\nu$ | transcendental functions [29] |
| $K$ | constant based on elastic properties of bearing steel |
| $P_N$ | normal ball load |
| $W_t$ | bearing thrust load |
| $\beta$ | contact angle |
| $\ell$ | effective roller length |

For bearing steel on bearing steel, $K = 1.58\times10^{-3}$ for $S_{\max}$ in GPa and $K = 23.58$ for $S_{\max}$ in ksi. The values for the transcendental functions $\mu$ and $\nu$ vary with conformity $f$ and are found in [29]. Values of their product $\mu\nu$ can be found in Table 4.

# References


1. Stribeck, R., 1900. Reports from the central laboratory for scientific investigation. Translation by H. Hess, 1907, *ASME Trans*., **29**, 420–466.
2. Goodman, J., 1912. Roller and ball bearings. *Proc. Inst. Civil Engrs*., **189**, 82–166.
3. Colvin, F.H., and Stanley, F.A., 1914. *American Machinist Handbook and Dictionary of Shop Terms*, 2nd ed., McGraw-Hill, New York, pp. 381–386.
4. Palmgren, A., 1924. Die Lebansdauer von Kugellagern (The Service Life of Ball Bearings). *Zeitschrift des Vereines Deutscher Ingenieure*, **68**, 14, 339–341 (NASA TT–F–13460, 1971).
5. Palmgren, A., 1945. *Ball and Roller Bearing Engineering*, 1st ed., Translation by G. Palmgren and B. Ruley, SKF Industries, Philadelphia, PA.
6. Weibull, W., 1939. A statistical theory of the strength of materials. *Inginiors Vetenskaps Adademien* (Proc. Royal Swedish Academy of Engr.), 151.
7. Weibull, W., 1939. The phenomenon of rupture. *Inginiors Vetenskaps Adademien* (Proc. Royal Swedish Academy of Engr.), 153.
8. Thomas, H.R., and Hoersch, V.A., 1930. Stresses due to the pressure of one elastic solid upon another with special reference to railroad wheels. Bulletin 212, Engineering Experimental Station, Univ. of Illinois, Urbana.
9. Lundberg, G., and Palmgren, A., 1947. Dynamic capacity of rolling bearings. *Acta Polytechnica Mechanical Engineering Series*, **1**, 3, Stockholm, Sweden.
10. Lundberg, G., and Palmgren, A., 1952. Dynamic capacity of roller bearings. *Acta Polytechnica Mechanical Engineering Series*, **2**, 4, Stockholm, Sweden.
11. Hertz, H., 1881. Uber die beruehrung elasticher koerper (On contact of elastic bodies). *Gesammelte Werke* (*Collected Works*), 1, Leipzig, Germany.
12. ISO 281:1990(E), 1990. Rolling bearing – Dynamic load ratios and rating life. International Organization for Standards, Geneva.
13. ANSI/AFBMA 9–1990, 1990. Load rating and fatigue life for ball bearings. The Anti-Friction Bearing Manufacturers Association, Washington, DC, USA.
14. ANSI/AFBMA 11–1990, 1990. Load rating and fatigue life for roller bearings. The Anti-Friction Bearing Manufacturers Association, Washington, DC, USA.
15. Zaretsky, E.V., 1997. *Tribology for Aerospace Applications*, STLE SP–37, Society of Tribologists and Lubrication Engineers, Park Ridge, IL, USA.
16. Ertel, A.M., 1939. Hydrodynamic lubrication based on new principles. Prikadnaya Matematika I Mechanika, **3**, 2 (in Russian).
17. Grubin, A.N., 1949. Fundamentals of the hydrodynamic theory of lubrication of heavily loaded cylindrical surfaces. *Investigation of the Contact Machine Components,* Kh. F. Ketova, ed., translation of Russian Book No. 30, Central Scientific Institute of Technology and Mechanical Engineering, Moscow (Available from Dept. of Scientific and Industrial Research, Great Britain, Trans. CTS–235, and from Special Libraries Association, Chicago. Transl. R-3554).
18. Zaretsky, E.V., 1992. *STLE life factors for rolling bearings*, STLE SP–34, Society of Tribologists and Lubrication Engineers, Park Ridge, IL, USA.

19. Styri, H., 1951. Investigators of rolling bearings at SKF Industries, Inc., Review of current and anticipated lubricant problems in turbojet engines. NACA Subcommittee on Lubrication and Wear, NACA RM 51D20, pp. 30–39.
20. Zaretsky. E.V., 1998. A Palmgren revisited – A basis for bearing life prediction. *Lubrication Engineering*, *J. STLE*, **54**(2), 18–24.
21. Anderson, W.J., 1964. Fatigue in rolling-element bearings. Advanced Bearing Technology, E.E. Bisson and W.J. Anderson, ed., NASA SP–38, pp. 371–450.
22. Langer, B.F., 1937. Fatigue failure from stress cycles of varying amplitude. *ASME J. Applied Mechanics*, **59**, A160–A162.
23. Miner, M.A., 1945. Cumulative damage in fatigue. *ASME J. Applied Mechanics*, **12**(3), A159–A164.
24. Johnson, L.G., 1964. *The Statistical Treatment of Fatigue Experiments*. Elsevier Publishing Co., Amsterdam, The Netherlands.
25. Tallian, T.E., 1962. Weibull distribution of rolling contact fatigue and deviations therefrom. *ASLE Trans.*, **5**(1), 183–196.
26. Weibull, W., 1951. A statistical distribution of wide applicability. *J. Applied Mechanics*, **18**(3), 292–297.
27. Weibull, W., 1962. Efficient methods for estimating fatigue life distribution of rolling bearings. *Rolling Contact Phenomenon*, (ed.: J.B. Bidwell), Elsevier, New York, NY, USA, pp. 252–265.
28. Zaretsky, E.V., Poplawski, J.V., and Peters, S.M., 1996. Comparison of life theories for rolling-element bearings. *STLE Trans.*, **39**(2), 237–248.
29. Jones, A.B., 1946. New departure – Analysis of stresses and deflections, vols. 1 and 2, New Departure Div., Gen. Motors Corp., USA.
30. Palmgren, A., 1959. *Ball and Roller Bearing Engineering*, 3rd ed., Translation by G. Palmgren and A. Palmgren, SKF Industries, Philadelphia, PA, USA.
31. Zaretsky, E.V., Poplawski, J.V., and Root, L.E., 2007. Reexamination of ball-race conformity effects on ball bearing life. *Trib. Trans.*, **50**(3), 336–349.
32. Ioannides, E., and Harris, T.A., 1985. A new fatigue life model for rolling bearings. *J. Tribol., Trans. ASME*, **107**(3), 367–378.
33. Tosha, K., Ueda, D., Shimoda, H., and Shimizu, S., 2008. A study on P–S–N curve for rotating bending fatigue test for bearing steel. *Tribology Trans*., **46**(4), 166–172.
34. ASME Tribology Division, 2003, Life Ratings for Modern Rolling Bearings: A Design Guide for the Application of International Standard ISO 281/2, *American Society of Mechanical Engineers*, New York, NY, USA.
35. ISO 281:1990/Amd 1 and 2:2000, 2002. *Rolling Bearings – Dynamic Load Ratings*. International Organization for Standardization, Geneva, Switzerland.
36. ISO 281:2007, 2007. *Rolling Bearings – Dynamic Load Ratings and Rating Life*. International Organization for Standardization, Geneva, Switzerland.
37. Ioannides, E., Bergling, G., and Gabelli, A., 1999. An analytical formulation for the life of rolling bearings. *Acta Polytechnica Scandinavica*, Mechanical Engineering Series, **137**, Finland.
38. Zaretsky, E.V., 1987. Fatigue criterion to system design, life and reliability. *AIAA Journal of Propulsion and Power*, **107**(3), 76–83.
39. Zaretsky, E.V., 1994. Design for life, plan for death. *Machine Design*, **66**(15), 55–59.

40. Vlcek, B.L., Hendricks, R.C., and Zaretsky, E.V., 2003. Determination of rolling-element fatigue life from computer generated bearing tests. *Tribology Trans.*, **46**(4), 479–493.
41. Zaretsky, E.V., Anderson, W.J., and Parker, R.J., 1962. The effect of contact angle on rolling-contact fatigue and bearing load capacity. *ASLE Trans.*, **5**(1), 210–219.
42. Takata, H., 1992. Fatigue life theory of rolling bearings considering the fatigue life of rolling elements. *Japanese J. Tribology*, **37**(12), 1605–1621.
43. Zaretsky, E.V., Poplawski, J.V., and Root, L.E., 2008. Relation between Hertz stress-life exponent, ball-race conformity, and ball bearing life. *Tribol. Trans.*, **51**(2), 150–159.
44. Parker, R.J., and Zaretsky, E.V., 1972. Reevaluation of the stress life relation in rolling-element bearings. NASA TN D–6745.
45. Styri, H., 1951. Fatigue strength of ball bearing races and heat treated 52100 steel specimens. *Proc. American Society for Testing and Materials*, **51**, 682–700.
46. Cordiano, H.V., Cochran, E.P., Jr., and Wolfe, R.J., 1956. A study of combustion resistant hydraulic fluids as ball bearing lubricants. *Lubrication Engineering*, **12**(4), 261–266.
47. McKelvey, R.E., and Moyer, C.A., 1963. The relation between critical maximum compressive stress and fatigue life under rolling contact. Paper 1, presented at the Institution of Mechanical Engineers Symposium on Fatigue in Rolling Contact, Mar. 28, 1963.
48. Townsend, D.P., Coy, J.J., and Zaretsky, E.V., 1978. Experimental and analytical load-life relation for AISI 9310 steel spur gears. *J. Mechanical Design*, **100**(1), 54–60.
49. Barwell, F.T., and Scott, D., 1956. Effect of lubricant on pitting failure of ball Bearings. *Engineering*, **182**, 4713, 9–12.
50. Butler, R.H., and Carter, T.L., 1957. Stress-life relation of the rolling-contact fatigue spin rig. NACA TN 3930.
51. Baughman, R.A., 1958. Experimental laboratory studies of bearing fatigue. ASME paper 58–A–235.
52. Scott, D., 1958. Lubricants at higher temperatures: assessing the effects on ball bearing failures. *Engineering*, **185**, 4811, 660–662.
53. Utsmi, T., and Okamoto, J., 1960. Effect of surface roughness on the rolling fatigue life of bearing steels. *J. Japan Society of Lubrication Engineers*, **5**(5), 291–296.
54. Greenert, W.J., 1962. The toroid contact roller test as applied to the study of bearing materials. *J. Basic Engineering*, **84**(1), 181–191.
55. Valori, R.R., Sibley, L.B., and Tallian, T.E. 1965. Elastohydrodynamic film effects on the load-life behavior of rolling contacts. ASME paper 65–LUBS–11.
56. Schatzberg, P., and Felsen, I.M., 1969. Influence of water on fatigue-failure location and surface alteration during rolling-contact lubrication. *J. Lubrication Technology*, **91**(2), 301–307.
57. Zaretsky, E.V., and Parker, R.J., 1967. Discussion to paper "On competing failure modes in rolling contact" by T.E. Tallian, *ASLE Trans.*, **10**(4), 436–437.
58. Lorosch, H.K., 1982. Influence of load on the magnitude of the life exponent for rolling bearings. *Rolling Contact Fatigue Testing of Bearing Steels* (ed.: J.J.C. Hoo), ASTM STP–771, American Society for Testing and Materials, Philadelphia, PA, USA, pp. 275–292.

59. Zwirlein, O., and Schlicht, H., 1982. *Rolling Contact Fatigue Testing of Bearing Steels* (ed.: J.J.C. Hoo), ASTM STP–771, American Society for Testing and Materials, Philadelphia, PA, USA, pp. 358–379.
60. Bamberger, E.N., and Signer, H., 1976. Endurance and failure characteristics of main-shaft jet engine bearing at $3\times10^6$ DN. *J. Lubrication Technology*, **98**(4), 580–585.
61. Parker, R.J., Zaretsky, E.V., and Bamberger, E.N., 1974. Evaluation of load-life relation with ball bearings at 500 °F. *J. Lubrication Technology*, **96**(3), 391–397.
62. Bamberger, E.N., and Zaretsky, E.V., 1971. Fatigue lives at 600 °F of 120-millimeter-bore ball bearings of AISI M–50, AISI, M–1, and WB–49 Steels. NASA TN D–6156.
63. Bamberger, E.N., Zaretsky, E.V., and Anderson, W.J., 1970. Effect of three advanced lubricants on high-temperature bearing life. *J. Lubrication Technology*, **92**(1), 23–33.
64. Zaretsky, E.V., Anderson, W.J., and Bamberger, E.N., 1969. *Rolling-Element Bearing Life from* 400 to 600 °F. NASA TN D–5002.
65. Townsend, D.P., Bamberger, E.N., and Zaretsky, E.V., 1976. A life study of ausforged, standard forged, and standard machined AISI M–50 spur gears. *J. Lubrication Technology*, **98**(3), 418–425.
66. Koistinen, D.P., 1964. The generation of residual compressive stresses in the surface layers of through-hardened steel components by heat treatment. *ASM Trans.*, **57**, 581–588.
67. Stickels, C.A., and Janotik, A.M., 1980. Controlling residual stresses in 52100 bearing steel by heat treatment. *Metallurgical Trans.* **11**(3), 467–473.
68. Almen, J.O., 1962. Effects of residual stress on rolling bodies. *Rolling Contact Phenomena* (ed.: J.B. Bidwell), Elsevier, pp. 400–424.
69. Gentile, A.J., Jordan, E.F., and Martin, A.D., 1965. Phase transformations in high-carbon, high-hardness steels under contact loads. *AIME Trans.*, **233**(6), 1085–1093.
70. Gentile, A.J., and Martin, A.D., 1965. The effect of prior metallurgically induced compressive residual stress on the metallurgical and endurance properties of overload-tested ball bearings. ASME paper 65–WA/CF–7.
71. Scott, R.L., Kepple, R.K., and Miller, M.H., 1962. The effect of processing-induced near-surface residual stress on ball bearing fatigue. *Rolling Contact Phenomena* (ed.: J. B. Bidwell), Elsevier, pp. 301–316.
72. Naisong, X., Stickels, C.A., and Peters, C.R., 1984. The effect of furnace atmosphere carbon potential on the development of residual stresses in 52100 steel. *Metallurgical Trans. A*, **15**(11), 2101–2102.
73. Jones, A.B., 1947. Metallurgical observations of ball bearing fatigue phenomena. *Symposium on Testing of Bearings*, American Society for Testing and Materials, Philadelphia, PA., USA, pp. 35–52.
74. Carter, T.L., 1960. A Study of Some Factors Affecting Rolling-Contact Fatigue Life. NASA TR R–60.
75. Akaoka, J., 1962. Some considerations relating to plastic deformation under rolling contact. *Rolling Contact Phenomena* (ed.: J.B. Bidwell), Elsevier, pp. 266–300.
76. Zaretsky, E.V., Parker, R.J., and Anderson, W.J., 1969. A study of residual stress induced during rolling. *J. Lubrication Technology,* **91**(2), 314–319.

77. Zaretsky, E.V., Parker, R.J., Anderson, W.J., and Miller, S.T., 1965. Effect of Component Differential Hardness on Residual Stress and Rolling-Contact Fatigue. NASA TN D–2664.
78. Foord, C.A., Hingley, C.G., and Cameron, A., 1969. Pitting of steel under varying speeds and combined stresses. *J. Lubrication Technology*, **91**(2), 282–293.
79. Cioclov, D., 1969, Discussion (pp. 290–291) of Foord, C. A., Hingley, C. G., and Cameron, A. 1969, "Pitting of Steel Under Varying Speeds and Combined Stresses," *J. Lubrication Technology*, **91**(2), 282–293.
80. Coe, H.H., and Zaretsky, E.V., 1987. Effect of interference fits on roller bearing fatigue life. *ASLE Trans*., **30**(2), 131–140.
81. Czyzewski, T., 1975. Influence of a tension stress field introduced in the elastohydrodynamic contact zone on rolling-contact fatigue. *Wear*, **34**(2), 201–214.
82. Zaretsky, E.V., Poplawski, J.V., and Miller, C.R., 2001. Rolling bearing life prediction – Past, present, and future. In *Proc. of the International Tribology Conf. Nagasaki*, 2000, Vol. 1, Japanese Society of Tribologists, Tokyo, Japan, pp. 101–107.
83. Vlcek, B.L., Hendricks, R.C., and Zaretsky, E.V., 2003. Determination of rolling-element fatigue life from computer generated bearing tests. *STLE Tribology Trans.*, **46**(3), 479–493.
84. Harris, T.A., 1995, "Final report-establishment of a new rolling bearing contact life calculation method. U.S. Naval Air Warfare Center, Aircraft Division Trenton, Contact No. N68335–93–C–0111.
85. Harris, T.A., and McCool, J.J., 1996. On the accuracy of rolling bearing fatigue life prediction. *ASME J. Tribology*, **118**(2), 297–310.
86. Lewicki, D.G., Black, J.D., Savage, M., and Coy, J.J., 1986. Fatigue life analysis of a turboprop reduction gearbox. *J. Mech. Trans. Autom. Des., Trans. ASME*, **108**(2), 225–262.
87. Zaretsky, E.V., Lewicki, D.G., Savage, M., and Vlcek, B.L., 2007. Determination of turboprop reduction gearbox system fatigue life and reliability. *Tribol. Trans.*, **50**(4), 507–516.
88. Coy, J.J., Townsend, D.P., and Zaretsky, E.V., 1975. Analysis of Dynamic Capacity of Low-Contact-Ratio Spur Gears Using Lundberg-Palmgren Theory. NASA TN D–8029.
89. Coy, J.J., and Zaretsky, E.V., 1975. Life Analysis of Helical Gear Sets Using Lundberg-Palmgren Theory. NASA TN D–8045.
90. Coy, J.J., Townsend, D.P., and Zaretsky, E.V., 1983. An Update on the Life Analysis of Spur Gears. In *Advanced Power Transmission Technology*, NASA, Cleveland, OH, USA, NASA CP–2210, pp. 421–434.
91. Poplawski, J.V., Peters, S.M., and Zaretsky, E.V., 2001. Effect of roller profile on cylindrical roller bearing life prediction – Part I: Comparison of bearing life theories, *STLE Tribology Trans.*, **44**(3), 339–350.
92. Poplawski, J.V., Peters, S.M., and Zaretsky, E.V., 2001. Effect of roller profile on cylindrical roller bearing life prediction – Part II: Comparison of roller profiles, **44**(3), 417–427.
93. Melis, M.E., Zaretsky, E.V., and August, R., 1999. Probabilistic analysis of aircraft gas turbine disk life and reliability. *J. Propulsion and Power*, *Trans. AIAA*, **15**, 658–666.